TRANSIENT ANALYSIS OF A GAS MANIFOLD SYSTEM

A Thesis Submitted

In Partial Fulfillment of the Requirements

For the Degree of

Master of Technology

by

Vineet Parolia

to

Department of Chemical Engineering

INDIAN INSTITUTE OF TECHNOLOGY

KANPUR

February, 2001

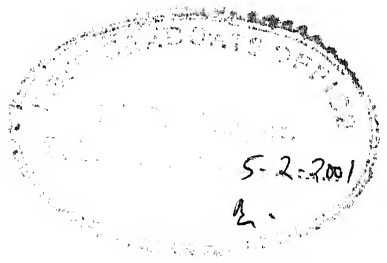

CERTIFICATE

It is certified that the work contained in the thesis entitled **Transient Analysis of a Gas Manifold System**, by **Vineet Parolia**, has been carried out under our supervision and that this work has not been submitted elsewhere for a degree.

Dr. Nishith Verma
Assistant Professor
Department of Chemical Engineering
Indian Institute of Technology
Kanpur

Dr. R. P. Chhabra
Professor
Department of Chemical Engineering
Indian Institute of Technology
Kanpur

February, 2001

ABSTRACT

For steady delivery of a gas to process tools, it is necessary that design considerations include implications of the steady as well as transient conditions that can arise during the operation of such systems. The start-up and shutdown, varying demand at the consumer ends, malfunctioning of equipments such as compressor and valve are just a few examples of the causes of transience in a gas delivery system. In the present work, numerical simulation has been carried out to analyze transient gas flow and pressure due to the above mentioned factors. A parametric study has also been done to determine the sensitivity of oscillations in pressure and mass flux to change in pipe dimensions, supply pressure and flow rate. The model simulation results show that larger pipe dimensions, higher gas requirements at the points-of-use (POU) and higher upstream pressure in the branch in which the disturbance is introduced, all result in relatively greater amplitude in mass flux and pressure oscillations in the neighboring branches. The duration of oscillations is also found to persist over longer periods. An analysis of transience occurring due to leakage and abrupt rupture in a gas pipeline has also been carried out. Depending upon the pressure conditions prevailing at the point of leakage or rupture, outflow is found to be sonic or subsonic. The present study has practical significance in the safe design and operation of a gas delivery system with multiple branches.

ACKNOWLEDGEMENT

I wish to express my deep sense of gratitude to Dr Nishith Verma, for his excellent guidance and all round assistance at every stage of my work.

I also express my sincere gratitude to Dr. R.P. Chabbra, for his valuable guidance and moral support throughout, which led to successful completion of this work.

I would also like to acknowledge the partial financial support obtained through a grant from All India Council of Technical Education (AICTE), New Delhi to my thesis Supervisor, Dr. Nishith Verma, to pursue the present study.

I would always remember the company of my friends, Deba, Kushal, Mukesh, and Shailesh for their lively company and co-operation throughout my tenure of my stay at IIT Kanpur.

The love, caring and constant encouragement from my parents are invaluable assets that I got throughout the course of study. Without them nothing would have been possible.

Vineet Parolia

Contents

List of Figures iii

List of Tables vi

List of Flow-sheets vii

Nomenclature viii

1. **Introduction**.....1
2. **Literature review**.....5
3. **Problem statement, formulation and governing equations**.....9
   - 3.1 Problem statement and formulation.....9
   - 3.2 Governing equations and methods of analysis.....10
   - 3.3 Non-dimensionalisation of Governing Equations.....12
   - 3.3.1 Two branch manifold.....12
   - 3.3.2 Initial and boundary conditions.....14
4. **Numerical formulation and solution procedure**.....15
   - 4.1 Discretization of Governing Equations.....15
   - 4.1.1 Discretization for case I.....16
   - 4.1.2 Discretization for case II.....18
   - 4.2 Effect of time step on solution.....20
5. **Results and discussion**.....31

   5.1 Effect of parametric variables on the dimensionless groups.....31

   5.2 Model Validation.....31

   5.3. Parametric study done on a two-branch manifold (Valve at node C is closed completely).....33

   5.3.1 Effect of change in mass flow rate in branch BC/BD.....33

   5.3.2Effect of change in upstream pressure at node A.....35

   5.3.3 Effect of change in diameter of branch BC and BD.....37

5.3.4 Effect of change in length of branch BC.....38

5.4 Effect of number of sub-branches on mass flux and pressure transience when valves at the downstream ends of the sub-branches are closed .....39.

5.5 Compressor shut down analysis.....40

5.6 Effect of change in mass flow rate in branch BC/BD.....40

5.6.1 Effect of change in upstream pressure at node A.....42

5.6.2 Effect of change in diameter of branch BD.....43

5.6.3 Effect of change in length of branch BD.....45

5.7 Compressor start-up analysis.....46

5.6.1 Change in mass flow rate in branch AB.....46

5.6.2 Effect of change in upstream pressure at node A.....49

5.6.3 Effect of change in diameter of branch BD.....50

5.6.4 Effect of change in length of branch BD.....51

5.7 Leakage Analysis.....52

5.8 Simulation of outflow from a rupture.....54

List of Figures

1 Schematics of a typical gas distribution system....4

2 Modeling scheme of an n-branch manifold....8

5.1a Effect of mass flow rate in branch BD on mass flux transience at node B in the main branch....56

5.1b Effect of length of branch BD on mass flux transience at node B in the main branch....56

5.2a Mass flux transience at node B for branch 1 (effect of change in mass flow rate of branch1)....57

5.2b Mass flux transience at node B for branch 2 57

5.2c Pressure transience at node D....58

5.2d Pressure transience at node B....58

5.2e Mass flux transience at node B for branch 1 (effect of change in mass flow rate of branch 2)....59

5.2f Mass flux transience at node B for branch 2 59

5.2g Pressure transience at node D....60

5.2h Pressure transience at node B....60

5.2i Mass flux transience at node B for branch 1 (effect of change in supply pressure at node A)....61

5.2j Mass flux transience at node B for branch 2 61

5.2k Pressure transience at node D....62

5.2l Pressure transience at node B....62

5.2m Mass flux transience at node B for branch 1 (effect of change in diameter of branch 1 and 2)....63

5.2n Mass flux transience at node B for branch 2 63

5.2o Pressure transience at node D....64

5.2p Pressure transience at node B....64

5.2q Mass flux transience at node B for branch 1 (effect of change in length of branch 2).....65

5.2r Mass flux transience at node B for branch 2 65

5.2s Pressure transience at node D.....66

ssure transience at node B.....66

ct of number of branches in manifold on mass flux at node A 67

ct of number of branches in manifold on pressure at node D 68

s flux transience at node B for branch 1(effect of change in mass flow rate in ich 2 in case of compressor shut down) 69

ss flux transience at node B for branch 2 69

ssure transience at node B 70

ssure transience at node A 70

ss flux transience at node B for branch 1(effect of change in supply pressure in nch 2) 71

s flux transience at node B for branch 2.....71

ssure transience at node B 72

ssure transience at node A 72

s flux transience at node B for branch 1(effect of change in diameter in branch case of compressor shut down) 73

s flux transience at node B for branch 2.....73

ssure transience at node B 74

ssure transience at node A 74

ass flux transience at node B for branch 1(effect of change in length in branch 75

5.4n Mass flux transience at node B for branch 2.....75

5.4o Pressure transience at node B 76

5.4p Pressure transience at node A 76

5.5a Mass flux transience at node C(change in mass flow rate in branch 2 in case of compressor start up) 77

5.5b Mass flux transience at node D.....77

5.5c Mass flux transience at node B for main branch 77

5.5d Pressure transience at node A 78
5.5e Pressure transience at node B.....78
5.5f Mass flux transience at node C(change in supply pressure in main branch) ...79
5.5g Mass flux transience at node D.....79
5.5h Mass flux transience at node B for main branch 79
5.5i Pressure transience at node A 80
5.5j Pressure transience at node B.....80
5.5k Mass flux transience at node C(change in diameter of branch 2) 81
5.5l Mass flux transience at node D.....81
5.5m Mass flux transience at node B for main branch 81
5.5n Pressure transience at node A 82
5.5o Pressure transience at node B.....82
5.5p Mass flux transience at node C(change in length of branch 2) 83
5.5q Mass flux transience at node D.....83
5.5r Mass flux transience at node B for main branch 83
5.5s Pressure transience at node A 84
5.5t Pressure transience at node B.....84
5.6 Leakage analysis:- Velocity, pressure and flow-rate variations at Sorzen after leakage 85
5.7a Rupture analysis:- Simulation of gas flow and pressure at the outlet in a low pressure pipeline (1st case).....86
5.7b Rupture analysis:- Simulation of gas flow and pressure at the outlet in a low pressure pipeline (2nd case).....87

List of Tables

1 Schematic representation of transient conditions studied in case of a manifold as well as in a single pipe.....21

2 Non-dimensionalized boundary conditions used in different scenarios of transient analysis in a manifold consisting of two or more branch and in a single pipe 23

3 Simulation of outflow as well as pressure at the point of rupture in a high-pressure gas pipeline 88

List of Flow-sheets

1. Solution procedure of a two branch manifold in which the valve is completely closed at node C.....24
2. Solution procedure of an n branch manifold in which valves are completely closed at the downstream ends of any of the sub-branches 25
3. Solution procedure of a two branch manifold in case of a compressor shut down.....26
4. Solution procedure of an n branch manifold in case of a compressor shut down.....27
5. Solution procedure of a two branch manifold in case of a compressor start up.....28
6. Solution procedure of an n branch manifold in case of a compressor start up.....29
7. Solution procedure of a leakage/rupture.....30

Nomenclature

d	diameter of pipe (m)
f	friction factor
g	acceleration due to gravity (m^2/s)
G	gas mass flux ($kg/m^2.s$)
L	length of pipe (m)
M	molecular weight of gas (kg/kmol)
p	Pressure (N/m^2)
R	universal gas constant ($m^3.Pa/kmol.K$)
t	time (sec)
T	temperature (K)
v	velocity (m/s)
z	axial distance (m)
Z	compressibility factor.

Subscripts

a,b,c,d	nodes A, B, C and D
z	z direction
b_1	branch 1
b_2	branch 2
b_m	main branch
f	final value
g	guess value
i	initial value
max	maximum value
min	minimum value
ss	steady state

Superscipt

*	dimensionless variables

Greek symbols

ρ	gas density (Kg/m^3)
μ	viscosity of gas (Kg/m.s)

ıapter 1

TRODUCTION

Transient flow of a gas in pipes and pipe networks is an important aspect in the effective design and safe operation of a gas distribution system. Actual operations riably encounter transient conditions. During transient condition in a gas delivery gas pressure and mass flow rate along the pipe length may drastically vary with . A change from steady flow conditions in a piping system occurs when there is a ge and/or failure in the operation of elements in the system such as valves, ɔressor, etc. Quite often these are terminals or boundaries of the pipe and maybe red to as boundary conditions. There are many opportunities to introduce transients fluid systems through changes in operating conditions. Rather than an exhaustive g of the possible causes of transients only a few different possibilities are mentioned

. Changes in valve settings, accidental or planned,
. Starting or stoppage of turbo-machines such as compressors, turbines, etc.
. Liquid vaporization or vapor condensation in supply pipeline due to change in ambient conditions
. Accidental leakage or abrupt rupture of safety valve-disk

The study of fluid transients quite often involves analysis of problems having one ore of these conditions. When a steady pattern of flow in a pipeline is disturbed by ging of the flow at either end, a pressure or mass flux wave is formed which travels from the source of disturbance. Friction reduces the peak velocity reached during successive mass flow waves or pressure waves propagating from the point of bance. Surges are the best known of all the transient phenomena in pipeline

systems. A surge is the conversion of the kinetic energy into potential energy, occurring when pressure drop across a pipeline is increased. In the rapid valve closure case, the transients generated may well be damaging and may last for a very long time; however a slower valve closure rate may result in little more than a mild oscillation in mass flow rate. Sudden valve closure at the downstream end of the pipe results in a well-known case of " water hammering" effect. This effect has been used quite frequently in our transient studies involving valve closure in manifolds and compressor shutdown. The above phenomenon generates the maximum amount of pressure transience, which is a useful feature while designing the thickness of pipe as well as surge tanks in the pipeline systems. Thus transient gas distribution model helps us to know a priori the various features before the pipeline system is actually put into operation. The analysis of pressure-velocity time relations may also be useful in predicting the transient performance of control valves and compressors and the response of compressor-station-control systems

Traditionally, the approach used is one of analysis rather than design or synthesis. A design is made, then the system is analyzed to see if it is satisfactory from a transient viewpoint. If not, alterations in the design are made and it is analyzed again, perhaps with such changes as an increase in the thickness of pipe walls or introduction of surge tanks, buffers, and so on which control or filter the extent of transience.

Thus in designing a new pipeline system, significant economy can be gained in many cases by a systematic analysis of transient-pressure distribution as demonstrated in the thesis.

As shown in Figure 1, a typical gas distribution system consists of a storage vessel, a flow and/or pressure control station which regulates the amount of the flow rate and pressure along the discharge lines and valve manifold boxes (VMBs) to vary the flow rate according to the existing demands of the process tools. Compressors are usually installed at intermediate distances in the pipeline to boost and maintain the supply pressure. Control stations and distribution junctions are connected to each other through pipes, valves, mass-flow controllers (MFC) and pressure regulators. The product delivered to the process tools can be stored either as a liquid or gas depending upon the

end requirements or for safety reasons. The POU requirements are usually specified in terms of flow and minimum pressure.

Objectives

The main objective of the present work is to develop a model for a gas distribution system of large-scale facility such as the one shown in Figure 1. In particular, consideration is given to study the transience in a gas manifold consisting of a main branch dividing into various sub-branches. Transience caused due to the following scenarios are studied: (a) change in gas demand at one of the POU's and its effect on the neighborhood branches are studied (b) one or more valve closure at the downstream end of sub-branches in a manifold and its effect on the remaining neighboring branches, (c) Start-up/shutdown of a compressor/pump which is installed at the upstream end of the main branch and its effect on the sub-branches and (d) leakage and rupture occurring at an intermediate point in the pipeline. In each case, the evolution of pressure and mass flux with time are studied and a detailed parametric study is performed to elucidate the sensitivity of the various operating variables by changing the available pressure drop across the pipes in the network and/or by changing the state of a valve or a turbo-machine on the mass flux and pressure transience.

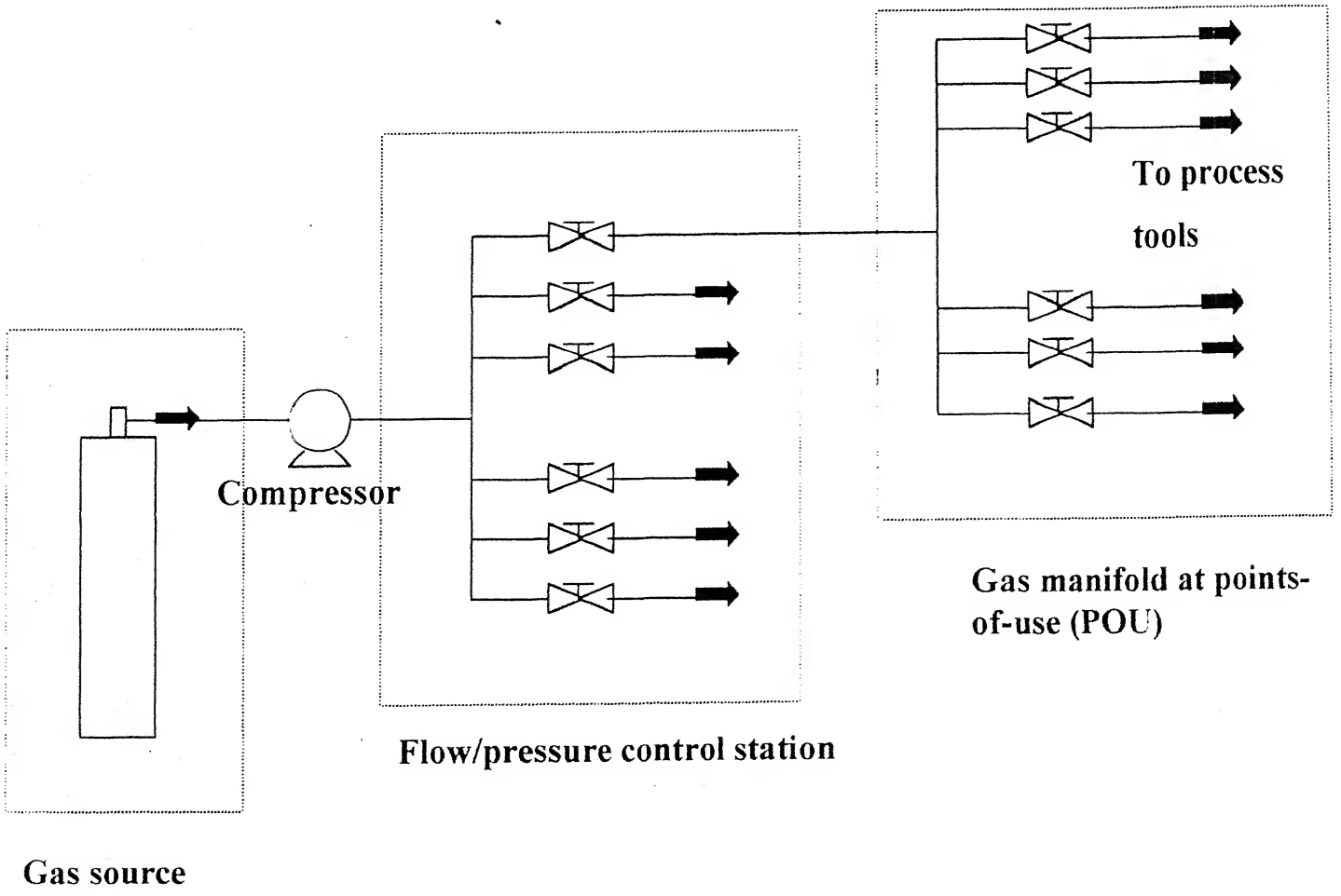

Figure 1: Schematics of a typical gas distribution system

CHAPTER 2

LITERATURE REVIEW

The subject of unsteady flow of liquids, which began in the middle of the nineteenth century, has expanded to other fluids, and has continued at an accelerated pace particularly after the mid-twentieth century. Consequently, well-developed ideas based on fundamental fluid mechanics are now available for the analysis of transient fluid flow in piping systems.

Many authors have investigated transience in gas pipelines. However, a vast amount of the available literature deals with the efficacy of various numerical methods employed for solving the unsteady flow problems in pipes. Not much is available in the open literature about the behavior of transience perse in a distribution system. Among some of the works done in 60s, during which period a large scale network of crude oil pipes was laid in the US, Burnett (1960) carried out a numerical study of the pressure-velocity-time relations at a fixed location in a long crude oil pipe line, especially with regards to the pressure surge and suggested that the performance of control valves and pumps and the response of pump-station-control system can be improved using his theoretical predictions. Batey et al. (1961) reported a rigorous mathematical analysis of gas pipeline for both steady state and transient and proposed various methods to control and/to to minimize the effects of transience. These include filtering the transients by two methods-active and passive. The pipeline section and compressor stations are used as passive and active filters respectively, in which the compressor horsepower is varied to keep the flow constant. Watters (1984), Wylie et al. (1993) and Simpson et al. (1997) have also carried out transient analysis in hydraulic systems and their works have especially focused on the so called "water hammering" caused by abrupt closure of a valve. In a recent work (Hati et al; 2001), a systematic numerical analysis has been

carried out to characterize the transient conditions in a horizontal pipeline under the conditions of a valve closure and opening at the two ends of a straight pipe. In the aforementioned work, eight representative cases were identified and simulated for unsteady-state situation.

Reviewing numerical methods, it is fair to note that the traditional explicit methods such as the method of characteristics (MOC) (Wylie et al; 1978), the Lax-Wendroff method (Bender, 1979), and the two-step Lax-Wendroff method ((Poloni et al; 1987) have been used to numerically solve the transient problems concerning a gas delivery system. Several numerical techniques based on implicit methods have also been developed. For instance, Guy (1967) proposed a partially implicit algorithm based on Crank-Nicolson method, in which the continuity and momentum equations are applied, to each node, alternatively. Rachford et al. (1975) developed an implicit technique using the Galerkin method. Schmidt (1977) used the Crank-Nicolson and the backward Euler methods alternately to avoid the spurious oscillations. Fincham et al. (1979) also developed a computer simulation model by employing a MOC and the Galerkin finite element method. It resulted in the development of a software package, PAN (Programme for the Analysis of Networks) that uses an implicit (Crank-Nicolson) finite difference scheme for the time variable and space variable. Some of these methods are adopted in commercial computer program used by the gas industry. Osiadacz (1984) applied a fully implicit method to the linearized equations, which were obtained by neglecting the inertia terms in the momentum equation.

The present work focuses on the pressure and flow transience in a gas delivery system consisting of a main branch and sub-branches connected to POUs. Disturbance in steady-state conditions is introduced by altering valve settings or start-up or shut down of a compressor installed upstream of the main branch or due to the accidental leakage or abrupt rupture. Figure 2 describes the modeling scheme of an n-branch manifold. The main branch AB splits into various sub-branches BC, BD, etc. Thus, it forms an open loop network in which any of the valves installed at the downstream end of a branch can be closed or opened partially or completely, and its effect on the mass flux and pressure in the remaining branches can be determined. Similar effects are also determined in

manifold consisting of several sub-branches for the start-up or shutdown of a compressor installed at the upstream end of the main branch.

Leakage or rupture occurring in a single pipeline is modeled using a two branch manifold and is described in detail later on. Thus a wide range of scenarios commonly encountered in the gas industry are covered here in and its parametric study greatly helps us to understand and analyze the situations better.

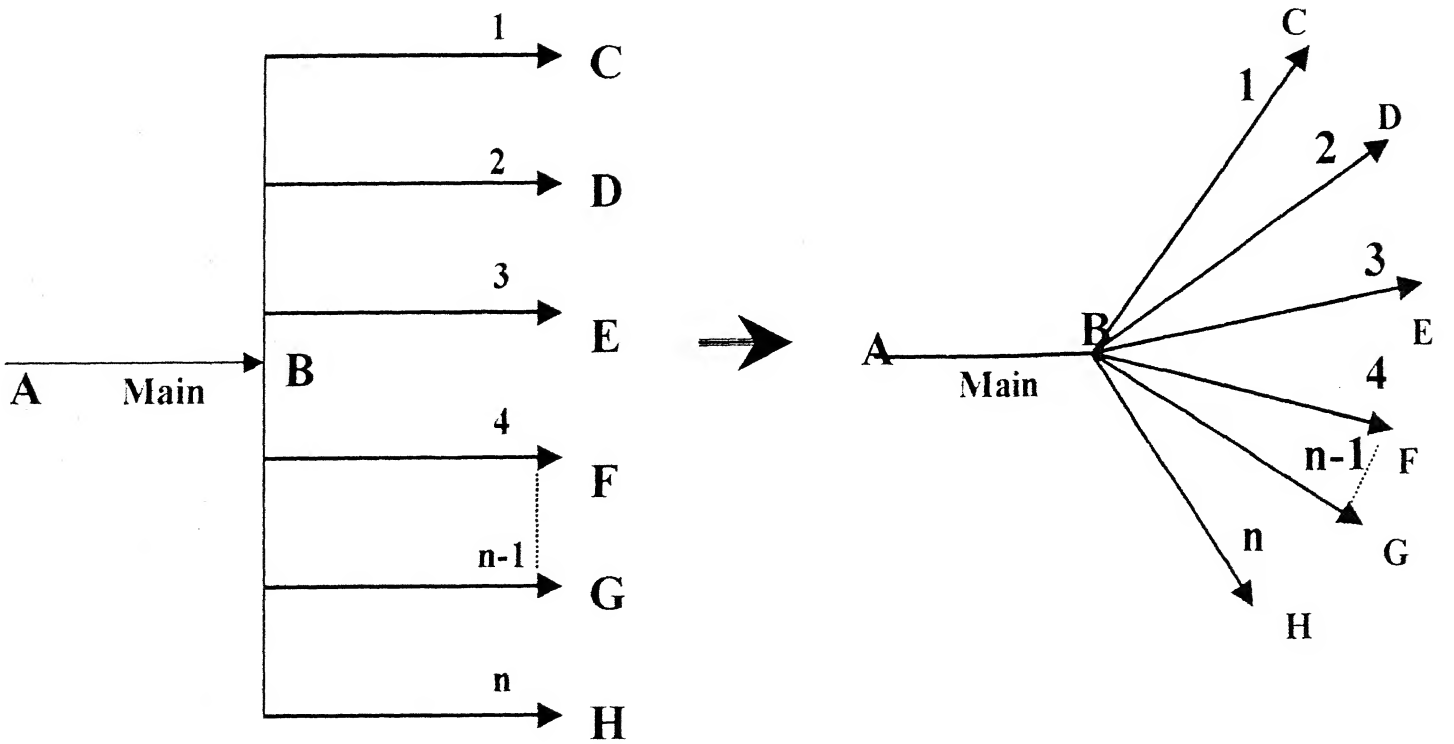

Figure 2: Modeling scheme of an n-branch manifold

CHAPTER 3

PROBLEM STATEMENT, FORMULATION AND GOVERNING EQUATIONS

3.1 Problem Statement and Formulation

The basis of the present work can be briefly categorized into eight representative cases in a single pipe. These cases differ with respect to their initial and boundary conditions because of the different starting and operating conditions respectively. In each case, the upstream end of the pipe is connected to a source or reservoir of gas at a constant pressure and the downstream end is connected to another pipe or to a point-of-use or sink, the pressure at which is usually determined by the process tools or customers demand. Depending upon the operation of the valve or the compressor, varying pressure and mass-flux profiles evolve in the pipelines.

The basic program for a single pipeline for different cases provides the fundamental elements that are necessary for the treatment of the more complex piping systems. Different types of boundary conditions may be introduced by changing only the part of the program that deals with the particular end condition. When the system contains more than one pipeline, the interior grid points of each pipeline are solved simultaneously for pressure and mass flux conditions at each instant of time. A non-pipe element such as a junction, reservoir, compressor, valve, etc. is referred to as a particular boundary condition and is solved simultaneously for all the grid points associated with that boundary condition. Additional boundary conditions (valve closure, compressor start up/shutdown, leakage/rupture) in a multi-pipe systems (manifold consisting of several branches) are also discussed.

At a junction where two or more pipe connections occur, the continuity equation must be satisfied at each instant of time, that is, there is no accumulation of mass at the junction.

A junction/node is visualized as a point connection of elements in a system, at which :re are two variables: a nodal flow, Q_m, and a nodal pressure. The elements connected at the ction/node may be any of the system facilities, such as valves, compressors, or pipelines. ere are two types of junctions or nodes:

1. A constant or prescribed pressure (i.e., a known value as a function of time) and hence the nodal flow must be a free variable.
2. A constant or a prescribed/specified flow, in which case the junction pressure must be a free variable.

3.2 GOVERNING EQUATIONS AND METHODS OF ANALYSIS:

All methods of analysis or synthesis of unsteady flow in conduits start with the equations iotion, continuity, or energy, along with the equation of state and the other physical property ionships. The methods commonly used are graphical, characteristics, algebraic, implicit, e element, linear analysis, etc.

The continuity and momentum equations, together with the equation of state under ermal conditions describing transients in gas pipelines yield a non-homogeneous system of linear hyperbolic conservation laws. The partial differential equations are approximated by raic finite-difference equations by use of either the implicit or the explicit formulations.

Under the assumptions of ideal gas behavior, 1-D isothermal compressible flow, friction r based on steady state flow, negligible expansion of pipe wall due to pressure changes and ontal pipe, the governing equations are developed as follows:

tion of Continuity:

$$\frac{\partial}{\partial z}(\rho v_z) = 0 \tag{3.1}$$

ion of motion:

$$+\rho v_z \frac{\partial v_z}{\partial z} = -\frac{\partial p}{\partial z} - \frac{2f\rho v_z^2}{d} + \mu \frac{\partial^2 v_z}{\partial z^2} + \rho g_z \tag{3.2}$$

ation (3.2), terms on left hand side are the inertial contributions respectively. The terms on ht hand are pressure, wall drag, viscous and gravitational forces respectively. For low of gases, the viscous term can be neglected in comparison to the wall drag. For a

horizontal pipe, gravitational term can also be dropped. Therefore, equation (3.2) is simplified as:

$$\rho\frac{\partial v_z}{\partial t}+\rho v_z\frac{\partial v_z}{\partial z}=-\frac{\partial p}{\partial z}-\frac{2f\rho v_z^2}{d} \tag{3.3}$$

Equation of state:

The gas is assumed to obey the ~~ideal~~ gas equation:

$$PM = Z\rho RT \tag{3.4}$$

Also the mass-flux (G), kg/m^{2}s, is given as:

$$G = \rho v_z \tag{3.5}$$

For steady state and for fixed pressure drop across the pipe, equations (3.1) and (3.2) are solved to obtain:

$$2\ln\frac{p_a}{p_b}-\frac{M}{G^2RTZ}(p_a^2-p_b^2)+4\frac{fL}{d}=0 \tag{3.6}$$

In equation (3.6), pressure (p) and mass flux (G) are dependant variables, whereas time (t) and space (z) are independent variables.

The density and velocity terms are eliminated from equation (3.1) and (3.3). Using equations (3.4) and (3.5), the following governing equations are obtained:

$$\frac{\partial p}{\partial t}=-\frac{ZRT}{M}\cdot\frac{\partial G}{\partial z} \tag{3.7}$$

$$\frac{\partial G}{\partial t}-\frac{G}{p}\frac{\partial p}{\partial t}+\frac{GZRT}{PM}\frac{\partial G}{\partial z}-\left(\frac{G^2ZRT}{p^2M}\frac{\partial p}{\partial z}\right)=\frac{\partial p}{\partial z}-\frac{2fpM}{ZRTd}\left(\frac{GZRT}{pM}\right)^2$$

$(\frac{\partial p}{\partial t})$ term from equation (3.7) is replaced and is rearranged, we get the following equation,

$$\frac{\partial G}{\partial t}+2\frac{GZRT}{pM}\cdot\frac{\partial G}{\partial z}-\left(\frac{G^2ZRT}{p^2M}-1\right)\frac{\partial p}{\partial z}=-\frac{2f}{d}\cdot\frac{G^2ZRT}{pM} \tag{3.8}$$

The partial differential equations (3.7) and (3.8) describe the transient flow of a gas in a pipe.

Due to the presence of the convective term, i.e., $(2\frac{GZRT}{pM}\cdot\frac{\partial G}{\partial z})$, equation (3.8) is hyperbolic in nature.

All three branches of the two branch manifold, i.e., main branch (AB), branch 1 (BC) and branch 2 (BD) can be considered as a single pipe and hence, equations, (3.7) and (3.8) are

)plied with appropriate boundary conditions in each branch to describe the transient behavior of e gas. Minor losses in bends and other fittings have been neglected.

3 Non-dimensionalisation of Governing Equations

3.1 Two branch Manifold

The governing equations and the boundary conditions have been non-dimensionalised ng the characteristic variables and the dimensions of branch 2nd sub-branch i.e., BD. For, ssure, however, respective pressure conditions in individual branch are used as the racteristic variables. The following dimensionless variables are introduced to render the verning equations and the boundary conditions dimensionless:

ne

$$= \frac{t}{t_{c,b2}} \quad where, t_{c,b2} = \frac{L_{b2}}{v_{ss,b2}} \tag{3.9}$$

the steady state velocity before the disturbance, is calculated based on the downstream ssure, i.e.,

$$_2 = \frac{G_{ss,b2} RTZ}{p_d M} \tag{3.10}$$

ninating $v_{ss,b2}$, $t_{c,b2}$ is written as:

$$= \frac{L_{b2} p_d M}{G_{ss,b2} RTZ} \tag{3.11}$$

$$\frac{t}{\frac{L_{b2} p_d M}{G_{ss,b2} RTZ}} \tag{3.12}$$

ss-flux

$$= \frac{G}{G_{ss,b2}} \tag{3.13}$$

tance in axial direction

$$= \frac{z}{L_{b2}} \tag{3.14}$$

erential operators

$$\frac{\partial}{\partial z^*} \equiv L_{b2} \frac{\partial}{\partial z} \tag{3.15}$$

$$\frac{\partial}{\partial t^*} \equiv \frac{L_{b2} p_d M}{G_{ss,b2} RTZ} \frac{\partial}{\partial t} \tag{3.16}$$

Finally, pressure is non-dimensionalised for each individual branch as follows:

Branch 1

$$p^* = \frac{p - p_c}{p_b - p_c} = \frac{p - p_c}{\Delta p_{b1}} \tag{3.17}$$

Branch 2

$$p^* = \frac{p - p_d}{p_b - p_d} = \frac{p - p_d}{\Delta p_{b2}} \tag{3.18}$$

Main Branch

$$p^* = \frac{p - p_b}{p_a - p_b} = \frac{p - p_b}{\Delta p_{bm}} \tag{3.19}$$

Introducing these dimensionless variables in the governing equations, (3.7) and (3.8), the non-dimensionalised equations are obtained as follows:

Branch 1:

$$\frac{\partial p^*}{\partial t^*} = -\frac{1}{A_{b1}} \cdot \frac{\partial G^*}{\partial z^*} \tag{3.20}$$

$$\frac{\partial G^*}{\partial t^*} + 2\frac{G^*}{(D_{b1} + p^* A_{b1})} \frac{\partial G^*}{\partial z^*} - \left[\frac{G^{*2} B_{b1}}{(D_{b1} + p^* A_{b1})^2} - M \right] \frac{A_{b1}}{B_{b1}} \frac{\partial p^*}{\partial z^*} = -2.C_{b1} \cdot \frac{G^{*2}}{(D_{b1} + p^* A_{b1})} \tag{3.21}$$

i.e., A_{b1}, B_{b1}, C_{b1} *and* D_{b1} are four dimensionless groups given as:

$$A_{b1} = \frac{Dp_{b1}}{p_{a2}}, B_{b1} = \frac{G_{ss,b2}^2 Z R T}{p_{d2}^2}, C_{b1} = f \frac{L_{b2}}{d_{b1}}, D_{b1} = \frac{p_c}{p_d}$$

Branch 2

$$\frac{\partial p^*}{\partial t^*} = -\frac{1}{Ab_2} \cdot \frac{\partial G^*}{\partial z^*} \tag{3.22}$$

$$\frac{\partial G^*}{\partial t^*} + 2\frac{G^*}{(D_{b2} + p^* A_{b2})}\frac{\partial G^*}{\partial z^*} - \left[\frac{G^{*2} B_{b2}}{(D_{b2} + p^* A_{b2})^2} - M\right]\frac{A_{b2}}{B_{b2}}\frac{\partial p^*}{\partial z^*} = -2.C_{b2}\cdot\frac{G^{*2}}{(D_{b2} + p^* A_{b2})} \tag{3.23}$$

i.e., A_{b2}, B_{b2}, C_{b2}, D_{b2} are four dimensionless groups given as:

$$A_{b2} = \frac{Dp_{b2}}{p_{d2}}, B_{b2} = \frac{G_{ss,b2}^2 Z R T}{p_{d2}^2}, C_{b2} = f\frac{L_{b2}}{d_{b2}}, D_{b2} = \frac{p_d}{p_d} = 1$$

Main Branch

$$\frac{\partial p^*}{\partial t^*} = -\frac{1}{A_{bm}}\cdot\frac{\partial G^*}{\partial z^*} \tag{3.24}$$

$$\frac{\partial G^*}{\partial t^*} + 2\frac{G^*}{(D_{bm} + p^* A_{bm})}\frac{\partial G^*}{\partial z^*} - \left[\frac{G^{*2} B_{bm}}{(D_{bm} + p^* A_{bm})^2} - M\right]\frac{A_{bm}}{B_{bm}}\frac{\partial p^*}{\partial z^*} = -2.C_{bm}\cdot\frac{G^{*2}}{(D_{bm} + p^* A_{bm})} \tag{3.25}$$

i.e., A_{bm}, B_{bm}, C_{bm} and D_{bm} are four dimensionless groups given as:

$$A_{bm} = \frac{Dp_{bm}}{p_{d2}}, B_{bm} = \frac{G_{ss,b2}^2 Z R T}{p_{d2}^2}, C_{bm} = f\frac{L_{b2}}{d_{bm}}, D_{bm} = \frac{p_b}{p_d}$$

3.3.2 Initial and Boundary Conditions

At the start of simulation, the flow is assumed to be in a steady state. The initial values *(G (x,0) & P (x,0))* therefore, are defined. For a two-branch manifold, six boundary conditions are required to solve the equations, two for each of three branches. From continuity, the incoming mass flow-rate through main branch at node, B, equals the sum of outgoing mass flow rates to branch 1 and 2. Assuming the pressure and mass-flux at node, B, to be *p(t)* and *G(t)*, respectively, a time varying pressure or mass-flux condition at node, B, is assumed to solve for transient pressure and mass flux profiles for branch 1 and 2. Various transient scenarios and their non-dimensionalized boundary conditions in their respective branches are described in Table 1 and 2 respectively.

Chapter 4

NUMERICAL FORMULATION AND SOLUTION PROCEDURE

4.1 Discretization of Governing Equations

As discussed previously, equations (3.7) and (3.8) are hyperbolic in nature. The main feature of hyperbolic equation is that, depending upon the characteristics of the equation the solution proceeds from left to right or vice-versa. For a set of equations, it can be shown that, the direction of solution depends upon the eigen values of the coefficient matrix of the equations.

For all cases involving valve closure, compressor start up and shut down and leakage transients, the basic discretization procedures of the governing equations are identical. The difference in the discretization procedure for different cases is only due to their respective boundary conditions. In the case of valve closure at the downstream end of one of the sub-branches, G, gas mass flux, is specified at the downstream end and hence P, supply pressure needs to be specified at the other end. While, in case of the compressor transience during start up or shut-down, G is specified at the inlet end of the main branch since compressor is installed at the upstream end and hence P, is specified at the other end. In all cases, the space variable (z), however, is divided into n grids and standard finite difference method is used to discretize the equations at each grid point. Due to the non-linear nature, the term, $G(\partial G/\partial z)$ in equation (3.8), an initial guess value of G is made at each time step and solutions are iterated till a specified convergence is attained.

Table 1 refers to the various scenarios of transience and their brief description. Referring to Table 2, **(Case I)** for cases 1 and 5, known pressure boundary conditions or a guess value of pressure is made at the inlet of the main branch i.e., branch AB, branch

BC for cases 1, 3 and 5 and branch BD for cases 1 and 3. Mass flux boundary conditions are known at the exit of the pipe. Thus, in all the cases and for the respective branches described above, coefficient matrix of the discretized equations is found to be identical as described below. Similarly, **(Case II)** for case 3, known or a guess value of mass flux is made at the inlet end of branch AB and for case 4, branch AB, BC and BD. The pressure boundary condition is specified at the other end. Thus, for these cases, the coefficient matrix of the discretized equations is similar.

4.1.1 Discretization for case I.

In this case, the governing equations have been solved for the mass-flux for grid-points, 1 to n-1 and pressure for 2 to n, since the mass-flux at 'n' and pressure at '1' are known from boundary conditions.

For z =2 to n, equation (3.7) is discretized as follows:

$$\frac{p_z^{*t+1}-p_z^{*t}}{\Delta t^*}=-\frac{1}{A_1}\cdot\frac{G_z^{*t+1}-G_{z-1}^{*t+1}}{\Delta z^*} \quad \text{or} \tag{4.1}$$

$$p_z^{*t+1}=p_z^{*t}-\frac{c}{A_1}\cdot\left(G_z^{*t+1}-G_{z-1}^{*t+1}\right)$$

For z =1 to n-1, equation (3.8) is discretized as follows:

$$\frac{G_z^{*t+1}-G_z^{*t}}{\Delta t^*}+2\frac{G_z^{*t+1}}{(D_1+p_z^{*t+1}A_1)}\cdot\frac{G_{z+1}^{*t+1}-G_z^{*t+1}}{\Delta z^*}-\left[\frac{G_z^{*t+1^2}B_1}{(D_1+p_z^{*t+1}A_1)^2}\right]\frac{A_1}{B_1}\cdot$$
$$\frac{p_{z+1}^{*t+1}-p_z^{*t+1}}{\Delta z^*}=-2C_1\cdot\frac{G_z^{*t+1^2}}{(D_1+p_z^{*t+1}A_1)} \tag{4.2}$$

For z=1, p_z^{*t+1} is known from boundary condition. Let this be P_1. The guess value of mass-flux at time step (t+1), i.e., G_z^{*t+1} to be $G_{g(z)}$.

For z =1, equation (4.2) can also be written as follows:

$$\frac{G_1^{*t+1}-G_1^{*t}}{\Delta t^*}+2\frac{G_{g(1)}c}{(D_1+P_1A_1)}\cdot\frac{G_2^{*t+1}-G_1^{*t+1}}{\Delta z^*}-\left[\frac{G_{g(1)}^{*t+1^2}B_1}{(D_1+p_1^{*t+1}A_1)^2}\right]\frac{A_1c}{B_1}(p_2^{*t+1}-P_1).$$
$$=-2C_1\cdot\frac{G_{g(1)}^2\Delta t^*}{(D_1+p_z^{*t+1}A_1)} \tag{4.3}$$

Assuming,

$$a_z = 2\frac{G_{g(z)}c}{(D_1 + d_z)}$$

$$b_z = \left(\frac{G_{g(z)}^2 B_1}{(D_1 + d_z)^2} - M\right)\frac{A_1 c}{B_1}$$

$$d_z = \left[p_z^{t+1} - \frac{c}{A_1}(G_z^{t+1} - G_{z-1}^{t+1})\right]A_1$$

Equation (4.3) can be rearranged to get the following equation:

$$G_1^{*t+1} - G_1^{*t} + a_1(G_2^{*t+1} - G_1^{*t+1}) - b_1(p_2^{*t+1} - P_1) \quad -2C_1\frac{G_{g,1}^2 \Delta t^*}{(D_1 + d_1)} \tag{4.4}$$

Also, p_2^{*t+1} at z =1 can be substituted from equation (4.1):

$$G_1^{*t+1} - G_1^{*t} + a_1(G_2^{*t+1} - G_1^{*t+1}) - b_1[\{(p_2^{*t} - \frac{c}{A_1}(G_2^{*t+1} - G_1^{*t+1})\} - P_1] \quad -2C_1\frac{G_{g,1}^2 \Delta t^*}{(D_1 + d_1)} \quad \text{or,}$$

$$\left(1 - a_1 - \frac{b_1 c}{A_1}\right)G_1^{*t+1} + \left(a_1 + \frac{b_1 c}{A_1}\right)G_2^{*t+1} \quad G_1^{*t} + b_1\left(p_2^{*t} - P_1\right) - 2C_1\frac{G_{g(1)}^2 \Delta t^*}{(D_1 + d_1)} \tag{4.5}$$

For grids 2 to n-1, on substitution of p_{z+1}^{*t+1} and p_z^{*t+1} from equation (4.1) into equation (4.2), the following equation is obtained;

$$G_z^{*t+1} - G_z^{*t} + 2\frac{G_{(g)z}c(G_{z+1}^{*t+1} - G_z^{*t+1})}{[1 + \{p_z^{*t} - \frac{c}{A_1}(G_z^{*t+1} - G_{z-1}^{*t+1})\}.A_1]} - \left[\frac{G_{g(z)}^2 B_1}{1 + \{p_z^{*t} \quad \frac{c}{A_1}(G_z^{*t+1} - G_{z-1}^{*t+1})\}.A_1]^2} - M\right]\frac{A_1.c}{B_1}$$

$$[\{(p_{z+1}^{*t} - \frac{c}{A_1}(G_{z+1}^{*t+1} - G_z^{*t-1})\} - p_z^{*t} - \frac{c}{A_1}(G_z^{*t+1} - G_{z-1}^{*t+1})\}] \quad -2C_1\frac{G_{g(z)}^2 \Delta t^*}{[1 + \{p_z^{*t} - \frac{c}{A_1}(G_z^{*t+1} - G_{z-1}^{*t+1})\}]} \tag{4.6}$$

Again, assuming

$$a_z = 2\frac{G_{g(z)}c}{(D_1 + d_z)}$$

$$b_z = \left(\frac{G_{g(z)}^2 B_1}{(D_1 + d_z)^2} - M\right)\frac{A_1 c}{B_1}$$

$$d_z = \left[p_z^{t+1} \quad \frac{c}{A_1} (G_z^{t+1} \quad G_{z-1}^{t+1}) \right] A_1$$

Equation (4.6) can be rearranged to get the following equation

$$\frac{b_z c}{A_1} G_{z-1}^{*t+1} + \left(1 - a_z - \frac{2b_z c}{A_1}\right) G_z^{*t+1} + \left(a_z + \frac{b_z c}{A_1}\right) G_{z+1}^{*t+1} \\ G_z^{*t} + b_z \left(p_{z+1}^{*t} - p_z^{*t}\right) - 2C_1 \frac{G_{g,z}^2 \Delta t^*}{(D_1 + d_z)} \tag{4.7}$$

For z =n, the boundary condition, $G^*=0$ when the valve is completely closed.

Therefore, equation (4.7) at z=n-1 can be modified as follows:

$$\frac{b_{n-1} c}{A_1} G_{n-2}^{t+1} + \left(1 - a_{n-1} - \frac{2b_{n-1} c}{A_1}\right) G_{n-1}^{*t+1} = G_{n-1}^{*t} + b_{n-1}\left(p_n^{*t} - p_{n-1}^{*t}\right) - 2C_1 \frac{G_{g,n-1}^2 \Delta t^*}{(D_1 + d_{n-1})} \tag{4.8}$$

4.1.2 Discretization for case II.

In this case, the governing equations have been solved for the mass-flux for grid-points, 2 to n and pressure for 1 to n-1, since the mass-flux at 'n' and pressure at '1' are known from boundary conditions.

For z =1 to n-1, equation (3.7) is discretized as follows:

$$\frac{p_z^{*t+1} - p_z^{*t}}{\Delta t^*} = -\frac{1}{A_1} \cdot \frac{G_{z+1}^{*t+1} - G_z^{*t+1}}{\Delta z^*} \tag{4.9}$$

or

$$p_z^{*t+1} = p_z^{*t} - \frac{c}{A_1} \cdot \left(G_{z+1}^{*t+1} - G_z^{*t+1}\right) \tag{4.10}$$

For z =1 to n-1, equation (3.8) is discretized as follows:

$$\frac{G_z^{*t+1} - G_z^{*t}}{\Delta t^*} + 2\frac{G_z^{*t+1}}{(D_1 + p_z^{*t+1} A_1)} \cdot \frac{G_z^{*t+1} - G_{z-1}^{*t+1}}{\Delta z^*} - \left[\frac{G_z^{*t+1^2} B_1}{(D_1 + p_z^{*t+1} A_1)^2}\right] \frac{A_1}{B_1} \cdot \\ \frac{p_z^{*t+1} - p_{z-1}^{*t+1}}{\Delta z^*} = -2C_1 \cdot \frac{G_z^{*t+1^2}}{(D_1 + p_z^{*t+1} A_1)} \tag{4.11}$$

For z =n, p_n^{*t+1} is known from boundary condition. Let this be P_n. The guess value of mass-flux at time step (t+1), i.e., G_z^{*t+1} to be $G_{g(z)}$.

For z =n, equation (4.11) can also be written as follows:

$$\frac{G_n^{*t+1}-G_n^{*t}}{\Delta t^*}+2\frac{G_{g(n)}c}{(D_1+P_nA_1)}\frac{G^{*t+1}_n-G^{*t+1}_{n-1}}{\Delta z^*}\left[\frac{G^2_{g(n)}B_1}{(D_1+P_nA_1)^2}-M\right]\frac{A_1c}{B_1}(P_n-p^{*t+1}_{n-1})-$$

$$2C_1\frac{G^2_{g(n)}\Delta t^*}{(D_1+P_nA_1)} \qquad (4.12)$$

Assuming,

$$a_n=2\frac{G_{g(n)}c}{(D_1+d_n)}$$

$$b_n=\left(\frac{G^2_{g(n)}B_1}{(D_1+d_n)^2}-M\right)\frac{A_1c}{B_1}$$

$$d_n=P_nA_1$$

Equation (4.12) can be rearranged to get the following equation:

$$G_n^{*t+1}-G_n^{*t}+a_n(G_n^{*t+1}-G_{n-1}^{*t+1})-b_n(P_n-p_{n-1}^{*t+1})-2C_1\frac{G^2_{g,n}\Delta t^*}{(D_1+d_n)} \qquad (4.13)$$

Also, p_{n-1}^{*t+1} at z = n-1 can be substituted from equation (4.10):

$$G_n^{*t+1}-G_n^{*t}+a_n(G_n^{*t+1}-G_{n-1}^{*t+1})-b_n\left[P_n\left\{(p_{n-1}^{*t}-\frac{c}{A_1}(G_n^{*t+1}-G_{n-1}^{*t+1})\right\}\right]-2C_1\frac{G^2_{g,n}\Delta t^*}{(D_1+d_n)} \quad \text{or,}$$

$$\left(-a_n-\frac{b_nc}{A_1}\right)G_{n-1}^{*t+1}+\left(1+a_n-\frac{b_nc}{A_1}\right)G_n^{*t+1}=G_n^{*t}+b_n\left(P_n-p_{n-1}^{*t}\right)-2C_1\frac{G^2_{g(n)}\Delta t^*}{(D_1+d_n)} \qquad (4.14)$$

For grids 2 to n-1 , on substitution of p_z^{*t+1} and p_{z-1}^{*t+1} from equation (4.10) into equation (4.11), the following equation is obtained;

$$G_z^{*t+1}-G_z^{*t}+2\frac{G_{(g)z}c(G_z^{*t+1}-G_{z-1}^{*t+1})}{[1+\{p_z^{*t}-\frac{c}{A_1}(G_{z+1}^{*t+1}-G_z^{*t+1})\}.A_1]}-\left[\frac{G^2_{g(z)}B_1}{1+\{p_z^{*t}-\frac{c}{A_1}(G_{z+1}^{*t+1}-G_z^{*t+1})\}.A_1]^2}-M\right]\frac{A_1.c}{B_1}$$

$$[\{(p_z^{*t}-\frac{c}{A_1}(G_{z+1}^{*t+1}-G_z^{*t+1})\}-\{p_{z-1}^{*t}-\frac{c}{A_1}(G_z^{*t+1}-G_{z-1}^{*t+1})\}]-2C_1\frac{G^2_{g(z)}\Delta t^*}{[1+\{p_z^{*t}-\frac{c}{A_1}(G_{z+1}^{*t+1}-G_z^{*t+1})\}]}$$

(4.15)

Again, assuming

$$a_z = 2\frac{G_{g(z)}c}{(D_1 + d_z)}$$

$$b_z = \left(\frac{G_{g(z)}^2 B_1}{(D_1 + d_z)^2} - M\right)\frac{A_1 c}{B_1}$$

$$d_z = \left[p_z^{*t} - \frac{c}{A_1}(G_{z+1}^{*t+1} - G_z^{*t+1})\right]A_1$$

Equation (4.15) can be rearranged to get the following equation

$$\left(-a_z + \frac{b_z c}{A_1}\right)G_{z-1}^{*t+1} + \left(1 + a_z - \frac{2b_z c}{A_1}\right)G_z^{*t+1} + \frac{b_z c}{A_1}G_{z+1}^{*t+1} = G_z^{*t} + b_z\left(p_z^{*t} - p_{z-1}^{*t}\right) - 2C_1\frac{G_{g(z)}^2 \Delta t^*}{(D_1 + d_z)} \quad (4.16)$$

For z =1, the boundary condition, $G^*=0$ when the valve is completely closed.

Therefore, equation (4.16) at $z = 2$ can be modified as follows:

$$\frac{b_2 c}{A_1}G_3^{*t+1} + \left(1 + a_2 - \frac{2b_2 c}{A_1}\right)G_2^{*t+1} = G_2^{*t} + b_2\left(p_2^{*t} - p_1^{*t}\right) - 2C_1\frac{G_{g(2)}^2 \Delta t^*}{(D_1 + d_2)} \quad (4.17)$$

Solution Procedure

The solution procedure for each time step for each of the transient scenarios is described in respective flow sheets.

4.2 Effect of time step on solution

Simulation was done for different scenarios of transience and it was found that decreasing the time step below 0.1s, the effect on mass flux and pressure is insignificant. But the computation time increased tremendously. So for all the cases, a time step of 0.1s was taken as an optimum time step.

Grid number was taken as 4000 for all the simulation results, which was considered to be optimum.

Table 1

Schematic representation of transient conditions studied in case of a manifold.

Figure	Description
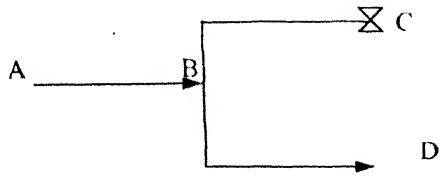 Valve closure in a two branch manifold	Initially there is a flow and then valve at node C is closed instantaneously. Pressure at node A and flow rate at node B are kept constant. (Case 1)
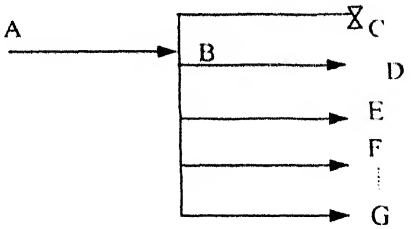 Valve closure in an n-branch manifold	Initially there is a flow and then valve at one or more ends of the downstream branch are closed instantaneously. Pressure at node A and flow rates in the remaining branches are kept constant. (Case 2)
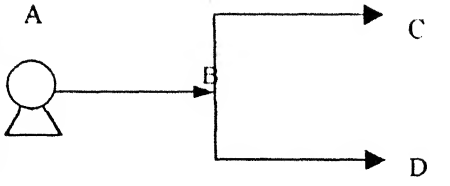 Compressor shut-down	Initially there is a flow and then compressor at A shuts off due to power failure and then valves at nodes C and D are closed as soon as compressor shuts down and the system becomes isolated. (Case 3)
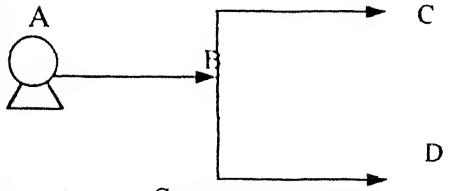 Compressor start-up	Initially there is no flow and then compressor at A starts from the initial line pressure and valves at nodes C and D are opened to final downstream pressures after the power is restored. (Case 4)

Various scenarios of transience studied in case of a single pipe.

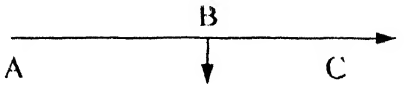 Leakage/Rupture analysis	Initially there is no leakage/rupture and the pipe is having a certain amount of flow. Then a leak/rupture develops at node B. Pressure at node A and mass flow rate at node C are fixed. (Case 5)

Table 2

Non-dimensionalized boundary conditions used in different scenarios of transient analysis in a manifold consisting of two or more branch and in a single pipe

(Case 1 refers to valve closure at the downstream end of branch BC, case 3 refers to compressor shutdown, case 4 refers to compressor start up and case 5 refers to leakage/rupture)

Case	Boundary Condition (For t^* 0)		
	Branch AB	Branch BC	Branch BD
1	At z^* 0, $p^* = 1$ At z^* 1, $G^* = \frac{G(t)}{G_{ss,b2}}$	At z^* 0, $p^* = \frac{p(t) - p_c}{p_b - p_c}$ At z^* 1, $G^* = 0$	At z^* 0, $p^* = \frac{p(t) - p_d}{p_b - p_d}$ At z^* 1, $G^* = 1$
3	At z^* 0, $G^* = 0$ At z^* 1, $p^* = \frac{p(t) - p_b}{p_a - p_b}$	At z^* 0, $p^* = \frac{p(t) - p_c}{p_b - p_c}$ At z^* 1, $G^* = 0$	At z^* 0, $p^* = \frac{p(t) - p_d}{p_b - p_d}$ At z^* 1, $G^* = 0$
4	At z^* 0, $G^* = \frac{G_{ssnew,bm}}{G_{ss,b2}}$ At z^* 1, $p^* = \frac{p(t) - p_b}{p_a - p_b}$	At z^* 0, $G^* = \frac{G(t)}{G_{ss,b2}}$ At z^* 1, $p^* = 0$	At z^* 0, $G^* = \frac{G(t)}{G_{ss,b2}}$ At z^* 1, $p^* = 0$
5	At z^* 0, $p^* = 1$ At z^* 1, $G^* = \frac{G(t)}{G_{ss,b2}}$	At z^* 0, $p^* = \frac{p(t) - p_d}{p_b - p_d}$ At z^* 1, $G^* = 1$	

Flow-sheet 1:- Solution procedure of a two branch manifold in which the valve is completely closed at node C

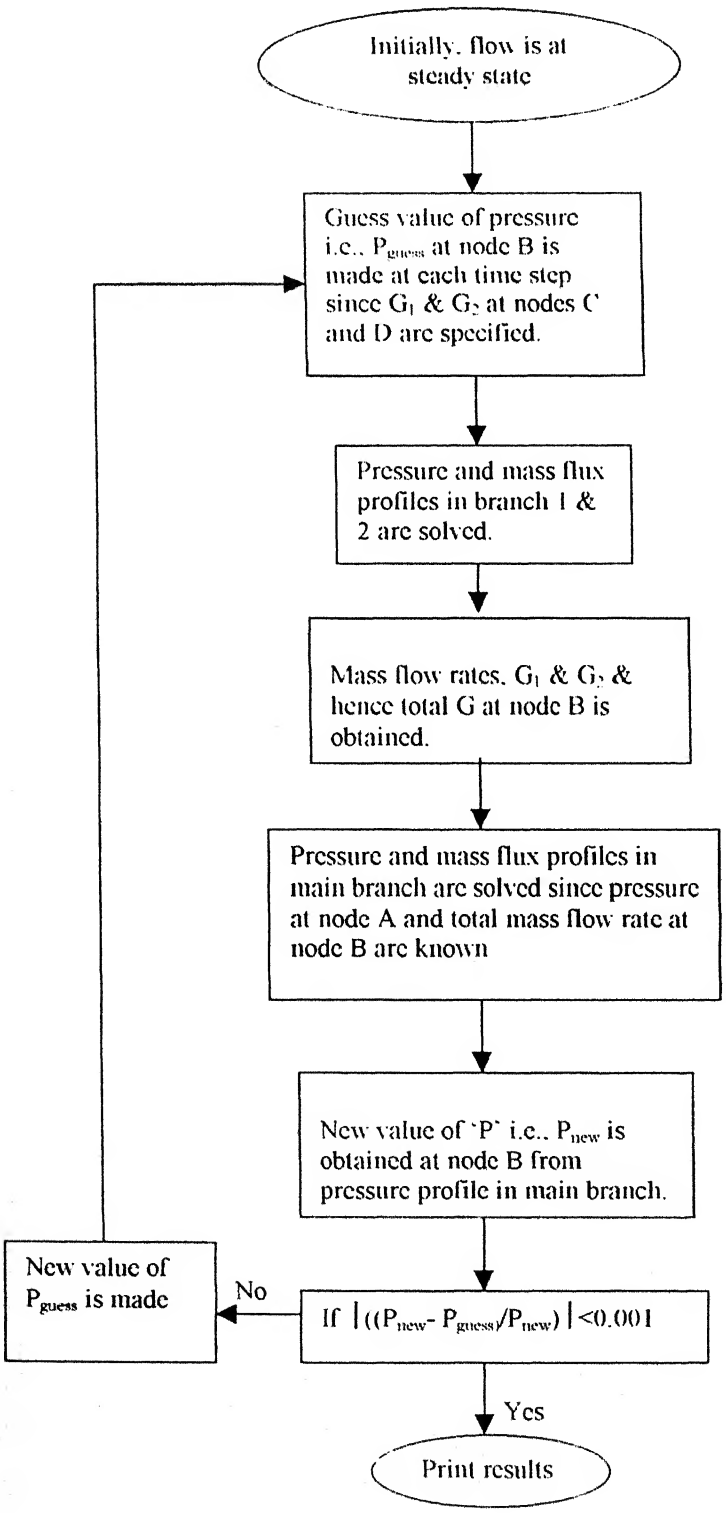

Flow-sheet 2:- Solution procedure of an n branch manifold in which valves are completely closed at the downstream ends of any of the sub-branches

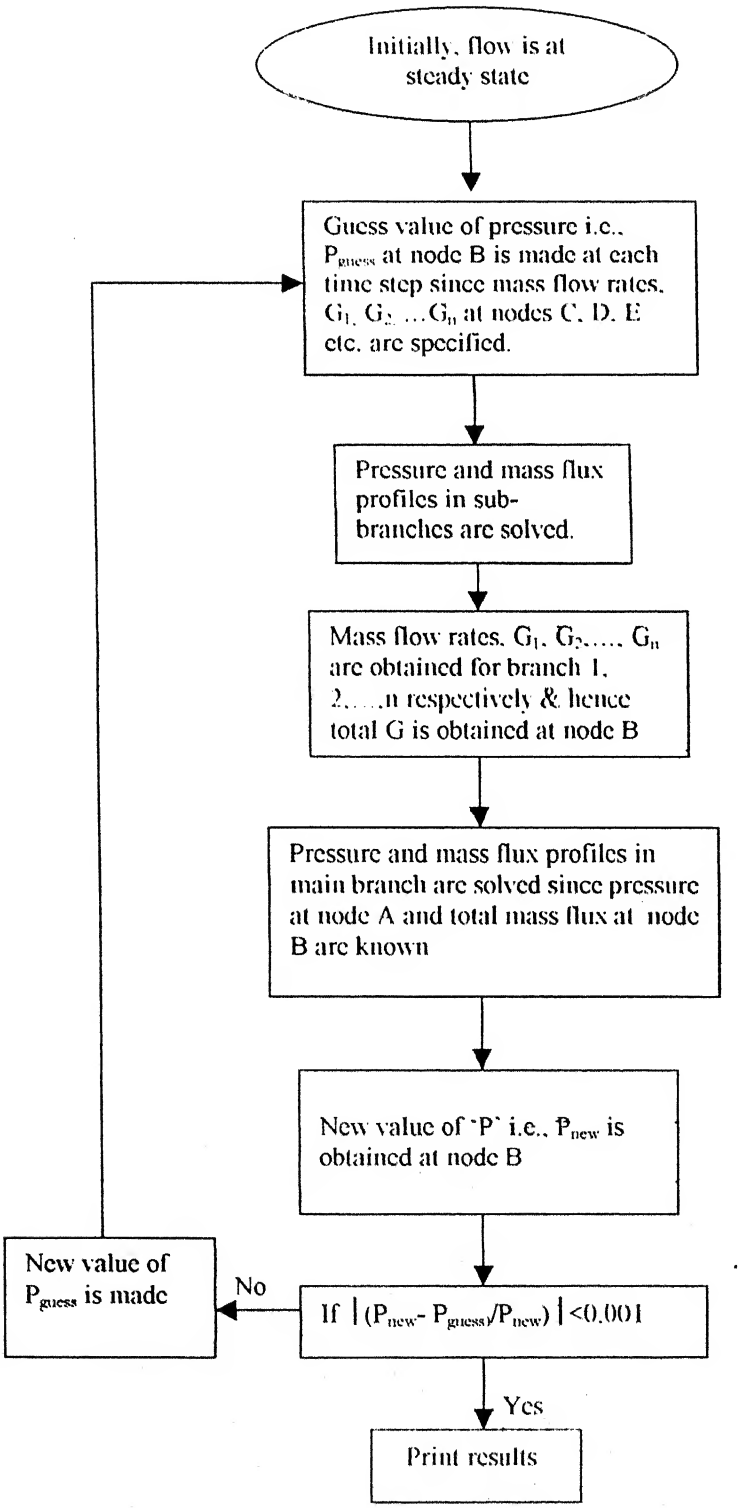

Flow-sheet 3:- Solution procedure of a two branch manifold in case of a compressor shut down

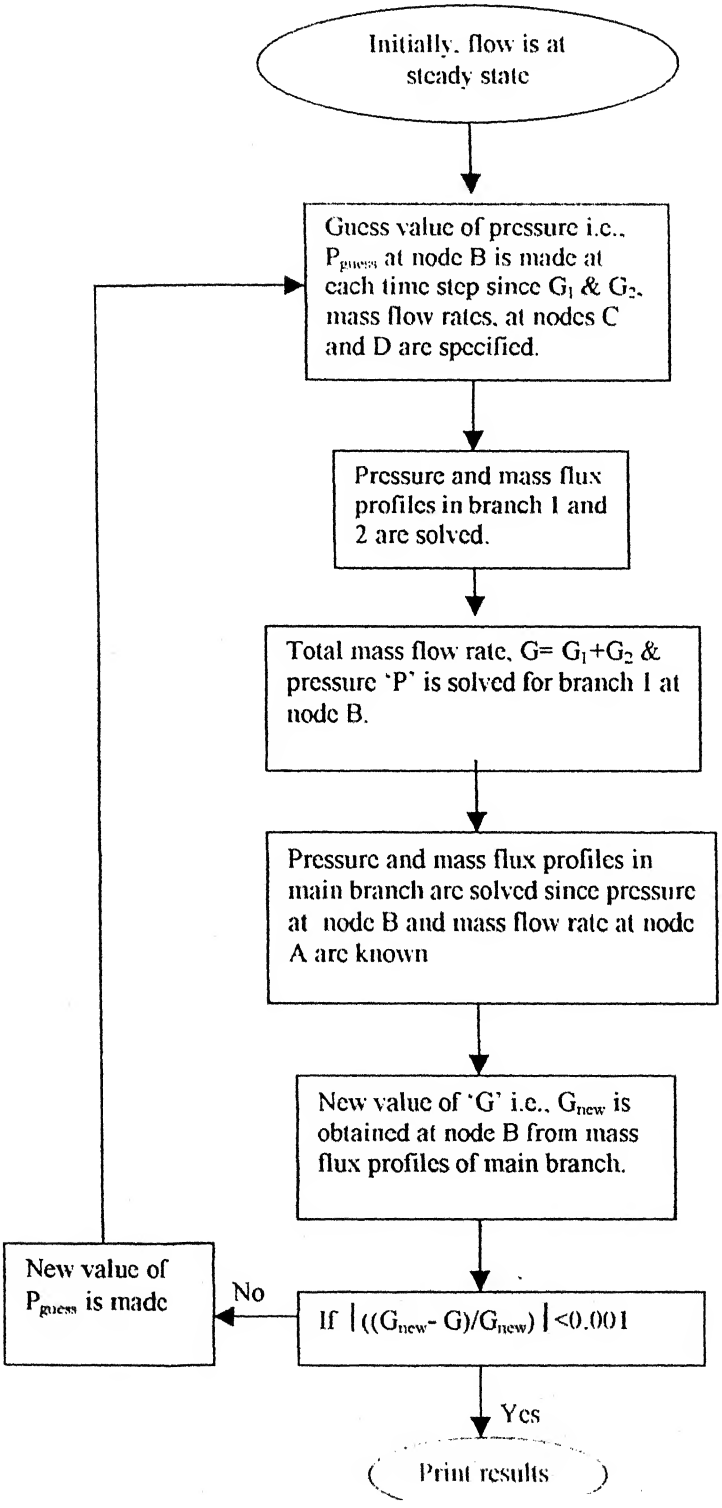

Flow-sheet 4:- Solution procedure of an n branch manifold in case of a compressor shut down

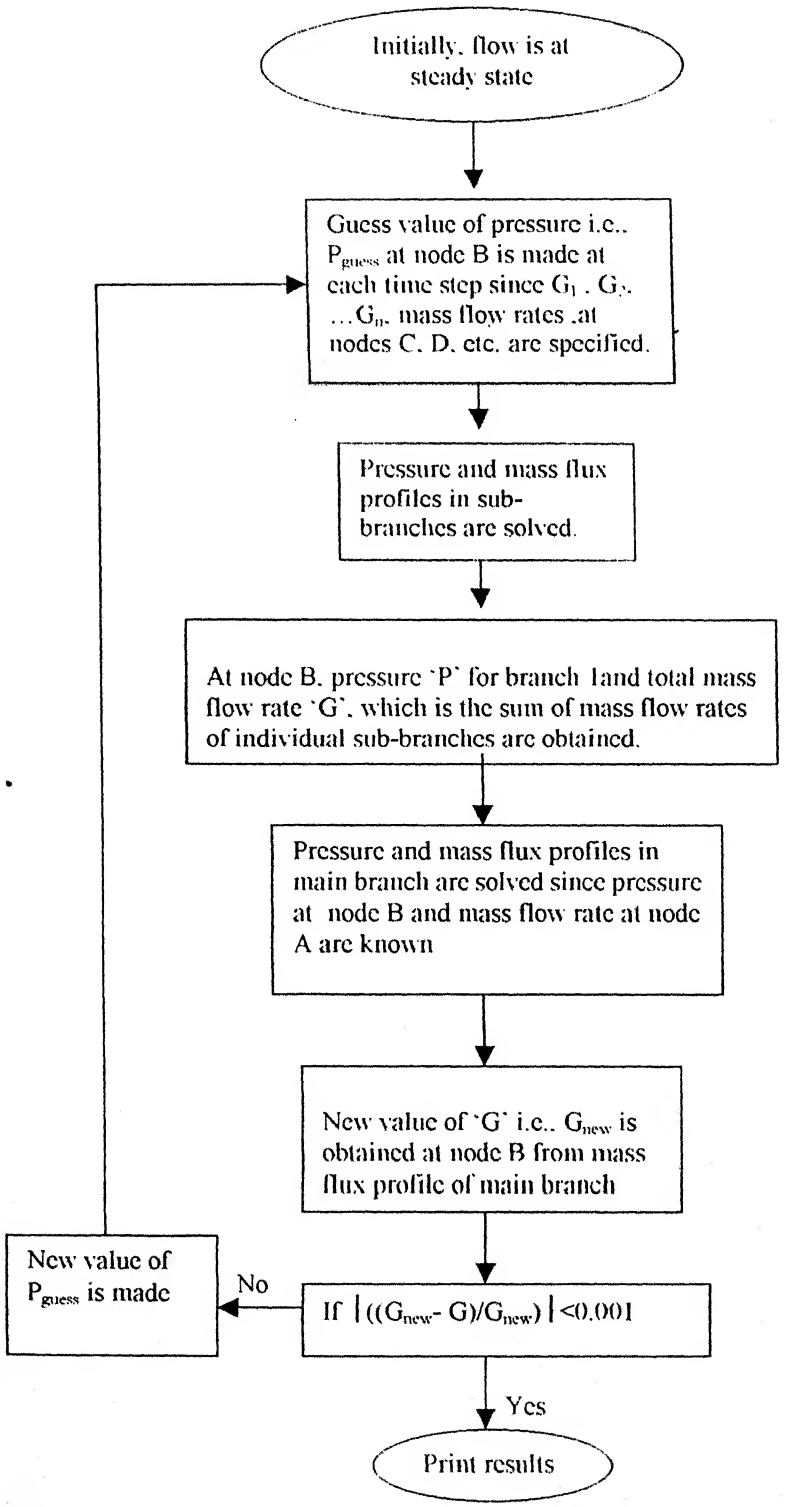

Flow-sheet 5:- Solution procedure of a two branch manifold in case of a compressor start up

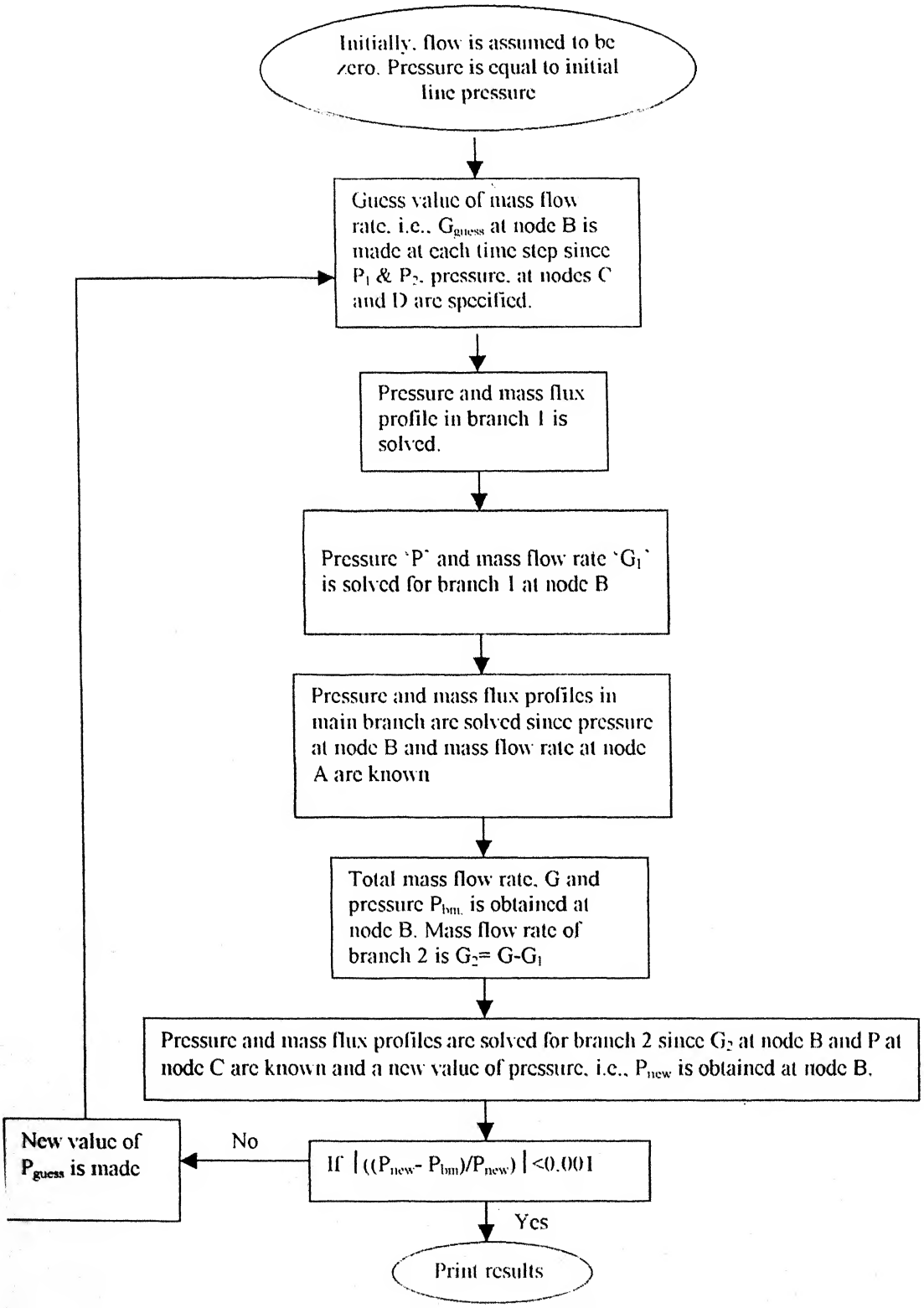

Flowsheet 6:- Solution procedure of an n branch manifold in case of a compressor start up

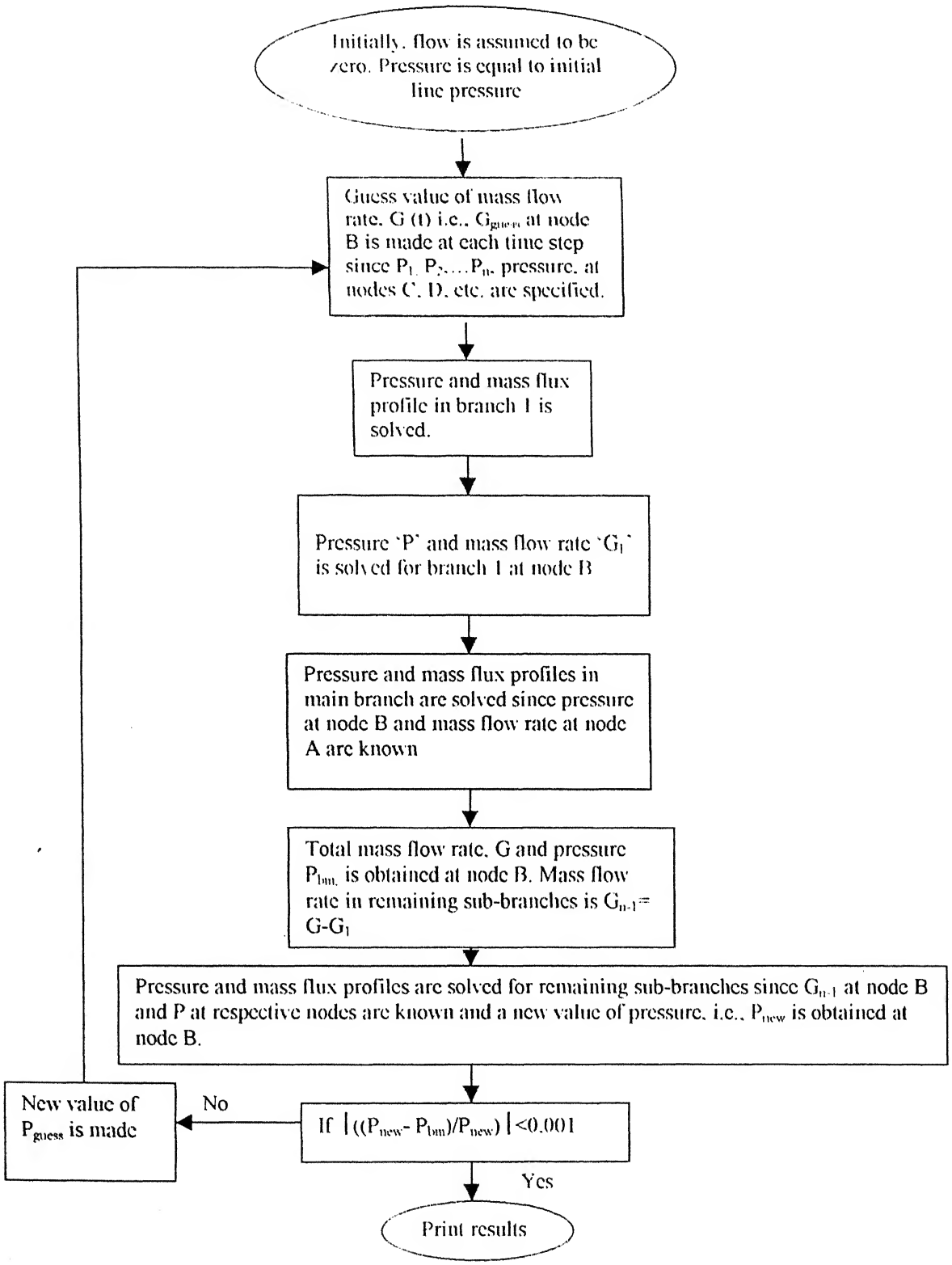

Flow-sheet 7:- Solution procedure of a leakage/rupture

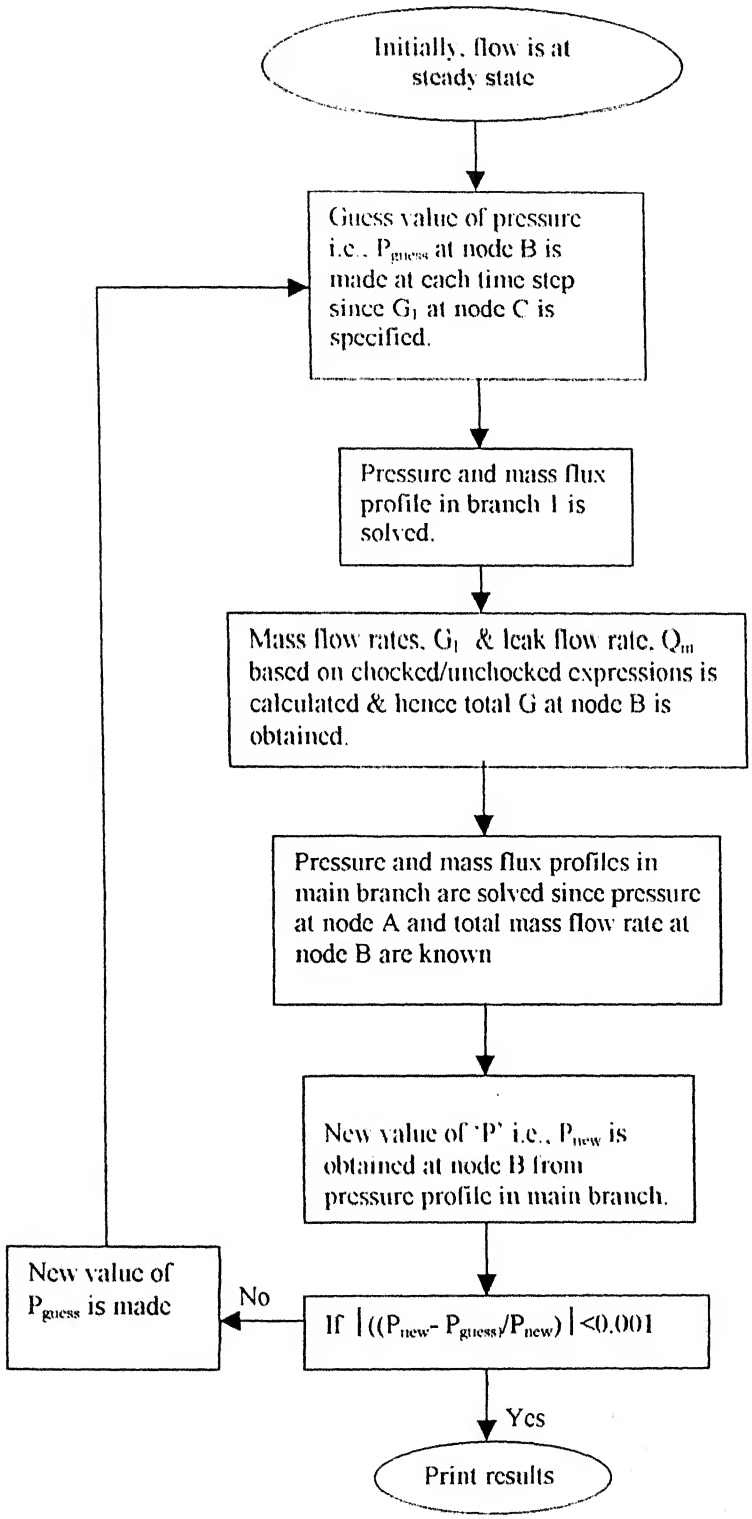

Chapter 5

Results and Discussion

In this chapter, the new extensive numerical results relating to a range of transient situations including leak and rupture are presented and discussed in detail. At the outset, it is, however, appropriate to validate the numerical solution procedure and to introduce the main dimensionless parameters effecting the transient gas flow in manifolds.

5.1 Effect of system variables on the dimensionless groups

The effect of system variables such as length, diameter, upstream pressure and mass flow rate on the dimensionless groups i.e., A_1, B_1 and C_1 on a single pipe was carried out. Since $A_1 = f(p_a, p_b)$ and $B_1 = f(G, p_b)$ and $C_1 = f(L, d)$, varying one of these variables and keeping the rest of the variables constant, it is observed that both pressure and mass flux are influenced simultaneously. For example, changing the length while keeping other variables constant results in a change in the downstream pressure i.e., p_b which occurs in both the dimensionless groups, i.e., A_1 and B_1. It was thus not possible to elucidate out the effect of diameter, length, upstream pressure and mass flow rate on a one particular dimensionless group and hence these key operating variable determine the transient behavior in a complex interactive manner.

5.2 Model Validation

A two-branch manifold is considered in which the main branch AB divides into two sub-branches BC and BD as shown schematically in Figure 5.1a. A valve is installed at the downstream end of branch BC and it is initially open. There is thus gas flow through the pipe corresponding to the prevailing pressure conditions at the two ends in each branch. A two-branch manifold can be reduced to a single pipe with a valve at its downstream end, choosing the lengths of branches AB and BD to be negligible as compared to that of the branch BC. Thus, the flow rate in branch BD is also negligible compared to that in branch BC.

A parametric study was done by varying the mass flow rate in branch BD and keeping the rest of the variables constant and by changing the length of branch BD and keeping rest of the variables constant. Thus a test two-branch manifold is assumed with lengths of branches AB and BD of 10 m and 1 m respectively and length of branch BC set at 500 m. The diameter of all pipes in the manifold is 203 mm. The mass flow rate in branch AB is set at 10.1 kg/s which is the total mass flow rate going inside the main branch. A mass flow-rate of 10 kg/s and 0.1 kg/s is flowing through pipes BC and BD respectively. The supply pressure at node A in the manifold is kept constant at 20 bar as is the flow rate at node D. Now the valve at node C is closed instantaneously which simulates the classical "water-hammering" case in branch BC, and the evolution of mass-flux and pressure at nodes A, B and C are followed. As seen from Figure 5.1a, mass flux oscillations start initially from mass flux value of 308.36 kg/m^{2}s before reaching its steady state value of zero flow. The oscillations continue for about 150 s and decrease monotonically.

Now a single pipe AB of length 510 m and diameter 203 mm is taken in which the mass flow rate of 10 kg/s (308.36 kg/m^{2}s) is flowing. The valve at the downstream end is now closed and its effect on mass flux transience at node B is plotted and compared with the two-branch manifold. The temperature of the entire system in the above simulations is kept constant at 303 K, a constant value of the Fanning friction factor of 0.003 was used which is consistent with the steady state flow conditions. The gas compressibility factor and gas specific gravity was taken as 1.0. The simulation was carried out for 100 s and with 4000 grid points. The physical properties of the gas have been approximated with those of air with a mean molecular weight of 28.97 kg/kmole. Pressure and mass flux were plotted at a distance of 500 m from the downstream end of the pipe. It was found that oscillations in mass flux and pressure were nearly of the same magnitude in both cases. Mass flux started initially from a value of 308.36 kg/m^{2}s and decreased monotonically to its steady state value of zero in about 150 s. Different cases involving a range of flow-rates as 10 kg/s, 5 kg/s and 1 kg/s were used and it was found that by decreasing the flow rate in pipe BD, the pressure and mass flux oscillations asymptotically approached the results for a single pipe.

Similar results were obtained in case of parametric study done on a two-branch manifold for different lengths of branch BD, and it can seen from Figure 5.1b, that decreasing the length of branch BD from initial 500 m to 1 m, the pressure and mass flux asymptotically approach the results for a single pipe. Similarly, a three-branch manifold can be reduced to a two-branch manifold by suitable choice of the operating conditions and the length of the branches.

5.3. Results for a two-branch manifold (Valve at node C is closed completely)

. The following results are based on a two branch manifold in which the main branch (AB) splits into two sub-branches (BC) and (BD). The base case which is described below for each transient scenario is used as a reference for comparison in rest of the cases. The temperature of the entire system for all our simulation purposes was kept constant at 303 K and a friction factor of 0.003 was used. The value of the compressibility factor of gas was assumed to be 0.98.

5.3.1 Effect of change in mass flow rate in branch BC/BD

Figures 5.2a and 5.2b show the transient behavior of a gas in the pipe for the effect of change in mass flow rate of branch BC on mass flux transience in branch 1 (BC) and 2 (BD) respectively when valve at C is completely closed

Base case: -The length of all branches i.e., AB, BC, BD is 500 m. The diameter of AB is 12"(0.3024 m) while that of the two sub-branches is 6"(0.1512 m). The upstream pressure of the main branch is fixed at 20 bar throughout the simulation. An initial steady state mass flow-rate of 10 kg/s (548.2 kg/m^{2}s) and 1 kg/s (54.82 kg/m^{2}s) through pipes BC and BD respectively is assumed and hence a total mass flow-rate in the main branch is 11 kg/s (150.76 kg/m^{2}s).

The valve at the node C is closed instantaneously as a result of which the flow becomes zero at node C. The gas supply at node D was kept constant throughout the simulation. As a result of valve closure, pressure rises at node C, causing disturbance in the line pressure and the mass-flux everywhere in the pipe, including nodes, A, B, and D. As seen from Figures 5.2a to 5.2d, an oscillatory behavior exists in both pressure and

mass-flux at the nodes, before steady state values are reached. For the case when mass flow rate in branch BC is 10 kg/s, dimensionless mass flux (which is non-dimensionlized with respect to initial steady state conditions in branch BD) starts from an initial value of 10 in case of branch BC. The gas flow in branch BC, at node B, temporarily reverses in direction with a minimum value of -3.5 at t=2.5 s. The flow rate goes through a maximum value of 1.8 at about t=10 s. The transient conditions appear to persist for about 80 s. In case of branch 2, referring Figure 5.2b, it is observed that dimensionless mass flux starts from a value of 1 and then it continuously decreases to a value of –4.2 in about 3.5 s. It then reverses in direction and reaches a maximum peak value of 4.8 in 7 s. The magnitude and the duration of oscillations can be compared with branch 1 and evidently, the amplitude of oscillations in branch 1 is larger and the oscillations are also seen to continue over a longer period.

Figures 5.2c and 5.2d depict the pressure transience at nodes D and B respectively for the case when the mass flow rate in branch BC is altered. In Figure 5.2c, the pressure starts from an initial value of 19.88 bar and reaches a maximum value of 20.5 bar at t=3 s, and thereafter it decreases to a value of 18.9 bar at t=5 s, ultimately attaining its steady state value of 19.88 bar in about 100 s. In Figure 5.3d, pressure starts from a value of 19.9 bar. At t=3 s, it reaches a maximum value of 20.35 bar and then it starts its downward trend and reaches a minimum value of 19.75 bar in 5 s, ultimately reaching its steady state value of 19.98 bar in about 100 s.

When the mass flow rate of branch BC is decreased by 90% with respect to the base case, i.e., to 1 kg/s while maintaining the rest of the parameters such as length, upstream pressure and diameter constant as in the previous case, it is seen that it results in the reduced fluctuations in mass-flux as compared to the previous as well as the base case. In Figure 5.2a, the dimensionless mass flux starts from a value of 1 and continues to oscillate for about 30 s before returning to a steady state. Qualitatively, similar trends are observed in branch BD. Thus the amplitude and duration of oscillations in base case for mass flux in both the branches are greater compared to the present case.

Again in Figures 5.2c and 5.2d, the pressure at node D starts from an initial steady state value of 19.91 bar and it oscillates a little compared to the base case before coming back to steady state value of 19.88 bar in about 50 s. Similar trend is observed at node B

which comes to a steady state value of 19.98 bar in about the same time period. Thus, the reduction in the flow rate tends to dampen the pressure and mass flux oscillations.

For the third case (Figure 5.2e), when the mass flow rate of branch of BD is decreased by 80% with respect to the base case i.e., to 0.2 kg/s keeping all other variables constant, the mass flux oscillations at node B for branch BC starts from an initial value of 50. The gas mass flux oscillations in this case are seen to be greater as compared to the base case. The flux is seen to reach a minimum value of about –22.3 in 2.5 s followed by a maximum value of 15.2 at t~10 s. Finally, it is seen to approach to the new steady state value of zero flow in about 120 s. Similar trends are obtained for branch BD. Thus, under these conditions, the oscillations amplify and persist for a longer time duration compared to the base case.

Figures 5.2g and 5.2h display pressure transience at nodes D and B respectively caused by changing the flow rate in branch 2. The pressure at node D starts initially from 19.96 bar and reaches a maximum of about 20.55 bar in 3 s and thereafter it starts decreasing and reaches a minimum value of 18.65 bar in 5 s. It is clearly seen in these figures that the pressure oscillations in the present case get amplified as compared to the base case. Similar trend is observed at node D.

Thus, an increased mass flow rate in the branch in which the disturbance is introduced due to valve closure or reduced flow rate in the neighboring branch results in enhanced disturbances in pressure and mass flux which also persist for a longer time period.

5.3.2.Effect of change in upstream pressure at node A

Figures 5.2i and 5.2j exhibit the transient behavior brought about by a change in the upstream pressure at node A on mass flux transience at node B for branch 1 (BC) and 2 (BD) respectively when valve at C is completely closed.

As seen in Figures 5.2i to 5.2l, an oscillatory behavior exists in both pressure and mass-flux at various nodes, before steady state values are reached. For the case when the upstream pressure is 30 bar, dimensionless mass flux starts from an initial value of 10 in case of branch BC (Figure 5.2i). The gas flow rate in the main branch BC, at node B, temporarily reverses in direction with a minimum value of -4.5 at t=3 s. The maximum

value of 2.2 is reached in about 12 s. It takes around 110 s for the flow in branch BC attain a steady state value of zero flow. In the case of branch 2, it is found that the dimensionless mass flux oscillations start from a value of 1 and then it continuously decreases to a value of –5.8 in about 4 s, followed by a reversal in direction to reach a maximum peak value of 6.0 at t=9 s.

Figures 5.2k and 5.2l display pressure transience at nodes D and B respectively when the upstream pressure at node A is 30 bar and 50 bar respectively. In Figure 5.2k, the line pressure at node D starts from an initial value of 29.89 bar and reaches a maximum value of 30.6 bar rather quickly i.e., in about 5 s. It then continues to decrease and at about 7 s, it reaches a minimum value of 28.6 bar. It then oscillates reaching a steady state value of 29.89 bar in about 110 s. Similarly, pressure at node B starts from a value of 29.9 bar, reaching a maximum value of 30.45 bar at t~3 s, followed a minimum value of 29.72 bar at t=5 s. It reaches its steady state value of 29.98 bar in about 110s.

In the case of increasing the upstream pressure at node A by 2.5 times with reference to the base case i.e., to 50 bar, it is seen that it results in increased fluctuations in mass-flux as compared to the previous as well as the base case. In Figure 5.2i, the dimensionless mass flux at node B for branch 1 starts from a value of 10 and continues to oscillate for around 130 s before coming back to a steady state value, attaining minimum value of –5.5 and the maximum 3.5, at t=3s and 14 s respectively. Similar trends are observed in branch BD. Thus, in this case also, the amplitude and the duration of oscillations are greater compared to the base and previous cases.

Figure 5.2l show pressure transience at nodes D and B respectively when the supply pressure is 50 bar. Pressure at node D starts from an initial steady state value of 49.88 bar and it oscillates a little before settling down to its steady state value of 49.91 bar in about 130 s. Similar trend is observed at node B which comes to a steady state value of 49.98 bar in about the same time.

Thus an increased supply pressure also tends to enhance the oscillatory nature of pressure and mass flux oscillations, which also last for a longer time.

5.3.3 Effect of change in diameter of branch BC and BD

Figures 5.2m and 5.2n describe the transient behavior in the pipe due to the change in diameter of branch BC and BD on mass flux transience at node B for branch 1 (BC) and 2 (BD) respectively when valve at C is completely closed.

Diameter of sub-branches BC and BD is decreased by one third with respect to the base case i.e., from 6" each to 4" (and keeping rest of the parametric variables constant). As seen from Figures 5.2m to 5.2p, an oscillatory behavior exists in both pressure and mass-flux at the nodes, before steady state values are reached. For the case when diameter of sub-branches are 4"(0.1016 m) each, dimensionless mass flux starts from an initial value of 10 in case of branch BC. The gas flow in main branch BC, at node B, temporarily reverses in direction with a minimum value of -5.0 at t=7 s. The maximum value of 3.0 is reached at t~10 s. It takes around 70 s for the flow in branch BC to come to a steady state of no flow. In the case of branch 2 (referring Figure 5.2n), it is seen that oscillations in mass flux start from a value of 1, decreasing to a value of –1.8 at t=10 s and reaching its maximum value of 3.9 at t~15 s. Thus, a reduction in pipe diameter results in weaker mass flux oscillations, which also die out quickly.

Figures 5.2o and 5.2p signify, the pressure transience at nodes D and B respectively when the diameters of sub-branches are changed. In Figure 5.2o, pressure starts from an initial value of 49.8 bar, reaches a maximum value of 50.5 bar at t~7 s and attains a minimum value of 48.6 bar at t~10 s. It then oscillates before coming to a steady state value of 49.89 bar in about 80 s. Similarly in Figure 5.2p, the pressure starts from a value of 49.96 bar. At t=5s, reaching a maximum value of 50.4 bar and a minimum value of 49.5 bar at t~10s. It reaches its steady state value of 49.98 bar in about 80s.

In case of increasing the diameter of sub-branches by the same amount, i.e., 33 % with reference to the base case i.e., to 8" (203.2 mm), it is seen that augments the fluctuations in mass-flux as compared to the previous two cases.

Again referring Figures 5.2o and 5.2p when the diameter of branch BC and BD are 8" each, the pressure at node D starts from an initial steady state value of 49.91 bar and it oscillates more compared to the base case before coming back to steady state value of 49.95 bar in about 150 s. Same trend is observed at node B which comes to a steady state

value of 49.98 bar in the same time. Thus increased diameter tends to decrease the pressure oscillations but it continues to oscillate for a longer time period.

5.3.4 Effect of change in length of branch BC

Figures 5.2q and 5.2r describe the effect of change in length of branch BC on mass flux transience at node B for branch 1 (BC) and 2 (BD) respectively when valve at C is completely closed. The lengths of branch BC and BD are 100 m and 500 m respectively. In Figure 5.2q, it can be seen that mass flux oscillations are negligible compared to the base case and in branch BD. It takes around 30 s for the flow in branch BC to come to the no flow steady state. In the case of branch 2, it is seen that the mass flux oscillations start from a value of 1 and then it continuously decreases to a value of –3.0 in about 4 s and then followed by a maximum value of 3.8 in 12 s.

Figures 5.2s and 5.2t, signify pressure transience at nodes D and B respectively when the length of branch BC is changed. In Figure 5.2s, the pressure starts from an initial value of 49.89 bar and reaches a maximum value of 50.51 bar quickly i.e., in about 3 s. It continues to decrease reaching a minimum value of 49.2 bar at t~7 s. It then oscillates before coming to a steady state value of 49.89 bar in about 100 s. In Figure 5.2t, the pressure starts from a value of 49.9 bar. At t 7 s, it reaches a maximum value of 50.3 bar and then it starts its downward trend and reaches a minimum value of 49.8 bar in 10 s, eventually going to its steady state value of 49.98 bar in about 100s.

When the length of branch BC is increased by 100% with reference to the base case i.e., to 1000 m, it is seen that it results in the increased fluctuations in mass-flux as compared to the previous and base cases. In Figure 5.2r, the dimensionless mass flux at node B for branch 2 starts from a value of 10 and continues to oscillate for around 130 s before coming back to a steady state. The minimum value of mass flux in this case is –7.2 and the maximum are 7.0, attained at t=10s and t=20 s respectively. Similar trends are observed in branch BC. Thus the amplitude and duration of oscillations in the present case are larger compared to the base case.

In Figures 5.2s and 5.2t, the pressure at node D starts from an initial steady state value of 49.88 bar and it oscillates more compared to the base case before coming back to

steady state value of 49.91 bar in about 150 s. Similar trend is observed at node B which comes to a steady state value of 49.98 bar in about the same time.

Thus, an increased length tends to increase the magnitude as well as time duration of the pressure as well as mass flux oscillations.

5.4 Effect of number of sub-branches on mass flux and pressure transience when valves at the downstream ends of the sub-branches are closed

Figures 5.3a and 5.3b show the effect of number of branches in the manifold on mass flux and pressure at nodes A and D respectively. In the 1st case of two branch manifold, main branch AB divides into two sub-branches BC and BD. Length of all the pipes is 500 m, diameter of pipe AB is 12" (0.3048 m) whereas pipes BC and BD are of 6" (0.1524 m) each. An initial mass flow rate of 10 kg/s in pipe BC and 1 kg/s in pipe BD is specified. Now the valve at node C is closed completely and its effect on pressure and mass flux on neighboring branches is studied. Thus, the mass flow rate in this case reduces from 11 kg/s to 1 kg/s in the main branch. As seen in Figure 5.3a, mass flux oscillates for about 120 s before coming back to a steady state value of 1 kg/s.

In the 2nd case of a three branch manifold, the main branch AB splits into three sub-branches BC, BD and BE. The lengths of pipes AB, BC, BD is 500 m whereas the length of pipe, BE, is 600 m. The diameter of the main branch and sub branches are same as in the previous case. An initial mass flow rate of 10 kg/s is specified for pipe BC and 1 kg/s each for pipes BD and BE respectively. Valves at node C and D are closed completely. Hence, the mass flow rate in this case reduces from 12 kg/s to 1 kg/s in the main branch. In this case, we see that the mass flux starts from 12 kg/s and oscillates between the steady state value of 1 kg/s for about 130 s. In the 3rd case, a manifold consisting of five sub-branches is considered, i.e., the main branch AB branches into BC, BD, BE, BF and BG. The lengths of pipes AB, BC and BD are 500 m while that of pipes BE, BF and BG are 600, 700 and 800 m respectively. The diameters of main branch and all sub-branches are kept unchanged as the previous cases. Valves at nodes C, D, E and F are closed completely. Upstream pressure in all the cases is kept fixed at 50 bar. A mass flow-rate of 10 kg/s and 1 kg/s each are specified for branches BC and BD, BE, BF and BG respectively. Thus the flow rate is reduced from 14 kg/s to 1 kg/s after the valve

closure. As seen from Figure 5.3a, mass flux oscillations are of greater magnitude which also continue for longer duration compared to the previous cases. In this case the time duration is about 150 s before it comes back to a steady state value of 1 kg/s. Thus, increasing the number of branches results in increased fluctuations in mass flux.

As seen from Figure 5.3b, in the case of pressure fluctuations at node D, it is observed that in a two-branch manifold, the pressure fluctuates in between the final steady state value of 49.989. In case of three-branch manifold, the pressure oscillates in between the final steady state value of 49.991. In case of a five-branch manifold, the pressure oscillates in between the final steady state value of 49.992. Thus, there seem to be a minor effect of the number of branches on oscillations in pressure at node D.

5.5 COMPRESSOR SHUTDOWN ANALYSIS

Two Branch Manifold (Compressor at A and valves at node C and D are simultaneously closed)

5.5.1 Effect of change in mass flow rate in branch BC/BD

Figures 5.4a and 5.4b describe effect of change in the length of branch BC on mass flux transience at node B for branch 1 (BC) and 2 (BD) respectively when the compressor located at A fails due to power failure and the valves at C and D are closed quickly.

(Base case):- The length of all the three pipes i.e., AB, BC, BD is chosen to be 500 m. The diameter of AB is 12"(0.3024 m) while diameter of sub-branches is 6"(0.1512 m). The upstream pressure of the main branch is fixed at 10 bar. An initial steady state mass flow-rate of 2.5 kg/s (137.119 kg/m^{2}s) and 3 kg/s (164.54 kg/m^{2}s) in pipes BC and BD respectively and hence a total mass flow-rate of 5.5 kg/s (175.41 kg/m^{2}s) in the main branch is assumed.

The compressor at node A and valves at node C and D are closed as soon as possible due to which the flow becomes zero at nodes A, C and D. As a result of the valve closure, the pressure rises at nodes C and D, causing disturbance in pressure and mass-flux everywhere in the pipe. As seen in Figures 5.4a to 5.4d, an oscillatory behavior exists in both pressure and mass-flux at the nodes, before the new steady state values are reached. For the case when mass flow rate in branch BD is 3 kg/s (base case), referring to

Figure 5.4a, it can be seen that mass flux oscillations start initially from a value of 102.52 kg/m^{2}s. The maximum and minimum value are 127.26 kg/m^{2}s and –137.64 kg/m^{2}s respectively and it decreases after each successive oscillation to a steady state value of zero in about 120 s .In case of branch 2, we find that mass flux oscillations start from a value of 144.23 kg/m^{2}s and then it continuously decreases to a value of –161.23 in about 5 s, reversing and reaching a maximum value of 141.24 kg/m^{2}s in 10 s. It is clearly seen that the amplitude of oscillations in branch 2 are more severe than in branch 1 and these continue for longer time. Thus higher mass flux results in more mass flux oscillations, which continue for a longer period. The oscillations in branch 1 are nearly the same for all the cases involving different mass flow rates as can be seen from Figure 5.4a.

Figures 5.4c and 5.4d, signify, pressure transience at nodes B and A respectively when mass flow rate in branch BD is changed. In Figure 5.4c, pressure starts from an initial value of 9.87 bar and reaches a minimum value of 9.69 bar quickly i.e., in about 3 s, followed by a maximum value of 10.21 bar at t=5 s. It then oscillates before coming to a steady state value of 9.97 bar in about 100 s. Similarly in Figure 5.4d, the pressure starts from a value of 9.98 bar. At t=3 s, it reaches a maximum value of 10.21 bar and then it starts its downward trend and reaches a minimum value of 9.32 bar in 7 s. It also reaches its steady state value of 9.97 bar in about 100s. The new steady state pressure values obtained after compressor shut down are compared theoretically and are found to be in close agreement. In all the cases described above and the cases following this, the difference from the graphical value and the analytical value of final steady state pressure ranges from 0.1 % to 0.8%. In this case the analytical value is 9.903 bar.

In case of increasing the mass flow rate of branch BD by 67% with respect to the base case i.e., to 5 kg/s keeping rest of parameters such as length, upstream pressure and diameter constant as in the previous case, we see that it results in increased fluctuations in mass-flux as compared to the base case. Again referring to Figures 5.4a and 5.4b, mass flux for branch BD starts from an initial value of 244.23 kg/m^{2}s and then continues to oscillate before reaching the final steady state value in 110 s. The maximum value is 220.45 kg/m^{2}s and the minimum is –240.34 kg/m^{2}s. Oscillations are more compared to the base case. Referring to Figure 5.4c, the pressure at node B starts from an initial steady state value of 9.71 bar and it oscillates more compared to the base case before coming

back to steady state value of 9.87 bar in about 100 s. Qualitatively similar trend is observed at node A which comes to a steady state value of 9.87 bar in about the same time. Thus increased flow rate tends to increase the pressure oscillations. In this case the analytical value is 9.799 bar. For the third case in which the mass flow rate of branch of BD is increased to 7 kg/s, (Figure 5.4a), mass flux in branch BD starts from an initial value of 332.58 kg/m^{2}s and it can be clearly seen that oscillations are more and persist for a longer time compared to the previous cases. Thus increasing the mass flow rate results in increased fluctuations in mass-flux.

Again referring to Figures 5.4c and 5.4d, the pressure at node B starts initially from 9.62 bar and reaches a minimum of about 9.3 bar in 3 s and thereafter it starts increasing and reaches a maximum value of 10.16 bar in 5 s. The dotted line represents the base case and it is clearly seen in this figure that the pressure oscillations in the present case are more, especially at node A. Thus increased mass flow rate in branch BD results in more disturbances in pressure.

5.5.2 Effect of change in upstream pressure at node A

Figures 5.4e and 5.4f describe the effect of a change in the upstream pressure of branch AB on mass flux transience at node B for branch 1 (BC) and branch 2 (BD) respectively when compressor at A shuts-off due to power failure and valves at C and D are simultaneously closed.

The numerical values of the variables are same as in the previous cases, except that for the supply pressure. As seen from Figures 5.4c to 5.4h, an oscillatory behavior exists in both pressure and mass-flux at the nodes, before steady state values are reached. For the case when upstream pressure at node A is 20 bar, the mass flux starts from an initial value of 117.119 kg/m^{2}s in case of branch BC. The gas flow in branch BC, at node B, temporarily reverses in direction with a minimum value of -139.9 kg/m^{2}s in about 5 s. The maximum value is 123.5 kg/m^{2}s which it reaches in about 2.5 s. It takes around 110 s for the flow in branch BC to come to a steady state value, which is zero. In case of branch 2, we find that mass flux oscillations start from a value of 146.23 kg/m^{2}s and then it increases to a value of 148.23 kg/m^{2}s in about 2.5 s. It then reverses in direction and reaches a minimum value of -153.24 kg/m^{2}s in 5 s. Evidently, the amplitude of

oscillations in the present case are more and continue for longer time as compared to the base case. Thus, a higher upstream pressure intensifies mass flux oscillations, which continue for longer intervals of time.

Figures 5.4g and 5.4h, signify pressure transience at nodes A and B respectively for the case when upstream pressure at node A is 20 bar and 5 bar respectively. Referring to Figure 5.4g, the pressure at node A starts from an initial value of 19.78 bar and reaches a minimum value of 19.65 bar quickly i.e., in about 3 s. It then continues to increase and at about 5 s, it reaches a maximum value of 20.18 bar. It then oscillates before coming to a steady state value of 19.92 bar in about 110 s. The pressure at node B starts from a value of 20.23 bar. At t= 1.5 s, it reaches a maximum value of 20.28 bar and its minimum value is 19.45 bar is reached in 4 s. The steady state value of 19.92 bar is attained in about 110s. In this case the analytical value is 19.956 bar which compares rather well with the numerical value.

In the case of decreasing the upstream pressure at node A by 50% with reference to the base case i.e., to 5 bar, we see that it reduces fluctuations in mass-flux as compared to the previous case. The mass flux in branch BC starts from a value of 117.119 kg/m^2s and continues to oscillate for about 100 s before coming back to a steady state. Similar trends are observed in branch BD. Thus the amount and time duration of oscillation in base case are more compared to present case.

Figure 5.4h represent pressure transience at nodes A and B respectively when the supply pressure is 5 bar. Pressure at node A starts from an initial steady state value of 4.64 bar and it oscillates before coming back to steady state value of 4.84 bar in about 80 s..Same trend is observed at node B which comes to a steady state value of 4.84 bar in the same time. Thus increased supply pressure tends to increase the pressure oscillations. In this case the analytical value is 4.792 bar.

5.5.3 Effect of change in diameter of branch BD

Figures 5.4i and 5.4j describe the effect of change in diameter of branch BD on mass flux transience for branch 1 (BC) and branch 2 (BD) when compressor at A shuts-off due to power failure and valves at C and D are closed quickly. Parametric variables are same as previously described

Referring to Figures 5.4i and 5.4j, for the case when the diameter of branch BD is 4"(0.1016 m), mass flux starts from an initial value of 333.119 kg/m^{2}s in case of branch BD. The gas flow in branch BD, at node B, temporarily reverses in direction with a minimum value of -189.9 kg/m^{2}s in about 7 s and the maximum value of 353.5 kg/m^{2}s reached in about 2.5 s. It takes around 100 s for the flow in branch BD to become zero. In case of branch 1, we see that mass flux oscillations for cases involving different diameter of branch BD differ negligibly. Thus a smaller diameter results in more mass flux oscillations in the neighboring branch in which the disturbance is introduced and it continues for a longer duration.

Figures 5.4k and 5.4l, signify pressure transience at nodes A and B respectively when the diameter of branch BD is changed. Referring to Figure 5.4k, the pressure starts from an initial value of 9.78 bar and reaches a minimum value of 9.52 bar quickly i.e., in about 3 s. It then continues to increase and at about 5 s, it reaches a maximum value of 10.11 bar. It then oscillates before coming to a steady state value of 9.78 bar in about 110 s. Referring to Figure 5.4l, the pressure starts from a value of 10.06 bar. At t=3 s, it reaches a maximum value of 10.18 bar and then it starts its downward trend and reaches a minimum value of 9.32 bar in 7 s. It reaches its steady state value of 9.78 bar in about 110s. The corresponding analytical value is 9.768 bar.

In case of increasing the diameter of branch BD by 33% i.e., to 8"(0.2032 m) keeping rest of parameters such as length, mass flow rate and upstream pressure constant as in the previous case, we see that it results in reduced fluctuations in mass-flux in branch BC and BD. Thus increasing the diameter results in reduced mass flux oscillations.

Again referring to Figures 5.4k and 5.4l, pressure at node A starts from an initial steady state value of 9.78 bar and it oscillates before coming back to steady state value of 9.92 bar in about 90 s. Similar trend is observed at node B which comes to a steady state value of 9.92 bar in the same time. Thus increased diameter tends to decrease the pressure oscillations. In this case the analytical value is 9.93 bar.

5.5.4 Effect of change in length of branch BD

Figures 5.4m and 5.4n describe the effect of change in length of branch BD on mass flux transience at node B for branch 1 (BC) and branch 2 (BD) when compressor at A shuts-off due to power failure and valves at C and D are instantaneously closed.

The values of parameters of all the branches are maintained at the same level. As seen from Figures 5.4m and 5.4n, for the case when length of branch BD is 100 m, there is no appreciable difference in mass flux oscillations in branch BC for different cases of lengths of branch BD. In case of branch 2, we find that the magnitude and the duration of mass flux oscillations compared with the base case is negligible and these also die out quickly. Thus shorter length results in less mass flux oscillations, which last over a shorter duration.

Figures 5.4o and 5.4p, signify pressure transience at nodes A and B respectively when the length of branch BD is varied. Referring to Figure 5.4o, the pressure starts from an initial value of 9.78 bar and reaches a maximum value of 10.18 bar in about 5 s. It then oscillates before coming to a steady state value of 9.92 bar in about 95 s. Referring Figure 5.4p, pressure starts from a value of 10.01 bar. At t 3 s, it reaches a minimum value of 9.41 bar. It reaches its steady state value of 9.92 bar in about 95 s. The corresponding analytical value is 9.939 bar.

In case of decreasing the length of branch BD by 40% with respect to the base case i.e., to 300 m keeping rest of parameters such as diameter, mass flow rate and upstream pressure constant as in the previous case, we see that in case of branch BD, it decreases fluctuations in mass-flux as compared to the base case but more compared to the case when length of branch BD is 100 m. Thus the amount and time duration of oscillation in base case are more compared to present case.

Again referring to Figures 5.4o and 5.4p, for the case when length of branch BD is 300 m, pressure oscillations are similar in nature to the case when length of branch BD was 100 m except that the final steady state pressure in the this case is 9.91 bar. The corresponding analytical value is 9.927 bar.

5.6 COMPRESSOR START-UP ANALYSIS

Two Branch Manifold (Compressor at A starts and valves at node C and D are kept open at respective downstream pressures)

Parametric study

5.6.1 Change in mass flow rate in branch AB

Figures 5.5a, 5.5b and 5.5c describe the effect of change in mass flow rate of branch BD on mass flux transience at nodes C, D and B for branch 1 (BC), branch 2 (BD) and main branch (AB) respectively when compressor at A starts from an initial line pressure and valves at C and D are kept open to respective downstream pressures.

Base case:-The length of all the three pipes i.e., AB, BC, BD is assumed to be 500 m. The diameter of AB is 12"(0.3024 m) while diameter of sub-branches is 6"(0.1512 m). The upstream pressure of main branch is fixed at 10 bar. Initially flow in all branches is zero though at a particular line pressure. When the compressor starts, a steady state mass flow-rate of 5.5 kg/s (175.41 kg/m^{2}s) is maintained in the main branch. The flow splits into 2.5 kg/s (137.119 kg/m^{2}s) and 3 kg/s (164.54 kg/m^{2}s) corresponding to the final downstream pressures prevailing through pipes BC and BD respectively.

As a result of compressor start-up, mass flux greater than the final steady state value is experienced in all the branches. As seen from Figures 5.5a to 5.5e, an oscillatory behavior exists in both pressure and mass-flux at the nodes, before steady state values are reached. For the case when initial line pressure is 9.97 bar, at the compressor start up, a mass flux of 5.5 kg/s is supplied at node A. Thus mass flux starts from zero in case of branch AB .It reaches a maximum value of 176.34 kg/m^{2}s quickly i.e., in about 3 s. The gas flow in branch BC, at node C, temporarily reverses in direction with a minimum value of 136.8 kg/m^{2}s in about 5 s. It takes around 10 s for the flow in branch BC to come to a steady state value which is the mass flux corresponding to the final pressure drop prevailing in the pipe i.e., 137.14 kg/m^{2}s. In all these cases described below, it can be inferred from figures that there was no appreciable difference in mass flux of branch BC. In case of branch 2, we find that mass flux oscillations starts from zero and then it rises and reaches a maximum peak value of 423.58 kg/m^{2}s in about 7s. It then reverses in direction and reaches a minimum value of 13.24 kg/m^{2}s in 10 s before coming to a new steady state value of 164.54 kg/m^{2}s. In case of a main branch, we find that mass flux

oscillations starts of zero and then it continuously increases to a value of 164.45 in about 7 s. It then reverses in direction and reaches a minimum peak value of 62.34 kg/m^{2}s in 10 s before coming to a final steady state value of 75.45 kg/m^{2}s.

Figures 5.5d and 5.5e, signify pressure transience at nodes A and B respectively for the cases for effect of change in initial line pressure at compressor start up from an initial value of 5.5 kg/s at node A. In Figure 5.5d, pressure starts from an initial value of 10.18 bar and reaches a maximum value of 10.85 bar quickly i.e., in about 3 s. It then continues to decrease and at about 5s, it reaches a minimum value of 9.68 bar. It then monotonically oscillates before coming to a steady state value of 10.0 bar in about 30 s. In Figure 5.5e, pressure starts from a value of 10.20 bar. At t=3 s, it reaches a maximum value of 10.28 bar and then it starts its downward trend and reaches a minimum value of 9.93 bar in 7 s. It reaches its steady state value of 9.956 bar in about 15s.

In case of increasing the mass flow rate of branch AB by 67% i.e., to 7.5 kg/s keeping rest of parameters such as length, upstream pressure and diameter constant as in the previous case, we see that it in increases fluctuations in mass-flux as compared to the previous case. The flow divides into 2.5 kg/s (137.119 kg/m^{2}s) and 5 kg/s (274.54 kg/m^{2}s) corresponding to the final downstream pressures prevailing through pipes BC and BD respectively.

In case of branch 2, we find that mass flux oscillations start from a value of zero and then it rises and reaches a maximum value of 473.58 kg/m^{2}s in about 7s. It then reverses in direction and reaches a minimum value of 253.24 kg/m^{2}s in 10 s before coming to a new steady state value of 274.23 kg/m^{2}s. In this case the oscillations last for about 20s compared to the previous case when oscillations continue for 30 s. Thus starting with a higher mass flux results in more mass flux oscillations but these quickly die out. In case of main branch, we find that mass flux oscillations start from zero and then it continuously increases to a value of 204.45 in about 7 s. It then reverses in direction and reaches a minimum peak value of 70.34 kg/m^{2}s in 10 s. The final steady state value is 102.78 kg/m^{2}s.

Figures 5.5d and 5.5e, signify pressure transience at nodes A and B respectively for effect of change in initial line pressure. When compressor at A starts from an initial mass flow rate value of 5.5 kg/s (Figure 5.5d), pressure starts from an initial value of

10.18 bar and reaches a maximum value of 10.85 bar quickly i.e., in about 3 s. It then continues to decrease and at about 6 s, it reaches a minimum value of 9.75 bar. It then oscillates before coming to a steady state value of 10.0 bar in about 30 s. In Figure 5.5e, pressure at node B starts from a value of 10.20 bar. At t=3 s, it reaches a maximum value of 10.22 bar and then it starts its downward trend and reaches a minimum value of 9.94 bar in 7 s. It reaches its steady state value of 9.906 bar in about 15s.

When the flow at node A is increased to 7.5 kg/s, keeping rest of the parametric variables constant, we find that it results in higher peak value of mass flux in branch BD compared to the base case. In case of branch BC, mass flux oscillations are similar in magnitude to the base case. Pressure oscillations at nodes B and A (Figures 5.5c and 5.5d respectively), are also larger in magnitude compared to the base case and come to a steady state value of 9.87 bar.

In case of increasing the mass flow rate of branch AB by 133.33% i.e., to 9.5 kg/s keeping rest of parameters such as length, upstream pressure and diameter constant as in the previous case, we see that it results in increased fluctuations in mass-flux as compared to the base and previous cases. Now when the compressor starts, a steady state mass flow-rate of 9.5 kg/s (137.41 kg/m^2s) is flowing in the main branch. The flow divides into 2.5 kg/s (137.119 kg/m^2s) and 7 kg/s (384.54 kg/m^2s) corresponding to the final downstream pressures prevailing through pipes BC and BD respectively.

As seen from Figure 5.5a, 5.5b and 5.5c, for the case when the compressor starts with a mass flow rate of 9.5 kg/s at node A, for branch 2, we find that mass flux oscillations start from zero and then it rises and reaches a maximum peak value of 523.58 kg/m^2s in about 10s. It then reverses in direction and reaches a minimum value of 378.24 kg/m^2s in 10 s before coming to a new steady state value of 384.23 kg/m^2s. In this case the oscillations last for about 15s. Thus higher mass flux results in more mass flux oscillations but continue for a shorter time duration. In case of main branch, we find that mass flux oscillations starts from zero and then it continuously increases to a value of 234.45 in about 7 s. It then reverses in direction and reaches a minimum peak value of 102.34 kg/m^2s in 10 s before reaching a steady state value of 137.14 kg/m^2s.

Figures 5.5d and 5.5e, signifies pressure transience at nodes A and B respectively for effect of change in initial line pressure. Compressor at starts from an initial value of

9.5 kg/s at node A. In Figure 5.5d, pressure starts from an initial value of 10.22 bar and reaches a maximum value of 10.48 bar quickly i.e., in about 3 s. It then continues to decrease and at about 5s, it reaches a minimum value of 9.87 bar. It then monotonically oscillates before coming to a steady state value of 10.0 bar in about 15 s. In Figure 5.5e, pressure starts from a value of 9.92 bar. At t=3 s, it reaches a maximum value of 10.07 bar and then it starts its downward trend and reaches a minimum value of 9.83 bar in 7 s. It reaches its steady state value of 9.85 bar in about 15s.

5.6.2 Effect of change in upstream pressure at node A

Figures 5.5f, 5.5g and 5.5h describe the effect of change in upstream pressure of branch AB on mass flux transience at nodes C, D and B for branch 1 (BC), 2 (BD) and main (AB) respectively when compressor at A starts.

Now when the compressor starts, a steady state mass flow-rate of 5.5 kg/s (175.41 kg/m^{2}s) is supplied in the main branch. The supply pressure is 15 bar. The flow divides into 2.5 kg/s (137.119 kg/m^{2}s) and 3 kg/s (164.54 kg/m^{2}s) corresponding to the final downstream pressures prevailing through pipes BC and BD respectively.

In case of branch 1, mass flux oscillations are similar to the oscillations observed in the base case. In case of branch 2, we find that mass flux oscillations starts from zero and then it rises and reaches a maximum peak value of 623.58 kg/m^{2}s in about 7s. It then reverses in direction and reaches a minimum value of -523.24 kg/m^{2}s in 10 s before coming to a new steady state value of 164.23 kg/m^{2}s. In this case the oscillations last for about 30s. Thus higher mass flux results in more mass flux oscillations, which continue longer. In case of main branch, we find that mass flux oscillations start from a value of zero kg/m^{2}s and then it continuously increases to a value of 244.45 in about 7 s. It then reverses in direction and reaches a minimum value of -62.34 kg/m^{2}s in 10 s.

Figures 5.5i and 5.5j signifies, pressure transience at nodes A and B when initial line pressure is 14.92 bar and 4.86 bar respectively. Compressor at A starts from an initial value of 5.5 kg/s at node A. Referring to Figure 5.5i, pressure at node A starts from an initial value of 15.2 bar and reaches a maximum value of 15.62 bar in about 3 s. It then continues to decrease and at about 5s, it reaches a minimum value of 14.64 bar. It then oscillates before coming to a steady state value of 15.0 bar in about 30 s. Pressure at node B starts from a value of 15.15 bar. At t=3 s, it reaches a maximum value of 15.26 bar and

then it starts its downward trend and reaches a minimum value of 14.90 bar in 7 s. It reaches its steady state value of 14.97 bar in about 15s.

In the case of decreasing the supply pressure by 50% i.e., to 5 bar (and keeping rest of parameters such as length, mass flow rate and diameter constant as in the previous case), we see that it results in decreased fluctuations in mass-flux as compared to the previous case. Referring to Figures 5.5f to 5.5j, an oscillatory behavior exists in both pressure and mass-flux at the nodes, before steady state values are reached. For the case when initial line pressure is 4.86 bar, when the compressor starts, a mass flux of 7.5 kg/s is supplied at node A. In case of branch 2, we find that mass flux oscillations start from zero and then it rises and reaches a maximum peak value of 223.58 kg/m^{2}s in about 7 s. It then reverses in direction and reaches a minimum value of 153.24 kg/m^{2}s in 10 s before coming to a new steady state value of 164.54 kg/m^{2}s. In this case the oscillations last for about 15 s. Thus higher supply pressure results in more mass flux oscillations which continue for longer duration. In case of main branch, we find that mass flux oscillations start from zero and it oscillates negligibly as compared to the cases when the upstream pressure was 15 bar and 10 bar.

Figure 5.5j signify, pressure transience at nodes A and B respectively for the case when initial line pressure is 4.86 bar. Similar pressure trends at respective nodes A and B are observed. The pressure oscillates before coming to respective steady state values in each of the branches in about the same time.

5.6.3 Effect of change in diameter of branch BD

Figures 5.5k, 5.5l and 5.5m describe the effect of change in diameter of branch BD on mass flux transience at nodes C, D and B for branch 1 (BC), 2 (BD) and main (AB) respectively when compressor at A starts.

The parametric variables are in consistency as with the previous case. Referring to Figures 5.5k to 5.5o, an oscillatory behavior exists in both pressure and mass-flux at the nodes, before steady state values are reached. For the case when diameter of branch BD is 4", in case of branch 2, we find that mass flux oscillations start from zero and then it increases to a value of 643.23 kg/m^{2}s in about 5 s. It then reverses in direction and reaches a minimum value of 133.24 kg/m^{2}s in 10 s. The magnitude and the duration of oscillations can be compared with base case (diameter of branch BD is 0.1524 m) and it

is evident that the amount of oscillations in branch 2 in the present case are more and continue for longer time. Thus smaller diameter of branch BD results in larger mass flux oscillations, which continue longer. Similar trends are observed in branch BC and main branch.

Figures 5.5n and 5.5o signify pressure transience at nodes A and B respectively for the case when the diameter of branch BD is changed. Referring to Figure 5.5n, pressure starts from an initial value of 10.18 bar and reaches a maximum value of 10.53 bar in about 3 s. It then continues to decrease and at about 7 s it reaches a minimum value of 9.79 bar. It then oscillates before coming to a steady state value of 10.0 bar in about 30 s. Referring Figure 5.5o, pressure starts from a value of 10.02 bar . At t=3 s, it reaches a maximum value of 10.24 bar and then it starts its downward trend and reaches a minimum value of 9.92 bar in 7 s. It reaches its steady state value of 9.945 bar in about 15s.

In case of increasing the diameter of branch BD by 33% i.e., to 8"(0.2032 m) keeping rest of parameters such as length, mass flow rate and upstream pressure constant as in the previous case, we see that fluctuations in mass-flux are reduced below that in the base case. Also the amplitude and time duration of oscillation in base case are larger compared to the present case.

Again referring to Figures 5.5n and 5.5o for the present case, pressure at node A starts from an initial steady state value of 10.18 bar and it oscillates before coming back to steady state value of 10.0 bar in about 30 s. Similar trend is observed at node B which comes to a steady state value of 9.97 bar in 15 s. Thus increased diameter tends to decrease the pressure as well as mass flux oscillations.

5.6.4 Effect of change in length of branch BD

Figures 5.5p, 5.5q and 5.5r describe the the effect of change in length of branch BD on mass flux transience at nodes C, D and B for branch 1 (BC), 2 (BD) and main (AB) respectively when compressor at A starts.

Parametric variables are same as before. Referring to Figures 5.5p to 5.5t, an oscillatory behavior exists in both pressure and mass-flux at the nodes, before steady state values are reached. For the case when length of branch BD is 100 m, there is no

appreciable difference in mass flux oscillations in branch BC and branch AB compared to the base case where length of branch BD is 500 m. In case of branch 2, we find that mass flux oscillations starts from zero and then it progressively increases to a value of 548.45 kg/m^2s in about 5 s. It then reverses in direction and reaches a minimum value of -19.24 kg/m^2s in 9 s. The magnitude and the duration of oscillations can be compared with base case and it is evident that the amount of oscillations in branch 2 in the present case are more and continue for longer time duration. Thus lower length results in more mass flux oscillations but persist for a shorter duration

Figures 5.5s and 5.5t signify pressure transience at nodes A and B respectively when diameter of branch BD is changed. Referring to Figures 5.5s and 5.5t, we can see that the pressure oscillations in all the cases nearly overlap with each other. Thus changing the length of branch BD does not influence the magnitude or time duration of pressure oscillations.

In case of decreasing the length of branch BD by 40% with reference to the base case i.e., to 300 m keeping rest of parameters such as diameter, mass flow rate and upstream pressure constant as in the previous case, we see that it results in decreased fluctuations in mass-flux as compared to the base case but more compared to the previous case when length of branch BC was 100 m.

Referring to Figures 5.5s and 5.5t, we can see that at nodes A and B, pressure oscillations are similar in magnitude compared to the previous cases.

5.7 Leakage Analysis

A large-scale simulation was done on a 77.33-km long gas pipeline in Germany from Neustadt to Unterfohring through Sorzen (Figure 5.6) has been reported by Bisgaard et.al. The normal steady flow conditions (V_s = 5.094 m/s, M_s = 2.007 kg/s and P_s = 6.186 bar) were altered by decreasing the pressure by 0.02 bar at a position 4.76 km from Sorzen. The pressure drop corresponds to a sudden decrease in the mass flow of approximately 12 per cent. The volume flow at Unterfohring was kept constant throughout the simulation.

The temperature of the entire system was kept constant at 286 K. The gas compressibility factor of 0.98 and the gas molecular weight of 18.2 kg/kmole were used.

The velocity and pressure variations have been calculated for a position along the pipeline corresponding to Sorzen. The variations are given as percentages of the steady state values.

Figure 5.6 compares the simulated time variation of pressure in the pipe at Sorzen (4.76 km from the point of leakage) with the reported experimental values. In present simulations, upstream pressure at Neustadt was kept constant at 6.59 bar. The diameter starting from Neustadt upto the point of leakage was taken as 15.378"(0.3906 m). The corresponding steady state pressure obtained at the point of leakage from equation (5) is 6.281 bar. The diameter of pipe running from point of leakage to Unterfohring was taken as 13.394"(0.3402 m). The mass flow rate at Unterfohring was kept constant at 2.007 kg/s. The initial steady state pressure at the point of leakage is 6.186 bar. As seen in this figure, the experimental and simulated results are qualitatively similar, though the quantitative agreement is somewhat lacking. This is so partly due to the fact that not all details are available in the published work[5], nor is the experimental uncertainty mentioned in their paper. Bearing in mind these factors, the agreement seen in Figure 5.6 is regarded to be satisfactory and acceptable; the discrepancy is of the order of 1-2%, which is well within the accuracy of data in such cases.

As seen from Figure 5.6, M/M_s and V/V_s ratio remains constant for about 10 s before it starts decreasing and it reaches a minimum value of 96.3 at about 383 s after which it again starts increasing and reaches a steady state value of 99.8 in about 10000 s after which asymptotically reaches to a value of 100 in about 20000 s. In our simulations, it was seen that there is not much difference in oscillations in V/V_s and M/M_s. Based on the given leakage i.e., 12% of the total mass flow rate in the pipe, area of the leak and thus the diameter of the leak is calculated based on unchocked flow i.e., equation (12). P/P_s ratio starts initially from a value of 100 and decreases with time and reaches a value of 99.80 after a time of 300 s. It continues to decrease and at about 20000 s it reaches to a value of 99.75. It can be seen from Figure 5.6, V/V_s and M/M_s ratio in the published work reaches a minimum value of 96.5 and 96.25 respectively whereas in our simulation case, the time to reach the minimum value for the same values is about 380 s. The difference maybe due to unknown pressure condition at Neustadt after the leak

developed. Attempts using different values of pressure at Neustadt either by increasing or decreasing from the previous value were made to resolve the issue. But still no appreciable difference was obtained from the case when pressure at Neustadt was 6.59 bar. The reported simulated work and the present simulation results follow a similar trend as can be seen from the inset in Figure 5.6.

5.8 Simulation of outflow from a rupture

The rupture case as reported by Bisgaard et al. was tried in our simulation work. Qualitatively, it was possible to capture some results of chocked pressure as well as the rupture flow rate in the high-pressure pipeline as reported in Table 3, but quantitatively, it was not possible to match the results of variation of chocked pressure and rupture flow rate with time. This may again be due to the missing key operating variable, eg., the pressure history at the upstream end of the pipe, or the rupture diameter, etc.

The results of a simulation of outflow from a rupture on a horizontal low-pressure pipeline are described here. The outflow of gas into the atmosphere has been calculated until a new steady-state condition is attained.

The pipeline is in contact with a gas reservoir at one end. The rupture occurs 500 m from this end (Figure 5.7(a)). The fluid is assumed to behave like an ideal gas flowing through a convergent nozzle. Thus the magnitude of the velocity of the gas at the exit is equal to the local speed of sound as long as the pressure at the exit, P_t, exceeds the pressure of the surroundings, P_B, as given in the following equation:

$$P_t > \left[\frac{2}{\gamma+1}\right]^{\gamma/(\gamma-1)} P_B \qquad (5.1)$$

where the specific heat ratio, γ, equal to 1.28, and thus equation (5.1) can be re-written as: $P_t > 1.82\ P_B$.

During normal steady-state conditions, the pressure at the inlet of the pipe is 4 bar and the area of leakage is 61.5×10^{-4} m^2. Pressure corresponding to the point of rupture initially is 1.067 bar (P_t). Since $P_t > P_B$ initially, flow is unchocked initially and the corresponding flow rate of the leakage is 0.594 kg/s. The chocked pressure is the maximum downstream pressure resulting in maximum flow through the hole or pipe. The maximum flow is determined by the following equation:

$$Q_{choked} = C_0 A P_0 \sqrt{\frac{2M\gamma}{RT}\left(\frac{2}{\gamma+1}\right)^{\frac{(\gamma+1)}{(\gamma-1)}}} \tag{5.2}$$

For $P_t < P_b$, the flow becomes unchocked and is given by the following formula:

$$Q = C_0 A P_0 \sqrt{\frac{2M\gamma}{RT(\gamma-1)}\left(\frac{1}{P_0}\right)^{\frac{2}{\gamma}} - \left(\frac{1}{P_0}\right)^{\frac{\gamma+1}{\gamma}}} \tag{5.3}$$

where A is the cross section area of rupture or leak, C_0 is a constant discharge coefficient. For situations where C_0 is not known, the use of a conservative value of 1.0 is recommended (Streeter et al.) In the present simulations, it has been found that the outflow velocity is initially the local velocity of sound but after 5 s, outflow becomes sonic and thus chocked. The thermodynamic data and the dynamic viscosity of the gas used here are as follows: T=286 K, Z=0.98 and M_w=18.2 kg/kmole.

The evolution of outflow and the pressure at the rupture with time are depicted in Figure 5.7a, starting at t=0 when the rupture occurs and upto time period when the new steady-state condition is reached

Another case using different upstream pressure at the reservoir end and different diameter of the pipe and also the leak area was also attempted. The other parameters were assigned the same values as in the previous case except the upstream pressure now is 6 bar and the diameter of pipe was chosen as 4"(0.1016 m). The area of leak was 36.5×10^{-4} m^2. Thus the initial leak flow rate was 0.875 kg/s which varied with the pressure conditions prevailing at the point of rupture. At t=4 s, flow which was initially unchocked becomes chocked since the pressure at the point of leakage increases with time. The results for outflow and the pressure at the point of leakage are depicted in Figure 5.7b.

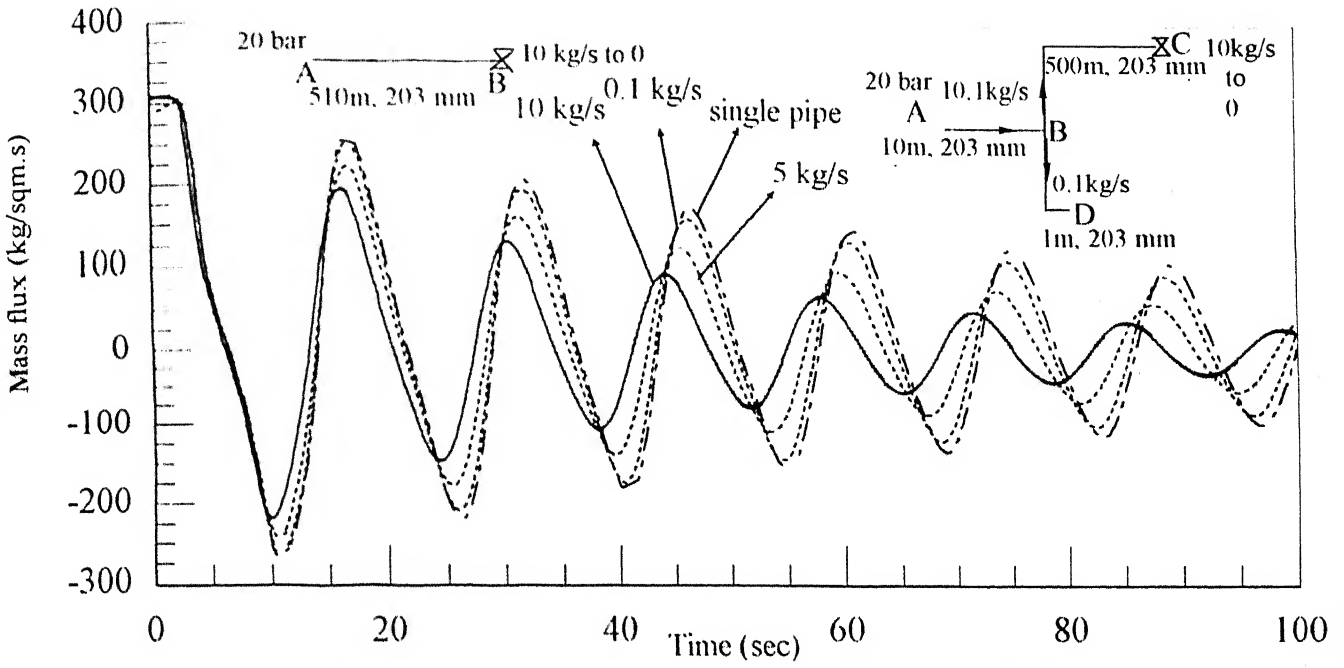

Figure 5.1a: Effect of change in mass flow rate in branch BD on mass flux transience at node B in main branch

(L_{mb}=10m, L_{b1}=500m, L_{b2}=1m, $d_{mb}=d_{b1}=d_{b2}$=6", m_{b1}= 10 kg/s)

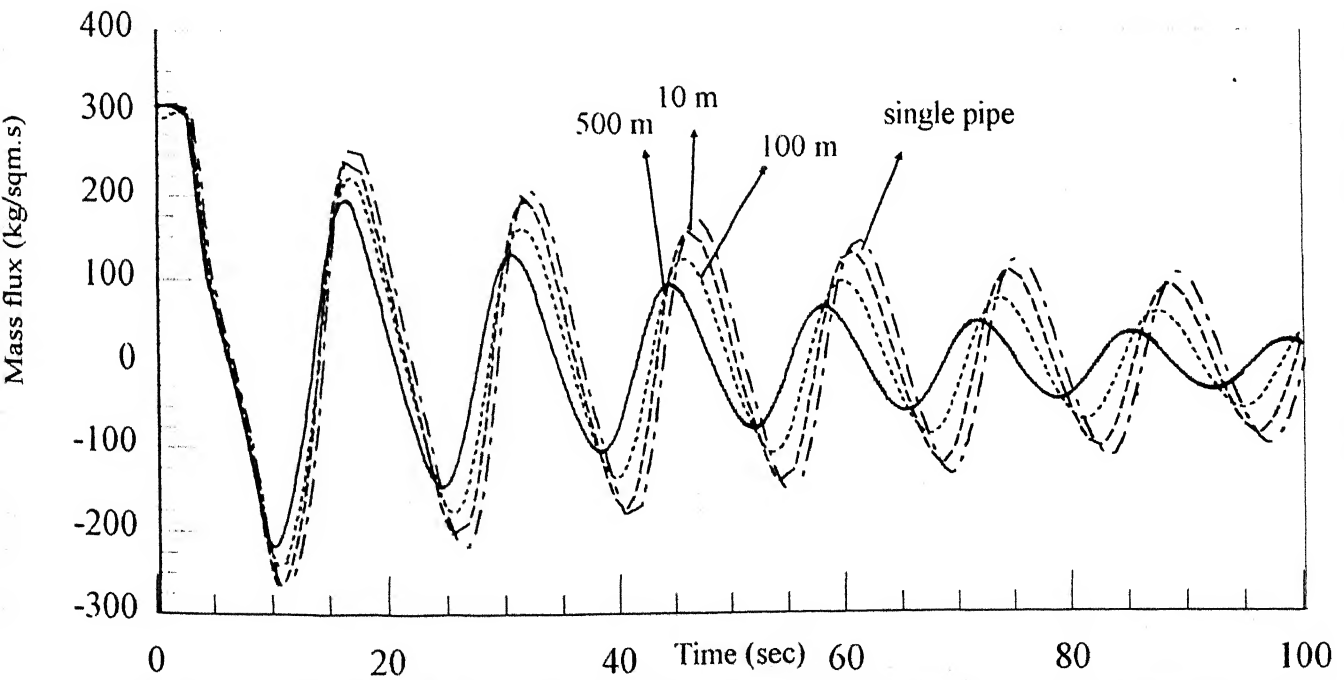

Figure 5.1b: Effect of length of branch BD mass flux transience at node B in main branch (Validation of model for two-branch manifold by that for a single pipe

(L_{mb}=10m, L_{b1}=500m, $d_{mb}=d_{b1}=d_{b2}$=6", m_{b1} = 10 kg/s, m_{b2}= 0.1 kg/s)

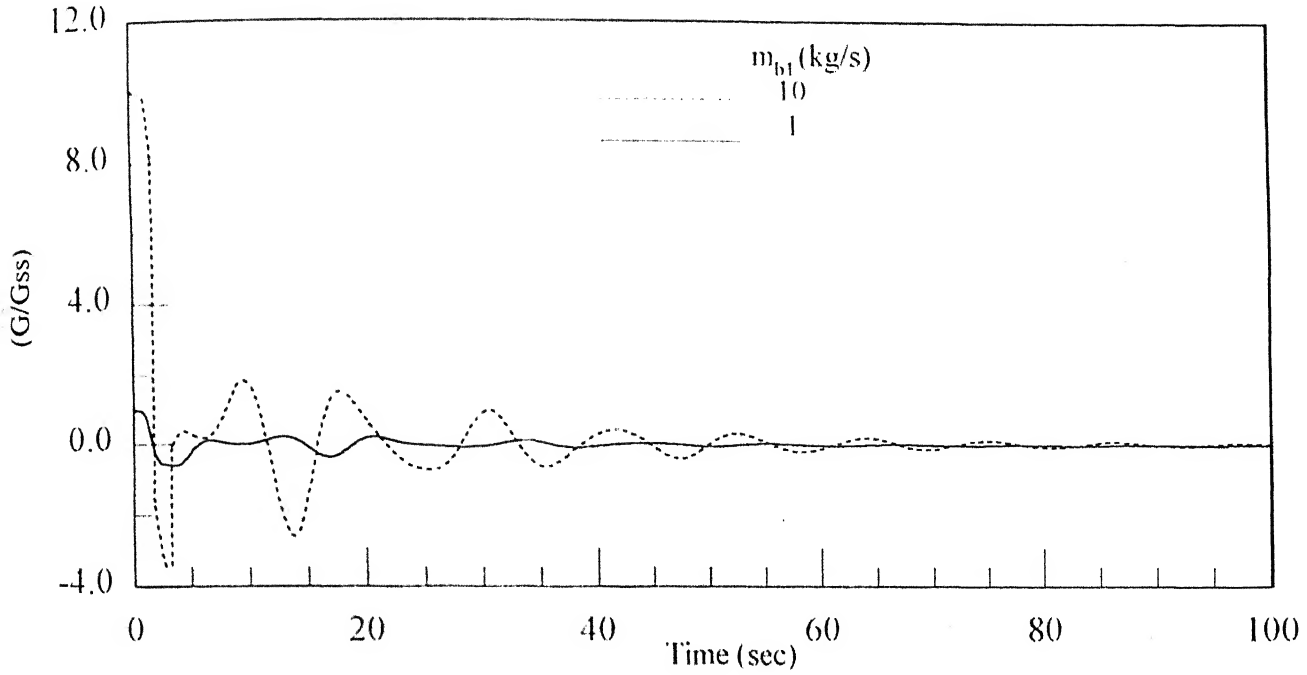

Figure 5.2 a: Mass flux transience at node B for branch 1

(L_{mb}=500 m, L_{b1}=500 m, L_{b2}=500 m, d_{mb}=12", d_{b1}=6", d_{b2}=6", P_{bm}=20bar, m_{b2}=1kg/s)

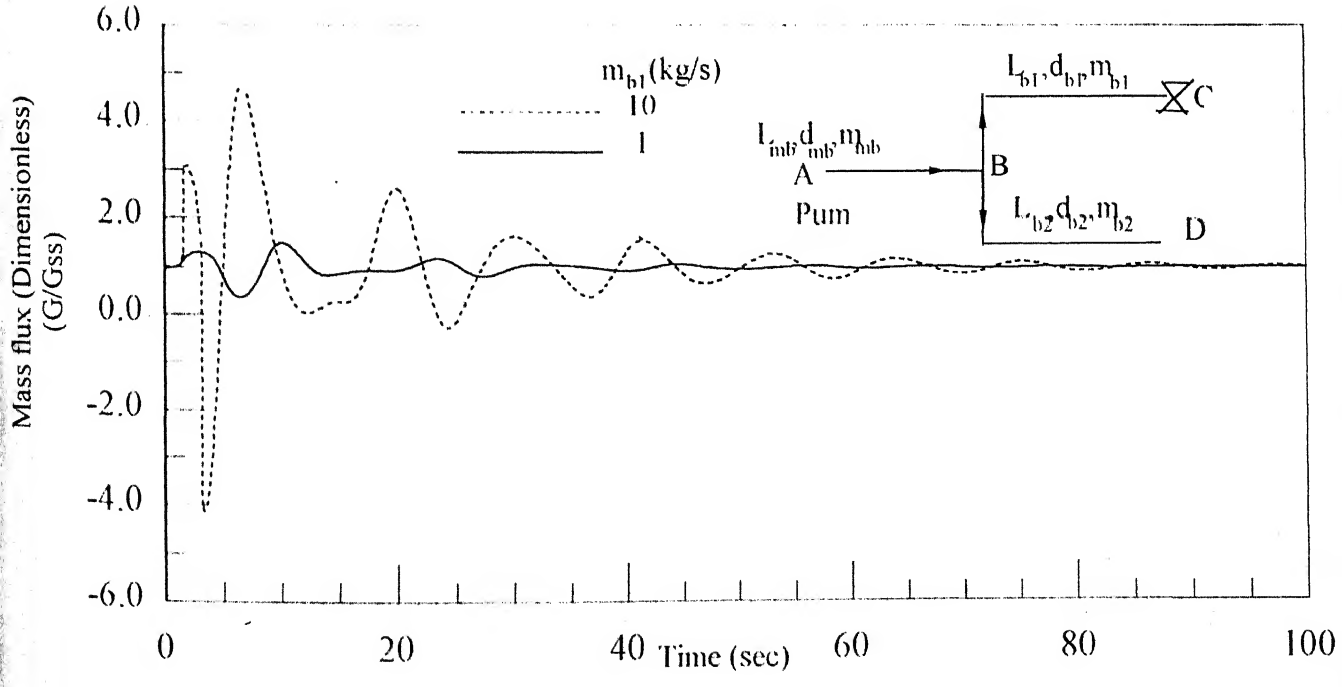

Figure 5.2b: Mass flux transience at node B for branch 2
(Effect of change in mass flow rate of branch 1 on mass-flux transience)
Conditon: Valve installed at the downstream end of branch 1 is closed completely

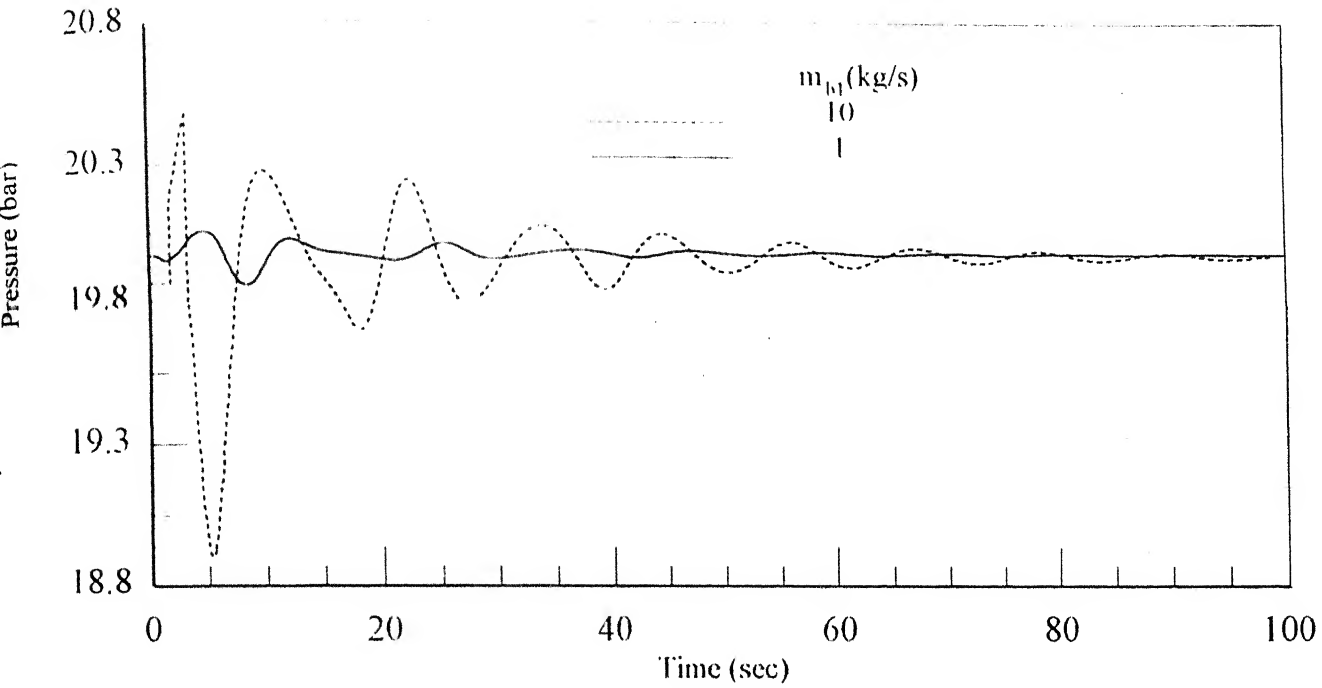

Figure 5.2c Pressure transience at node D

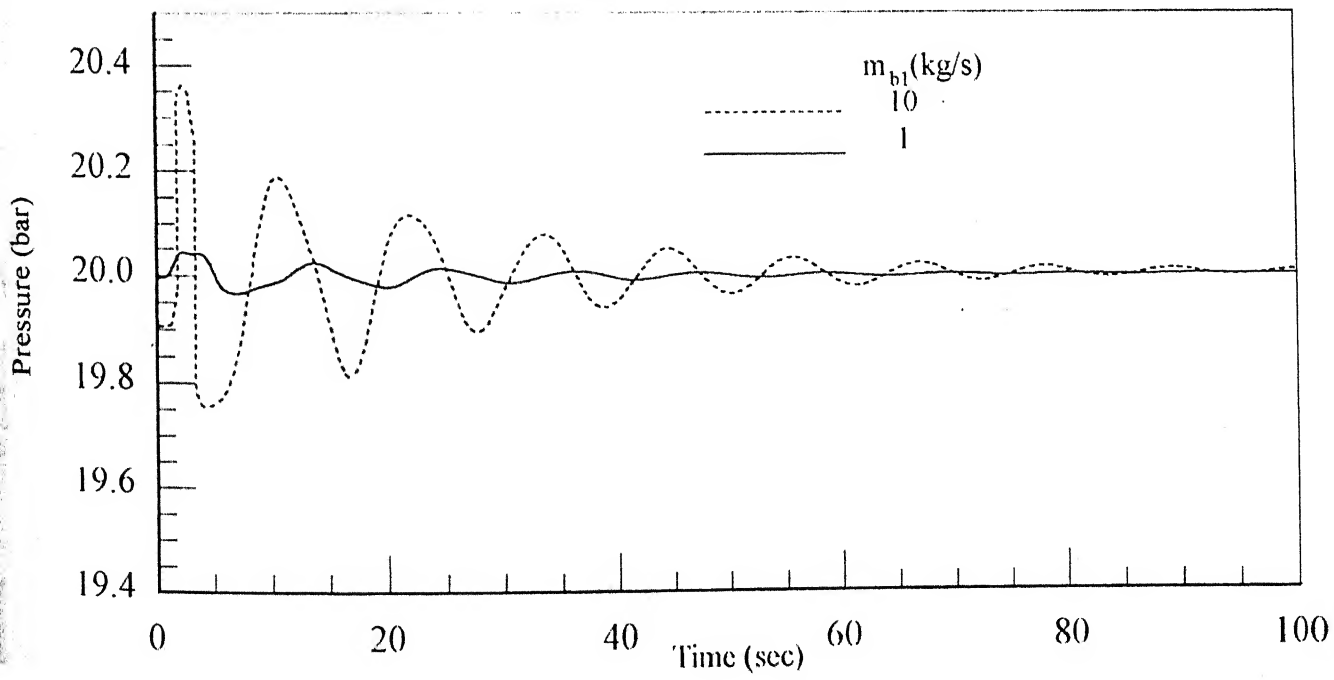

Figure 5.2d: Pressure transience at node B
(Effect of change in mass flow rate of branch 1 on pressure transience)
Conditon: Valve installed at the downstream end of branch 1 is closed completely

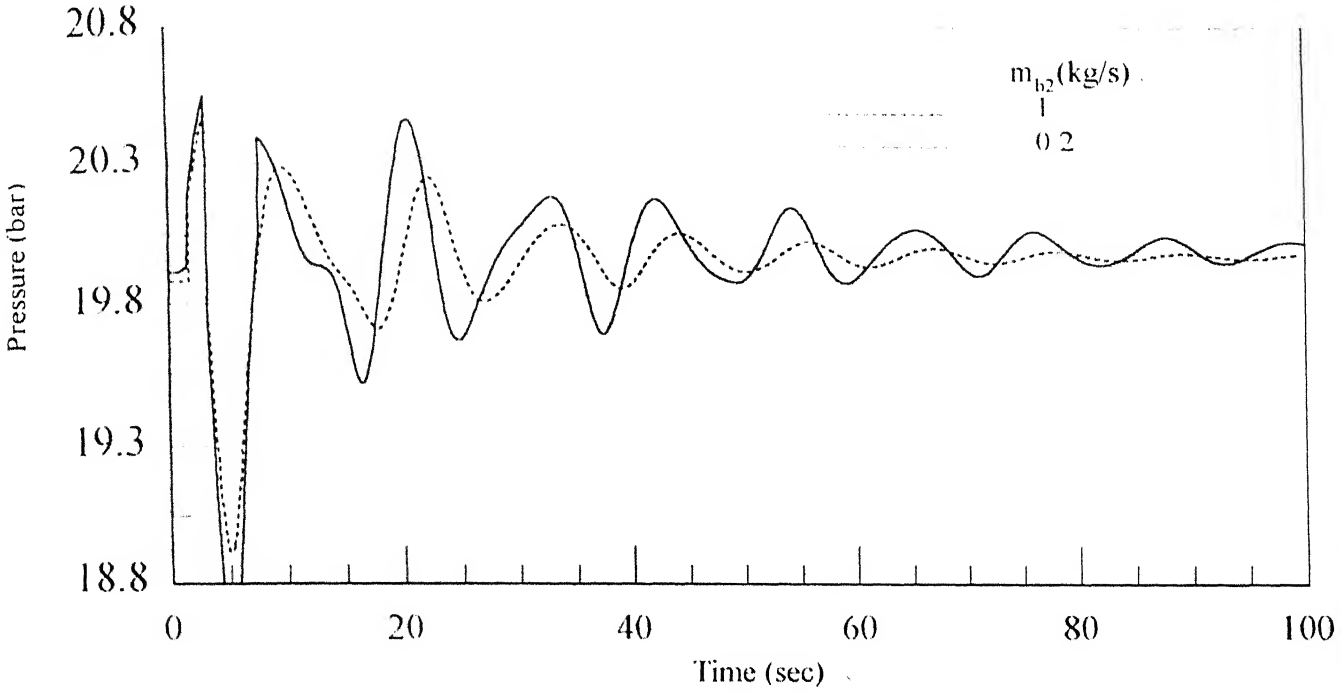

Figure 5.2g: Pressure transience at node D

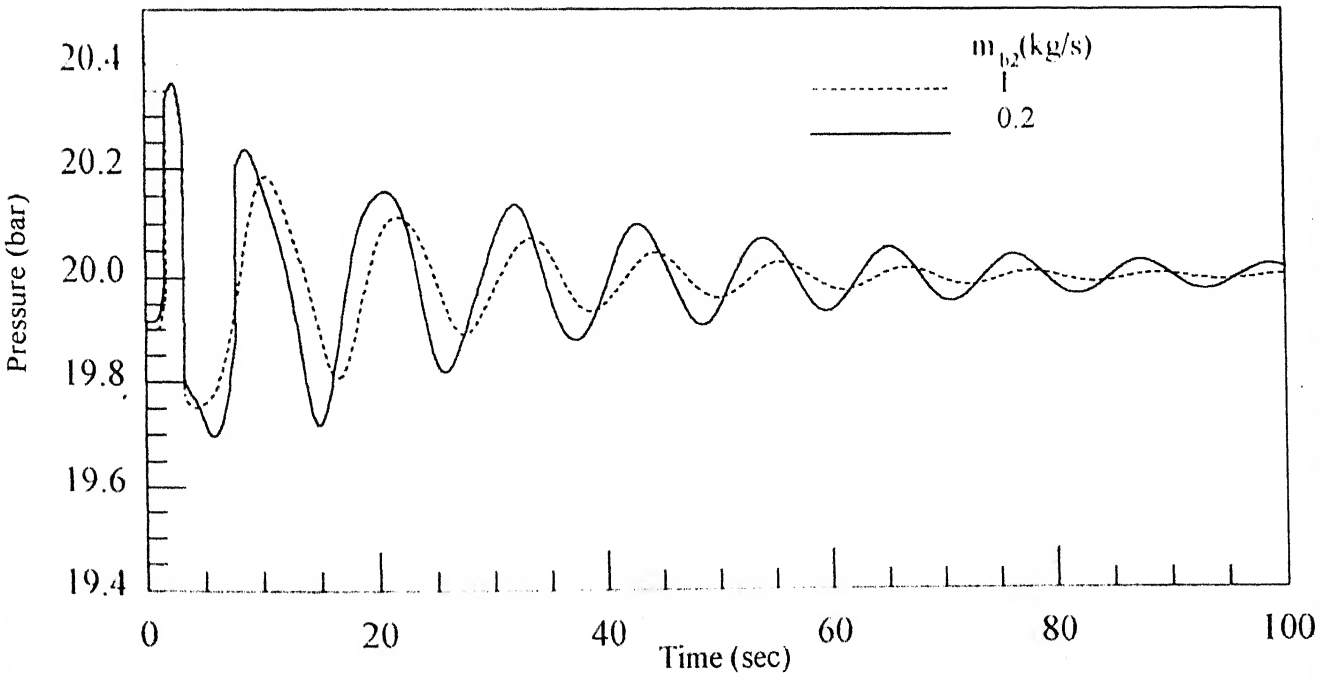

Figure 5.2h: Pressure transience at node B

(Effect of change in mass flow rate of branch 2 on pressure transience)

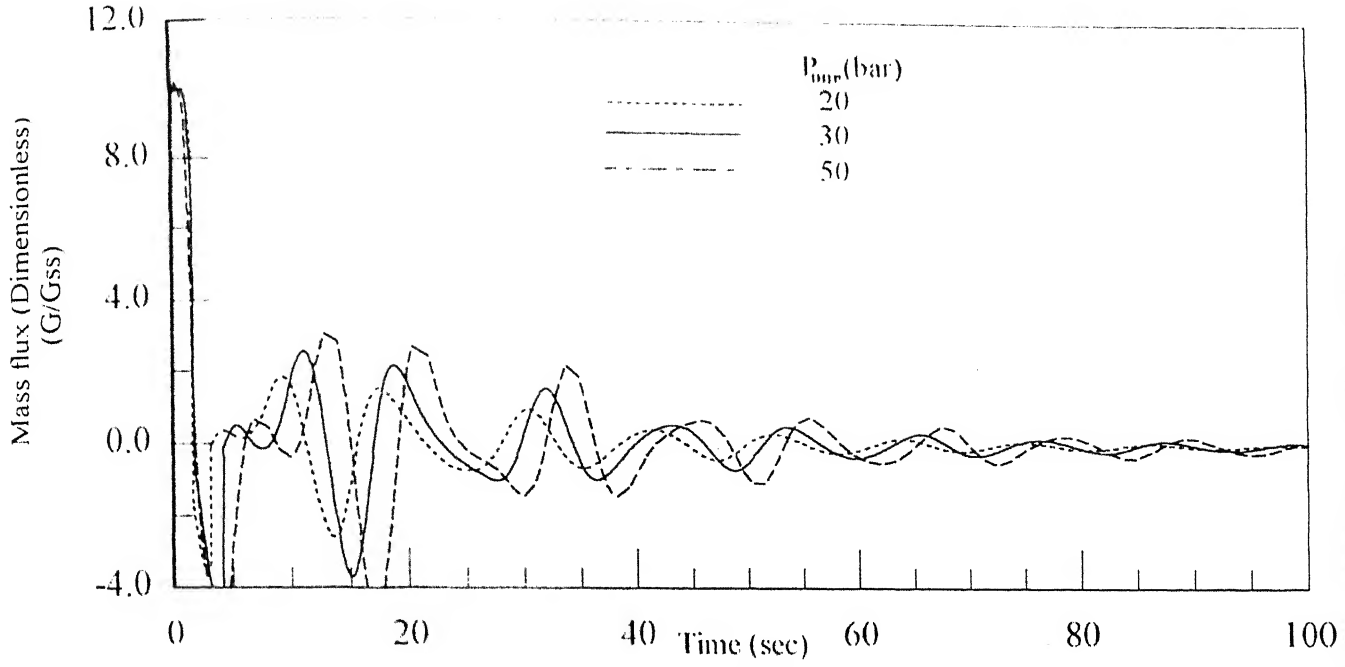

Figure 5.2i Mass flux transience at node B for branch 1

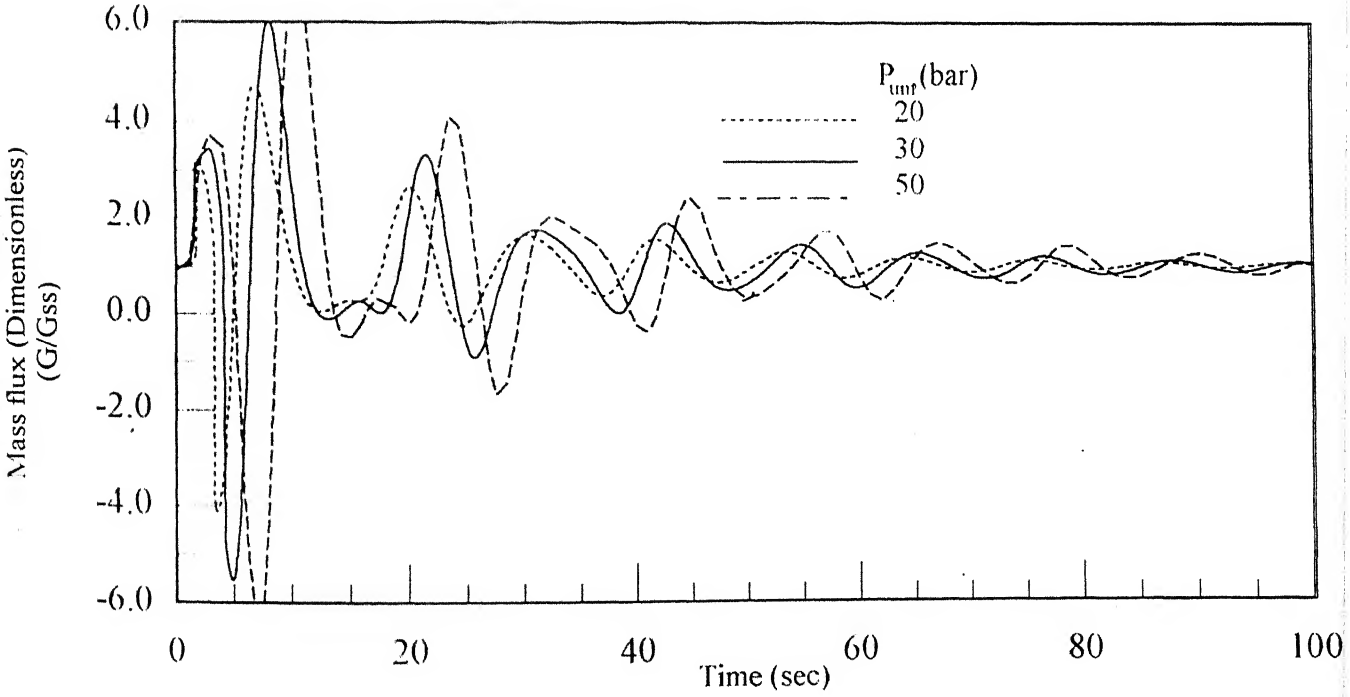

Figure 5.2j: Mass flux transience at node B for branch 2

(Effect of change in supply pressure on mass-flux transience)

(L_{mb}=500 m, L_{b1}=500 m ,L_{b2}=500 m, d_{mb}=12", d_{b1}=6" ,d_{b2}=6" ,m_{b1}=10 kg/s, m_{b2}=1kg/s)

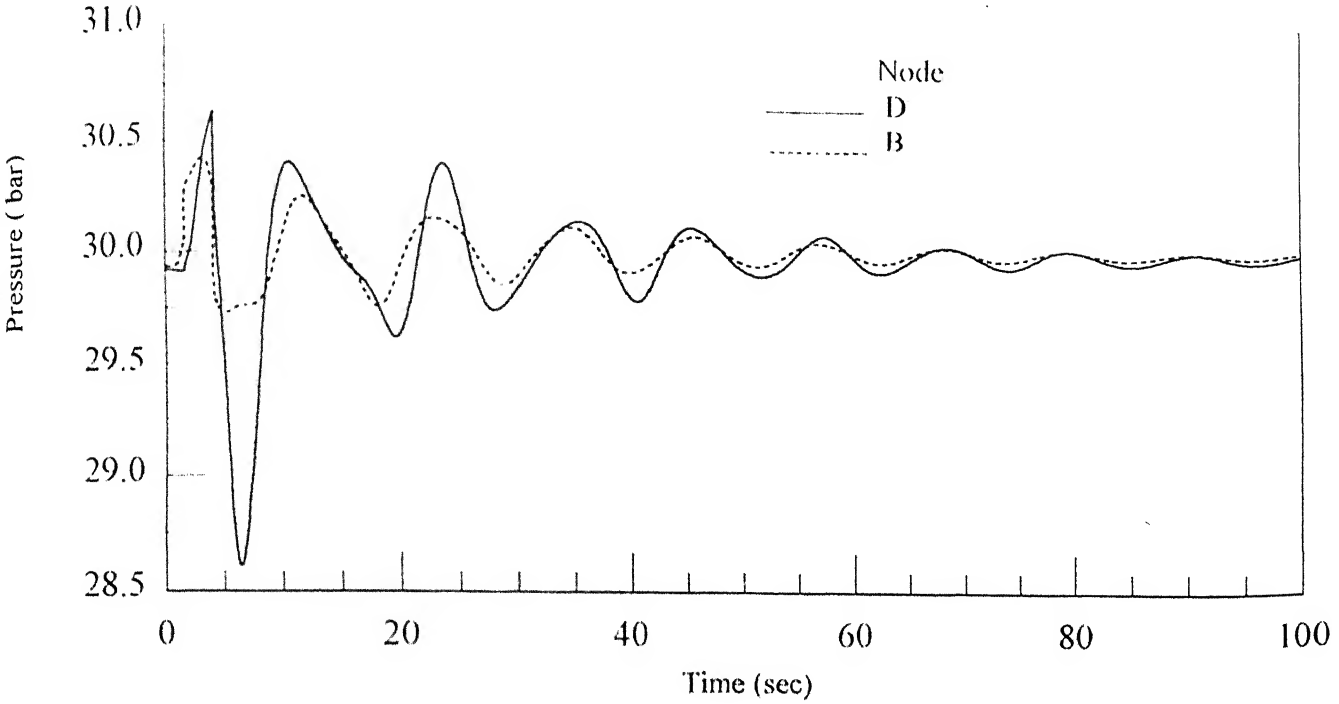

Figure 5.2k: Pressure transience at node D and B when upstream pressure at node A is 30 bar

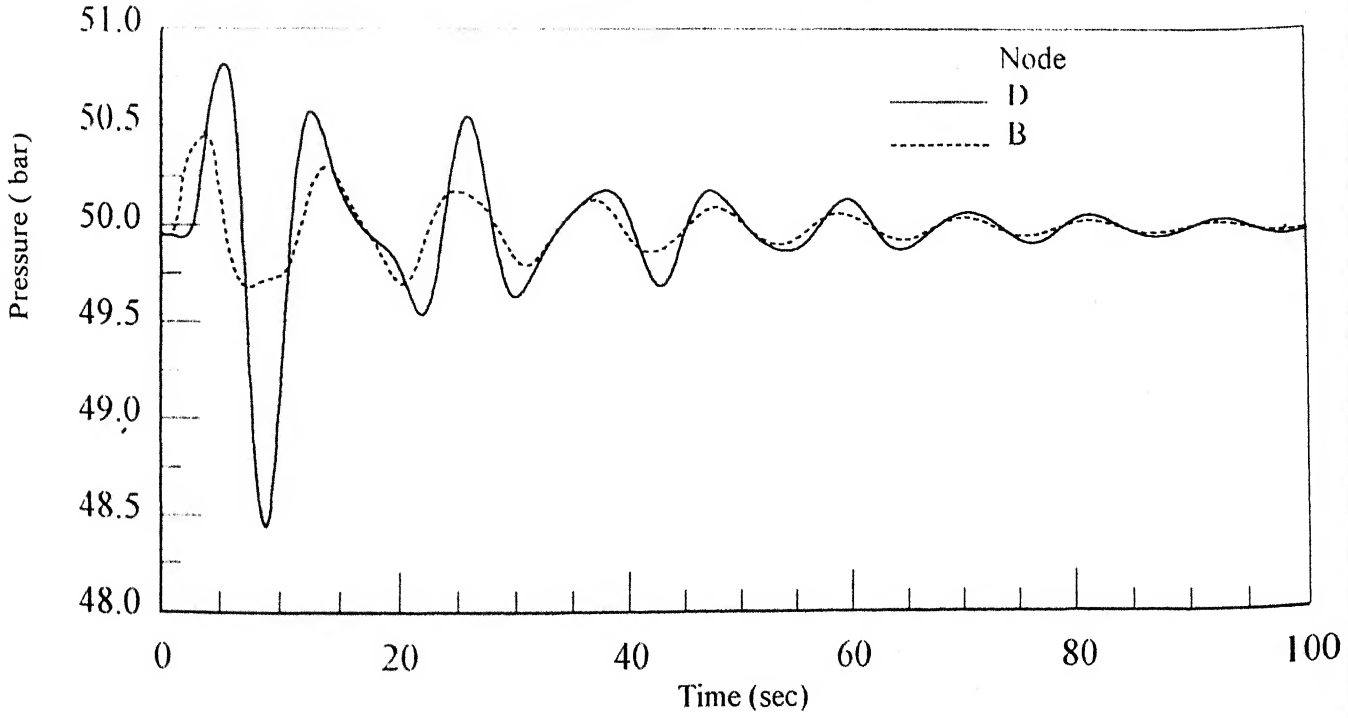

Figure 5.2l: Pressure transience at node D and B when upstream pressure at node A is 50 bar

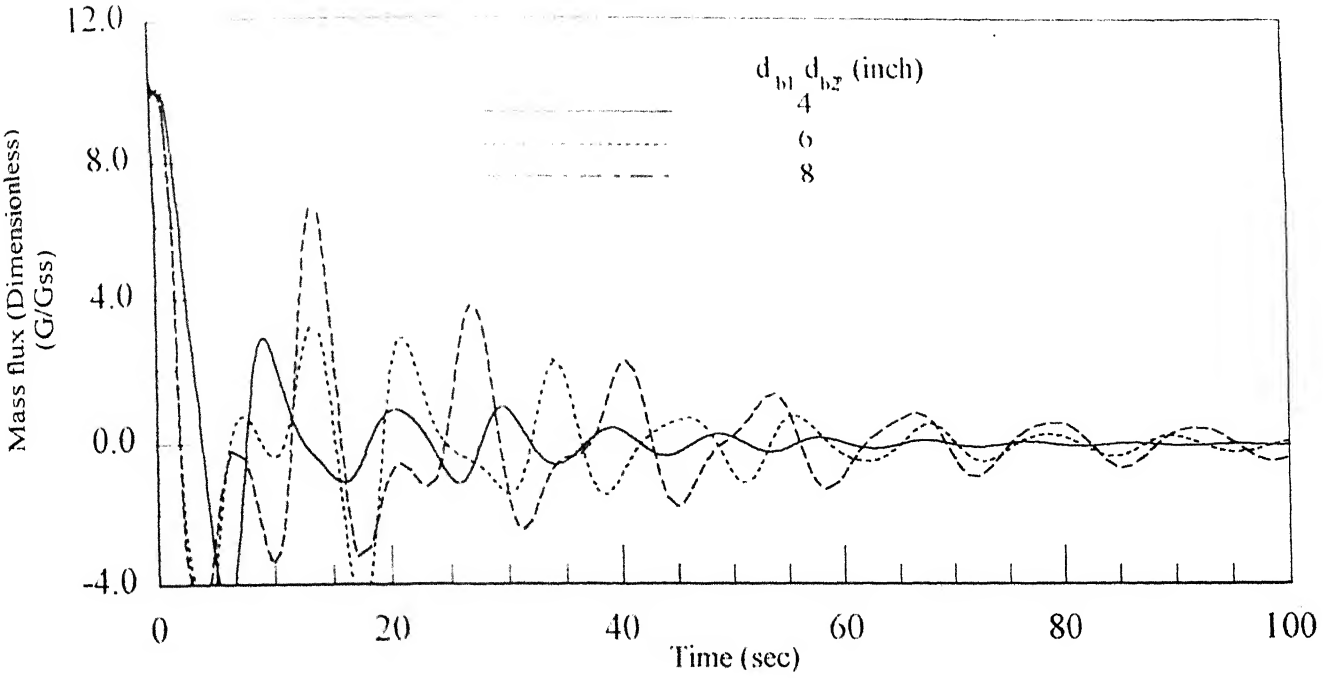

Figure 5.2m: Mass flux transience at node B for branch 1

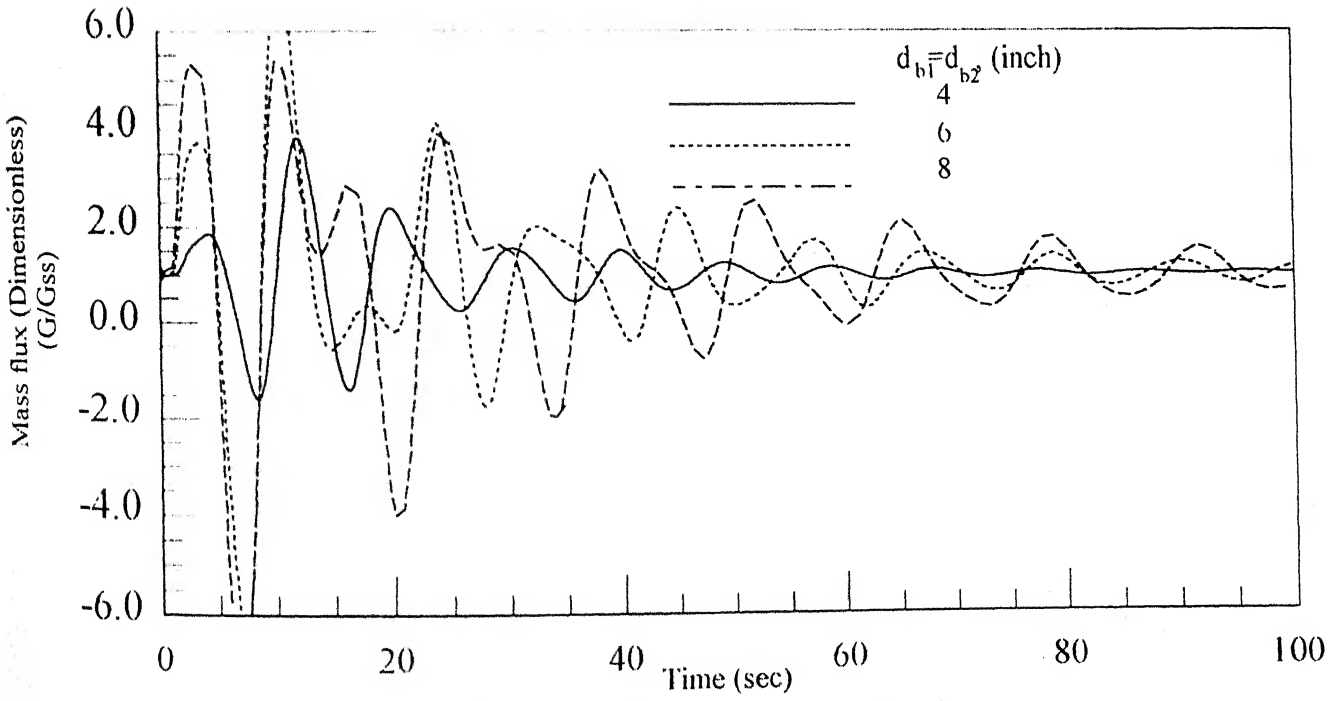

Figure 5.2n Mass flux transience at node B for branch 2

(Effect of change in diameter of branch 1 and 2 on mass-flux transience)

(L_{mb}=500 m, L_{b1}=500 m ,L_{b2}=500 m, d_{mb}=12" , P_{um}=20bar, $\dot{m}_{b1}$=10kg/s, $\dot{m}_{b2}$=1kg/s)

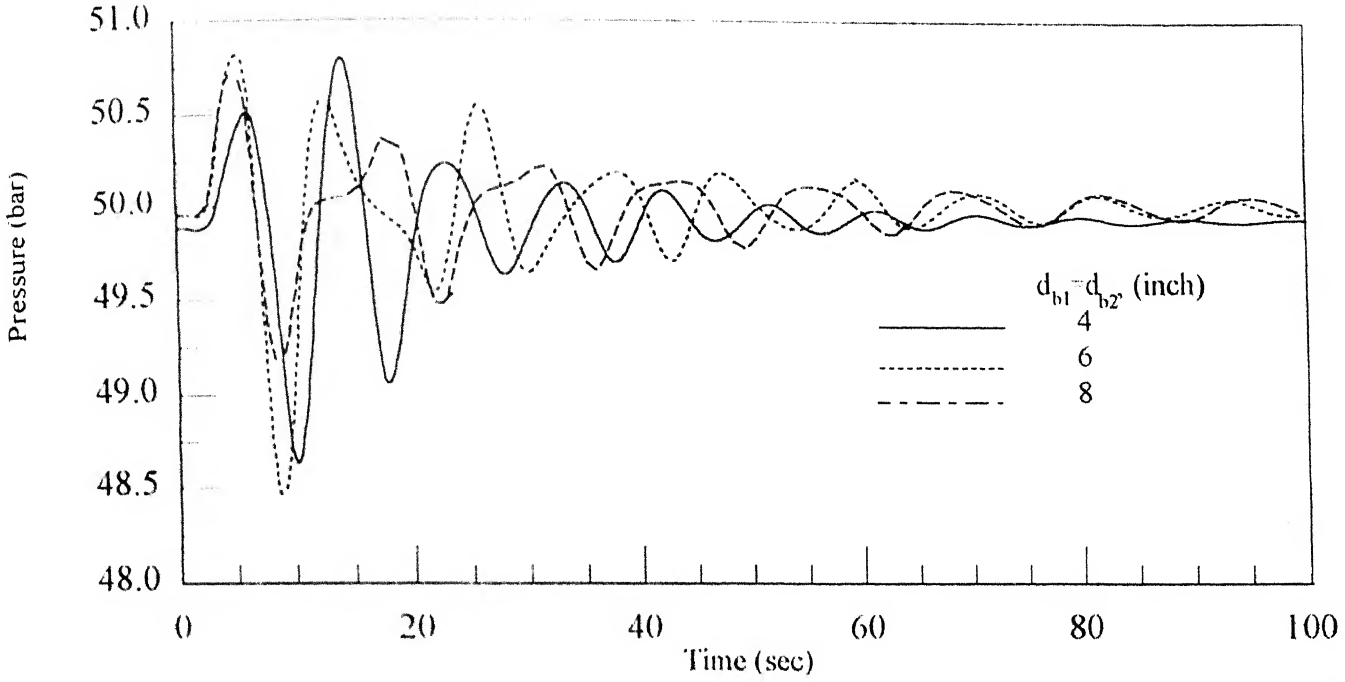

Figure 5.2o: Pressure transience at node D

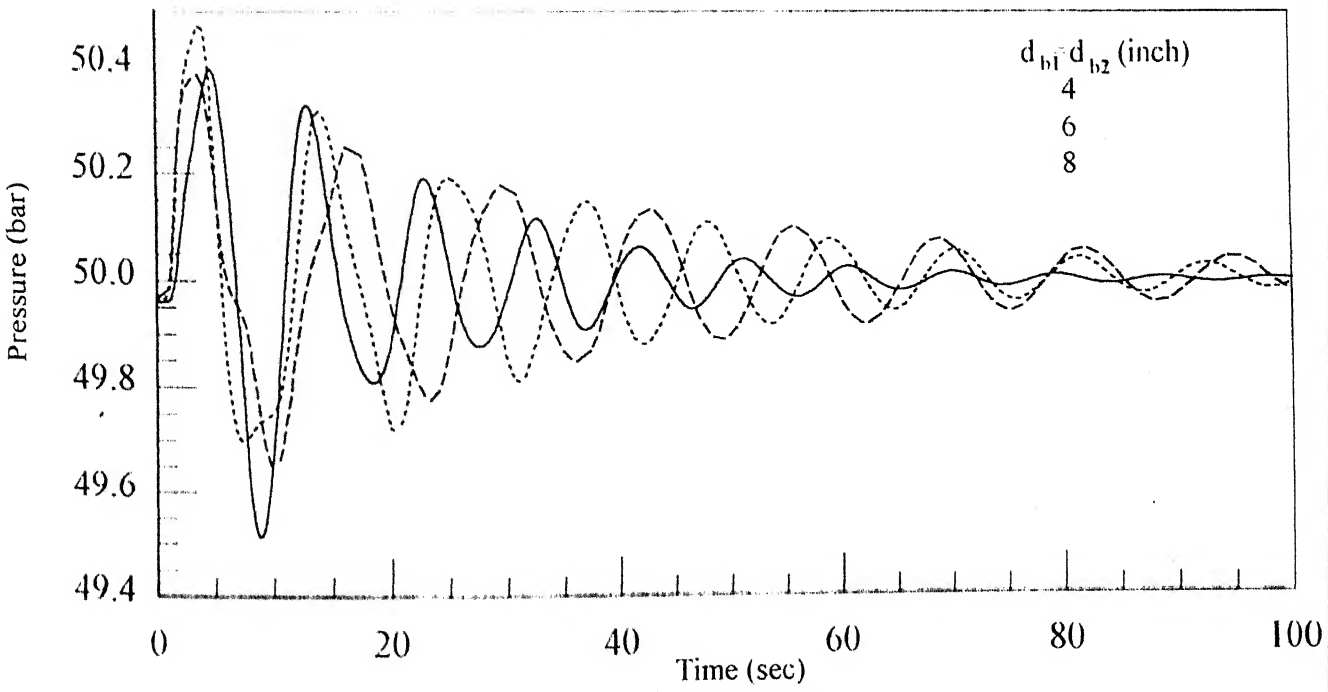

Figure 5.2p: Pressure transience at node B

(Effect of change in diameter of branch 1 and 2 on pressure transience)

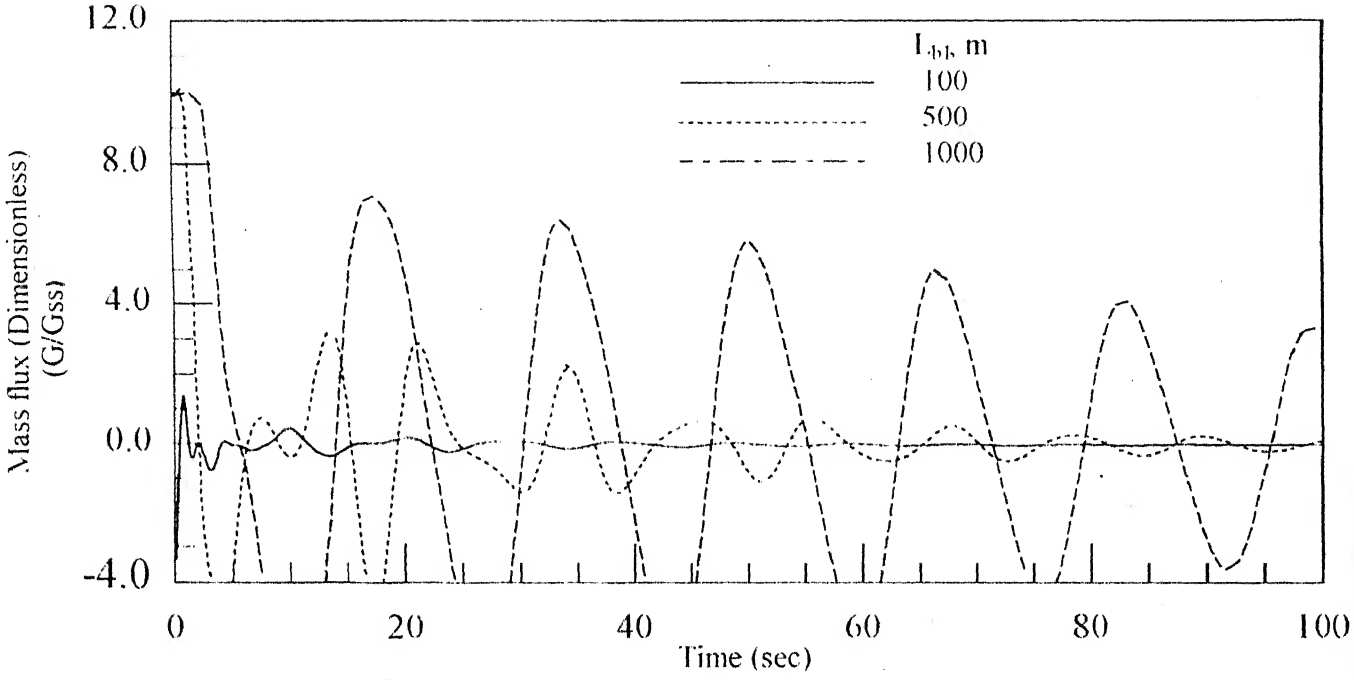

Figure 5.2q: Mass flux transience at node B for branch 1

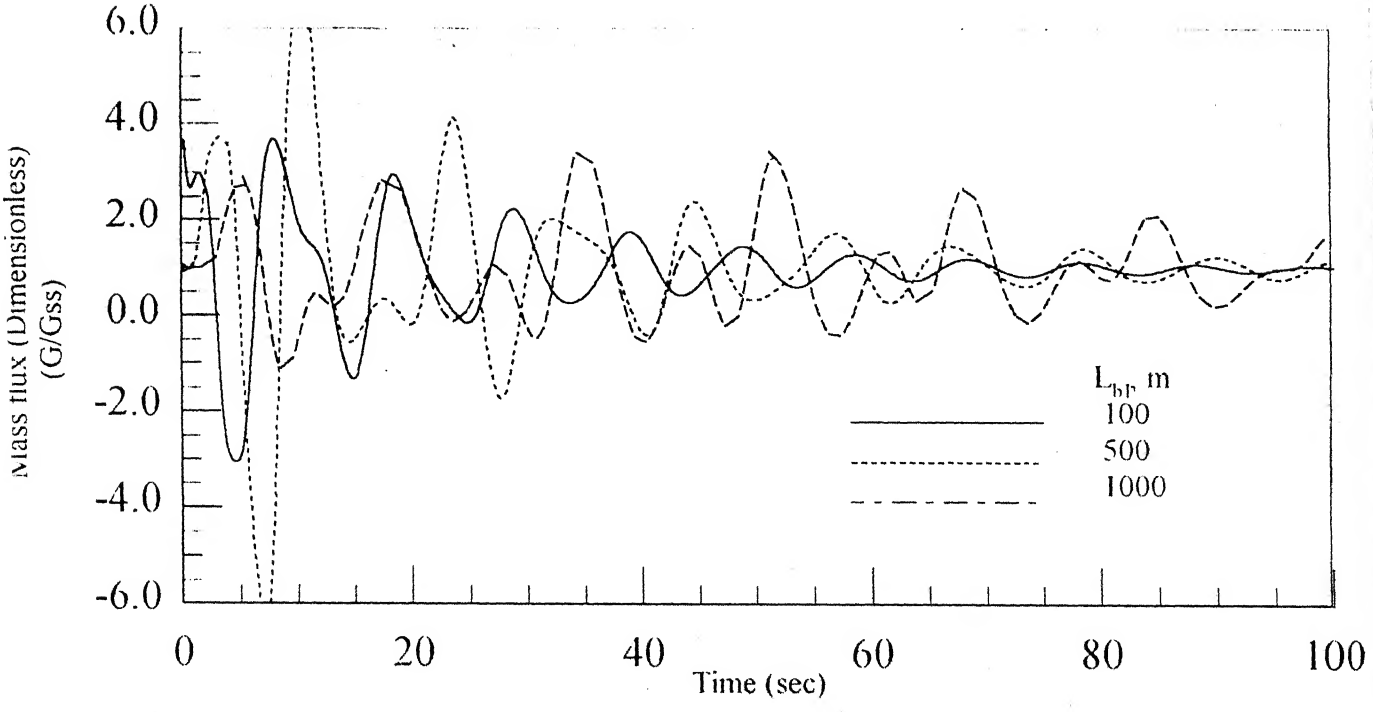

Figure 5.2r: Mass flux transience at node B for branch 2

(Effect of change in length of branch 1 on mass-flux transience)

(L_{mb}=500 , L_{b1}=500 m, d_{mb}=12", d_{b1}=6" ,d_{b2}=6" , P_{mm} 20bar, m_{b1} 10kg/s, m_{b2} 1kg/s)

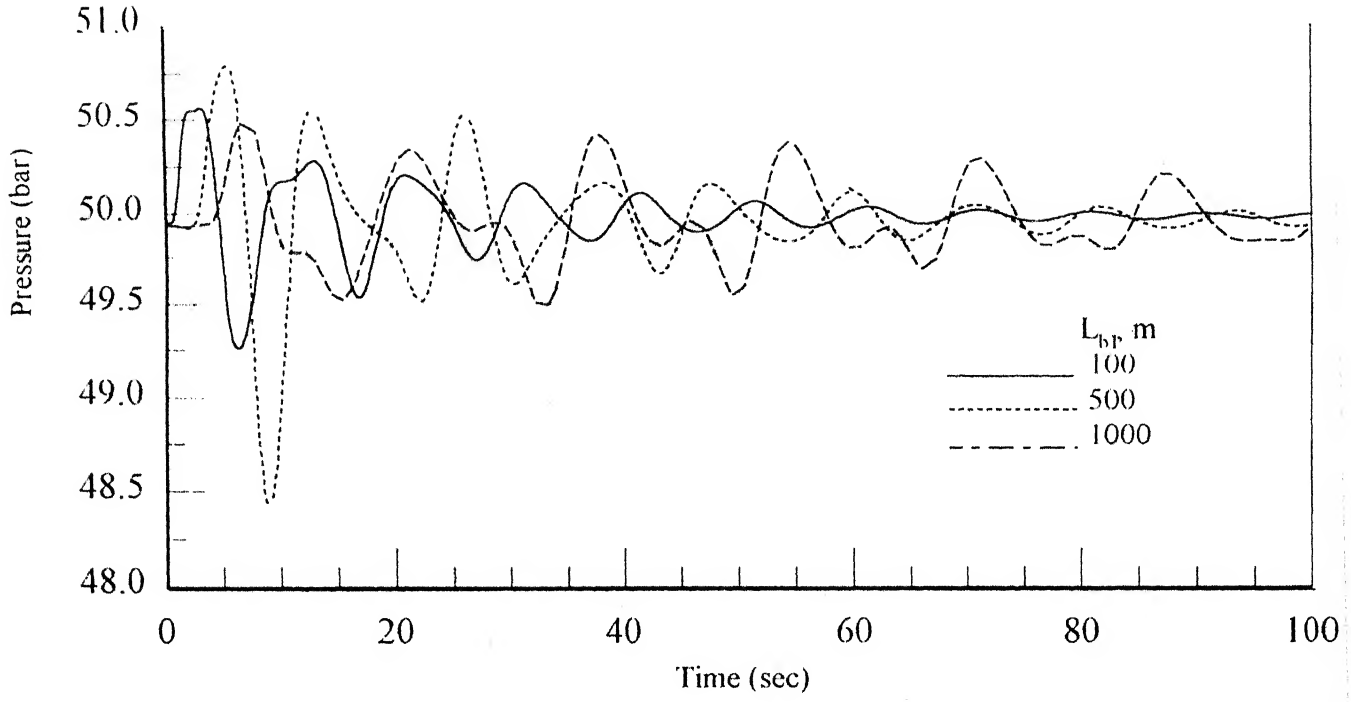

Figure 5.2s: Pressure transience at node D

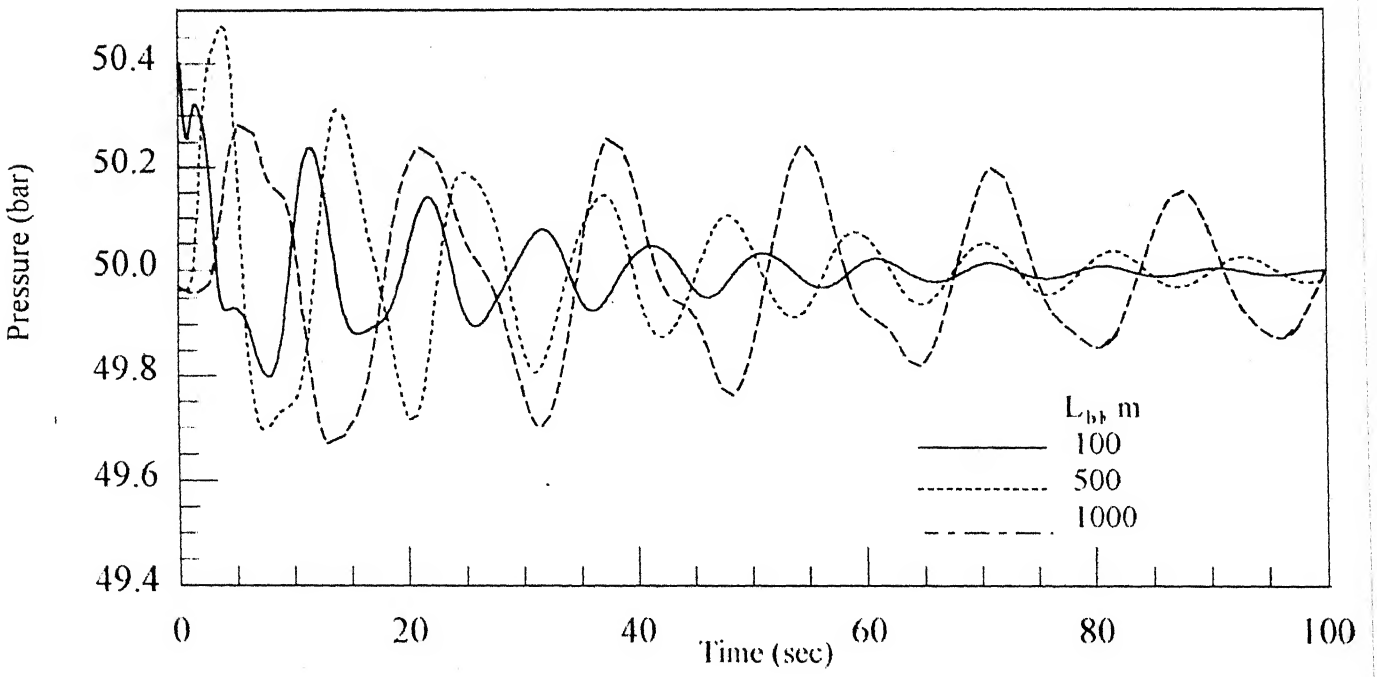

Figure 5.2t: Pressure transience at node B

(Effect of change in length of branch 1 on pressure transience)

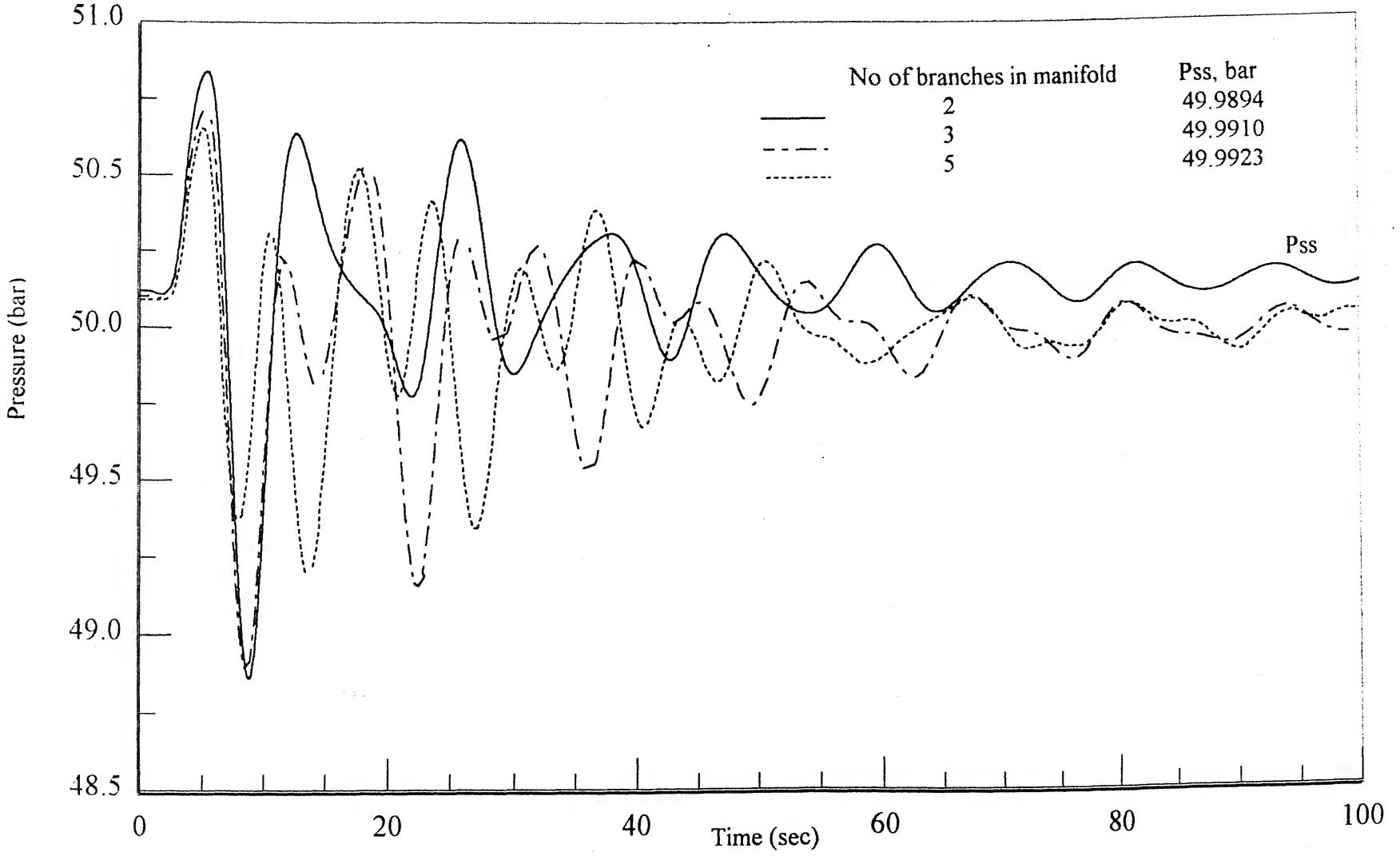

Figure 5.3b: Effect of number of branches in manifold on the pressure at node D

(Valves at the downstream end of branch BC, BD, BE, BF are completely shut-off)

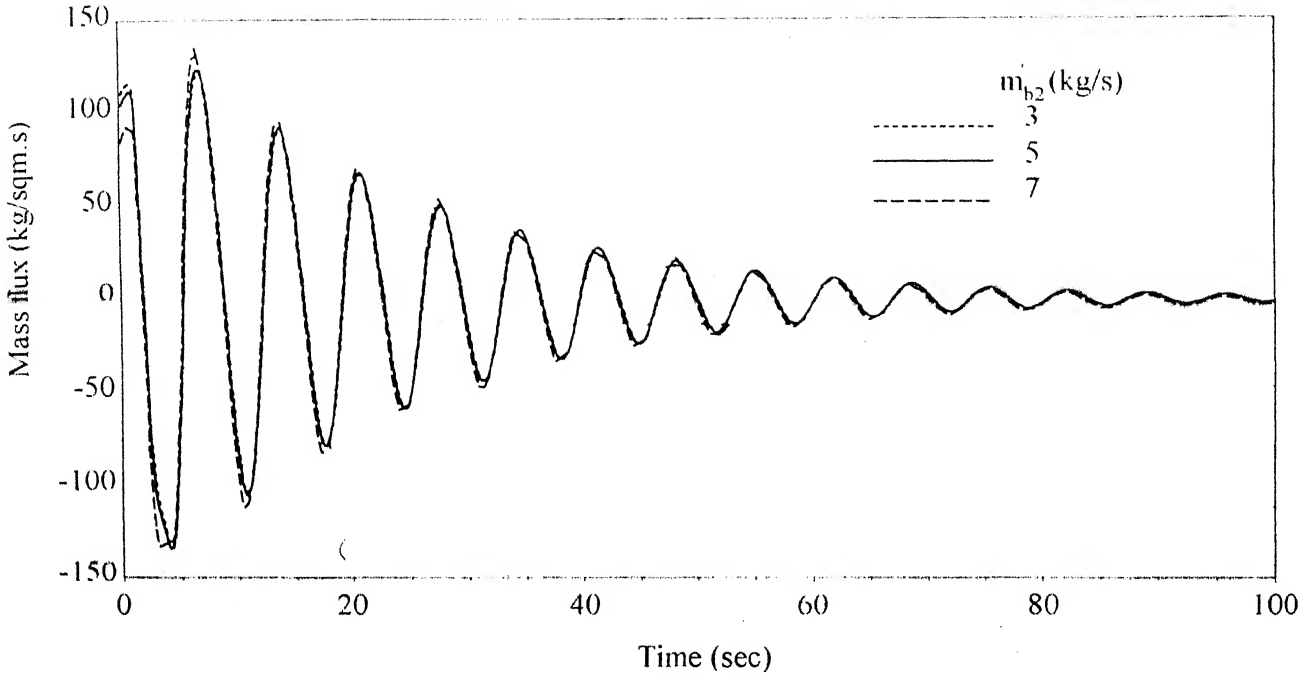

Figure 5.4a: Mass flux transience at node B for branch 1

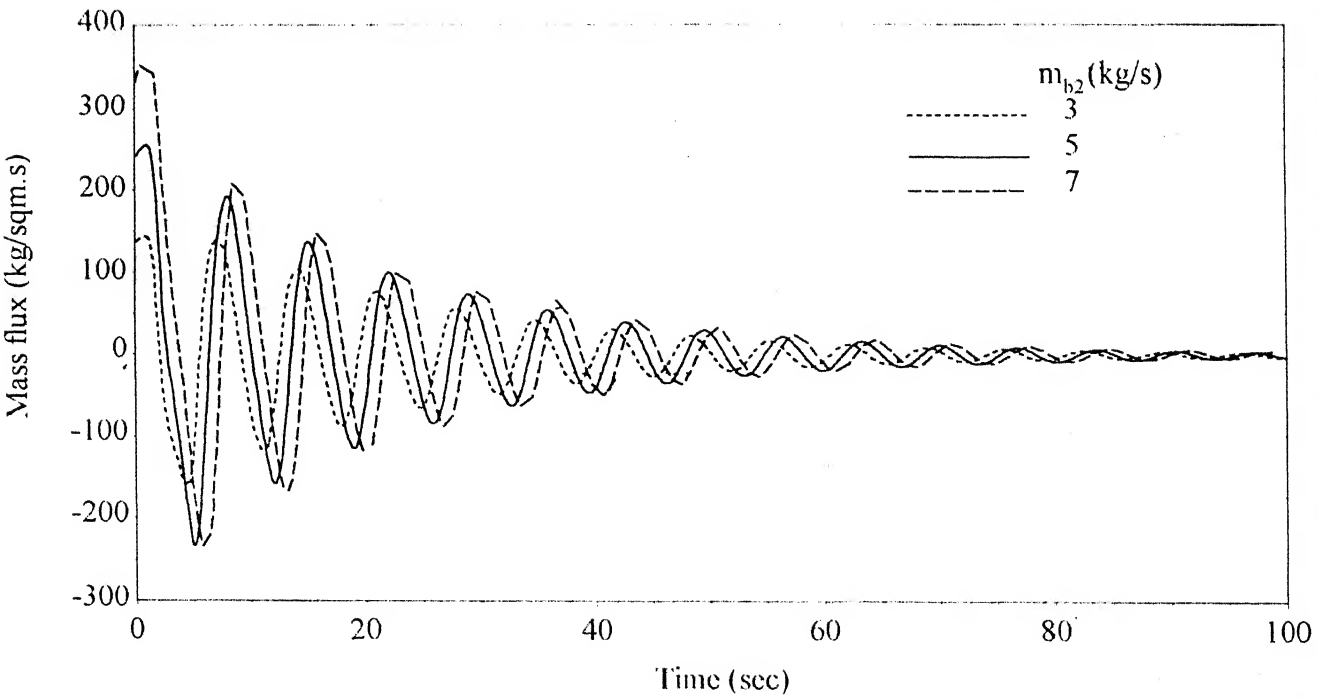

Figure 5.4b: Mass flux transience at node B for branch 2

(Effect of change in mass flow rate of branch 1 on mass-flux transience)

(L_{mb}=500 m ,L_{b1}= 500m, L_{b2}=500 m, d_{mb}=12", d_{b1}=6" ,d_{b2}=6" , P_{in}=10bar, m_{b1}= 2.5 kg/s)

Condition: Compressor at A shuts down and valves at C and D are closed simultaneously

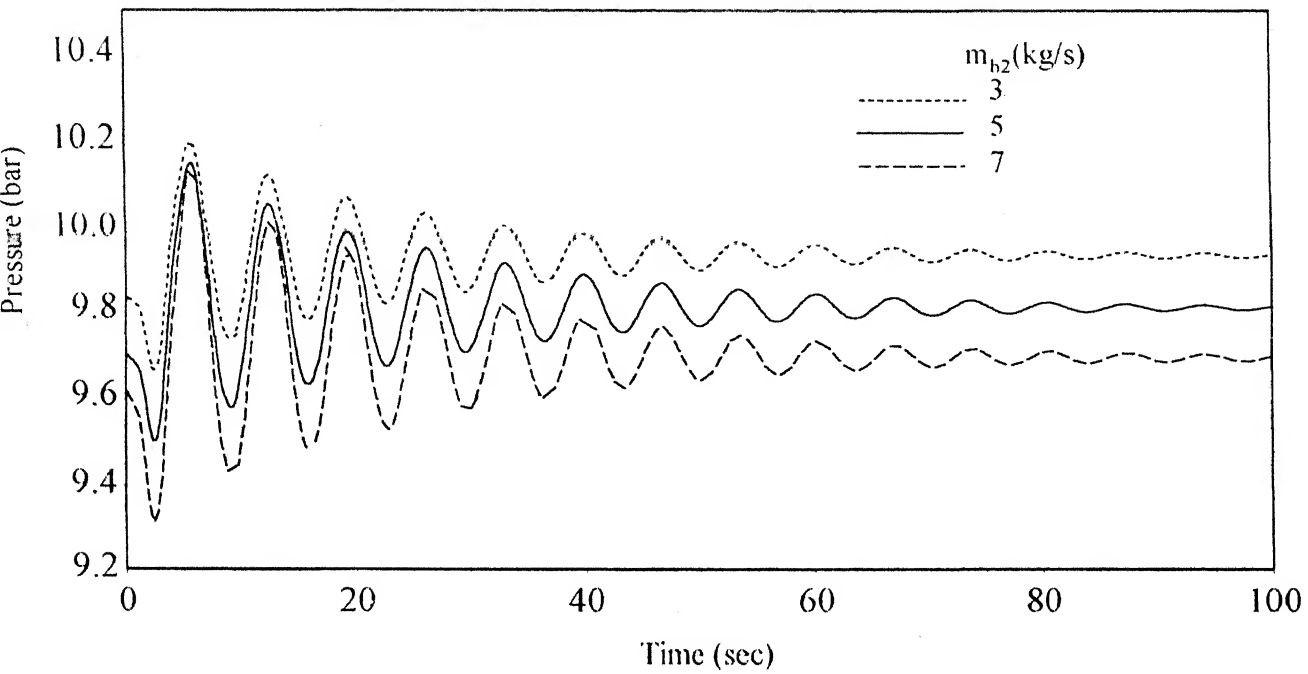

Figure 5.4c: Pressure transience at node B

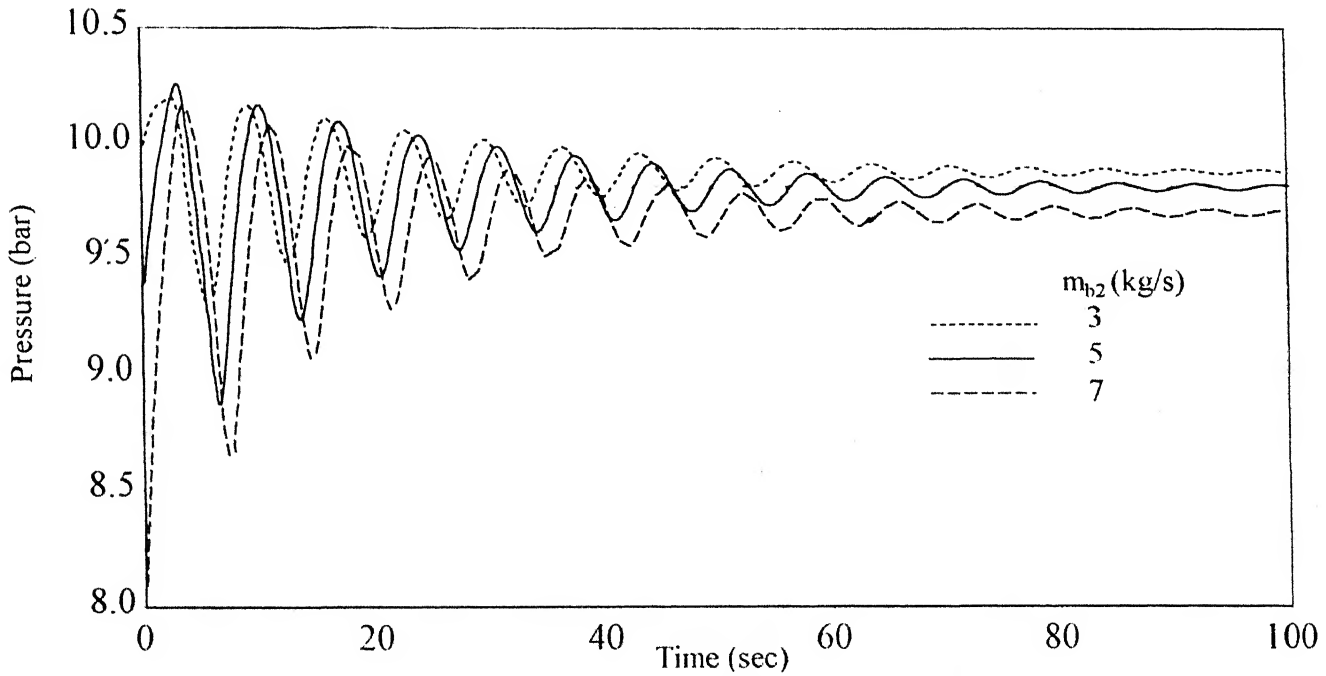

Figure 5.4d: Pressure transience at node A
(Effect of change in mass flow rate of branch 1 on pressure transience)
Condition: Compressor at A shuts down and valves at C and D are closed simultaneously

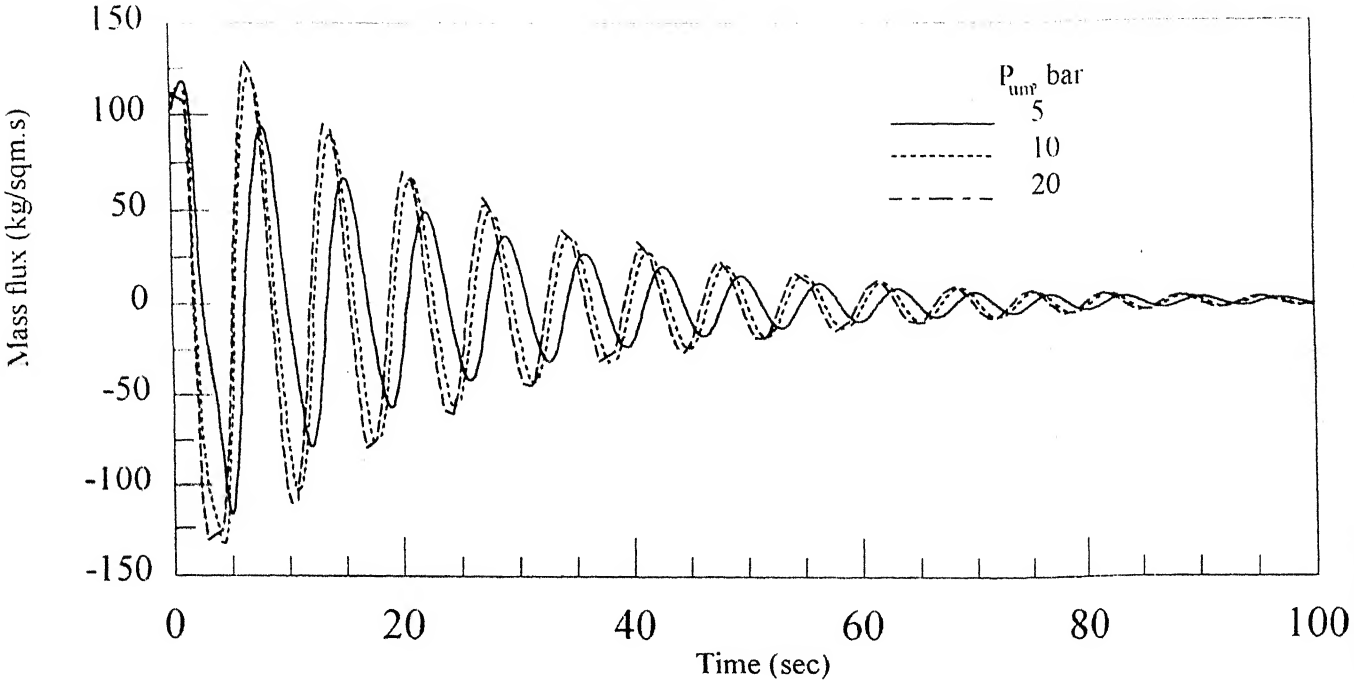

Figure 5.4e: Mass flux transience at node B for branch 1

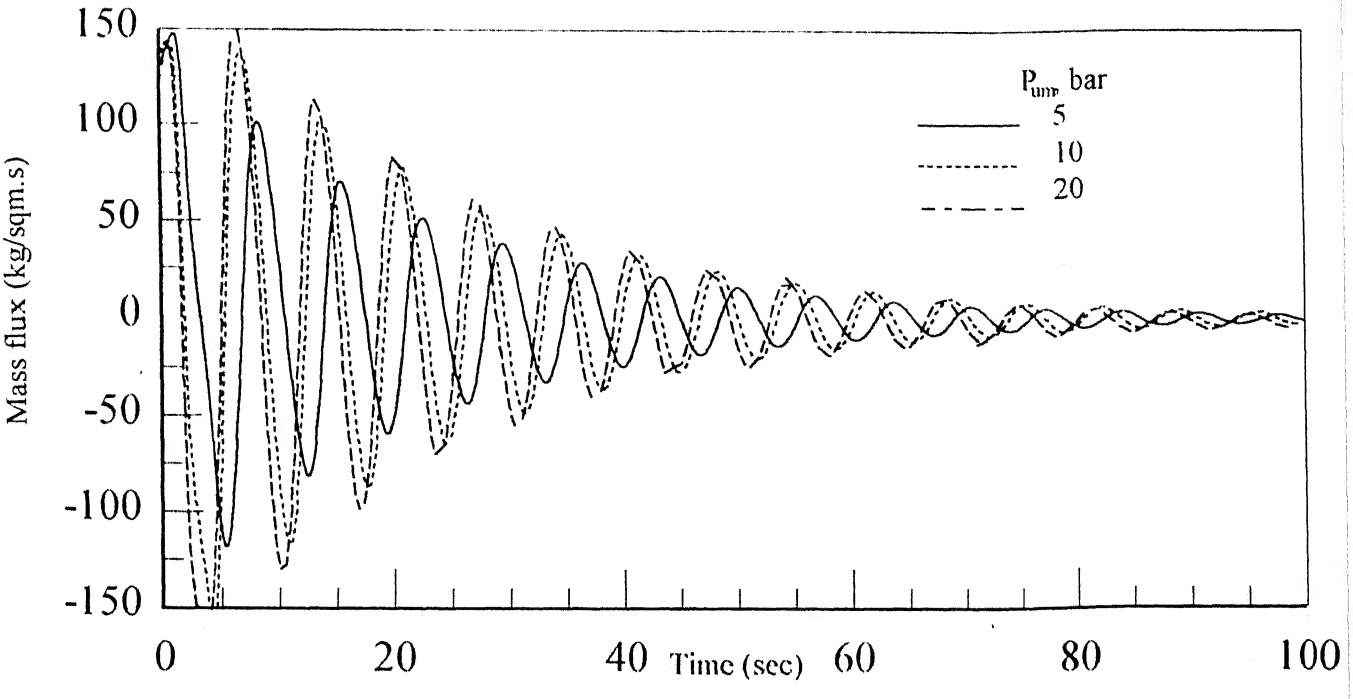

Figure 5.4f: Mass flux transience at node B for branch 2

(Effect of change in supply pressure on mass-flux transience)

(L_{mb}=500 m ,L_{b1}= 500m, L_{b2}=500 m, d_{mb}=12", d_{b1}=6" ,d_{b2}=6" , m_{b1}= 2.5 kg/s m_{b2}=3kg/s)

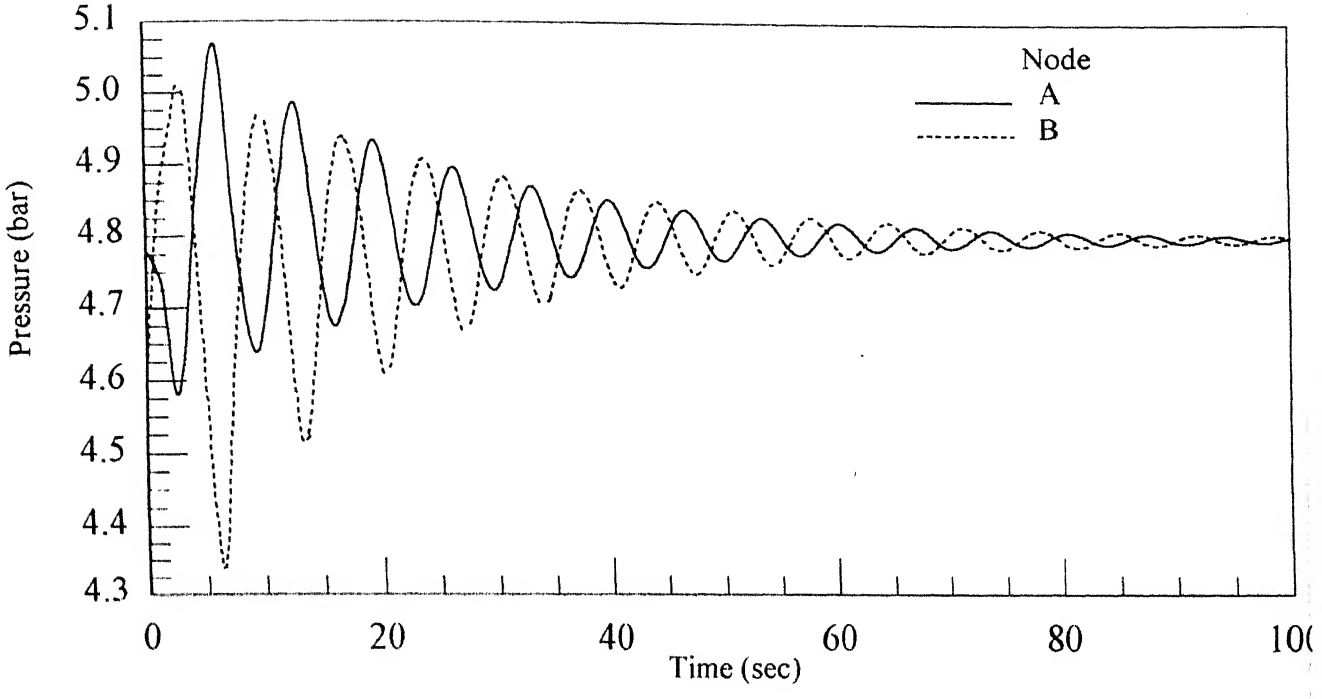

Figure 5.4g: Pressure transience at node A and B

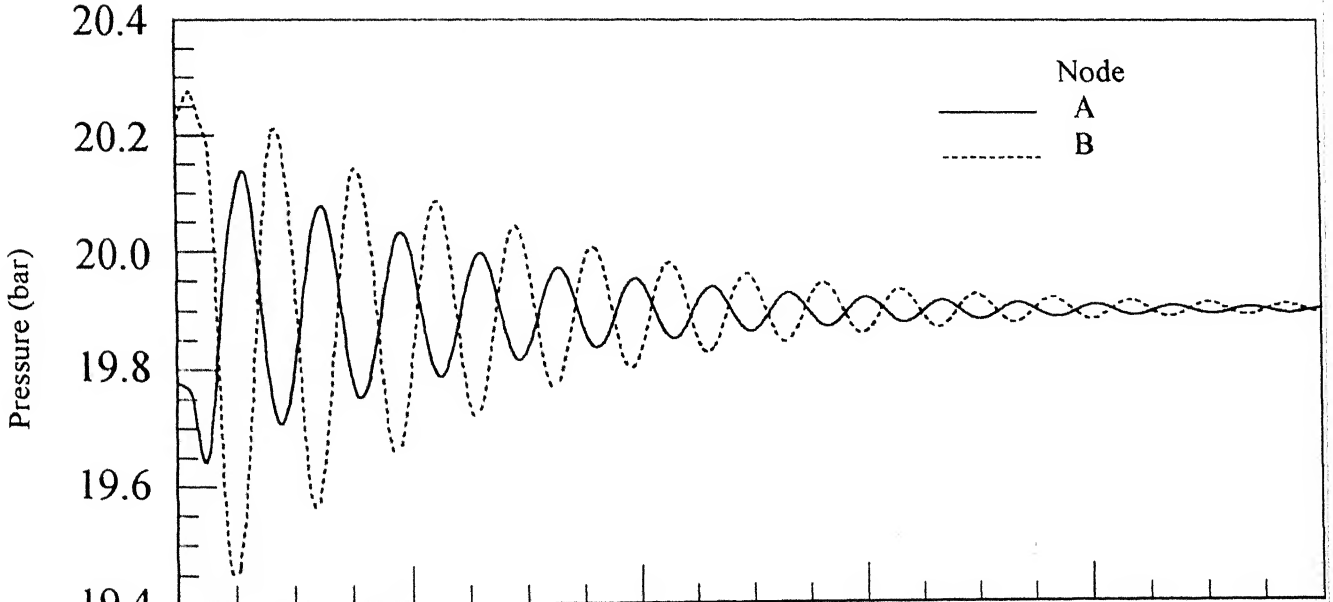

Figure 5.4h: Pressure transience at node A and B

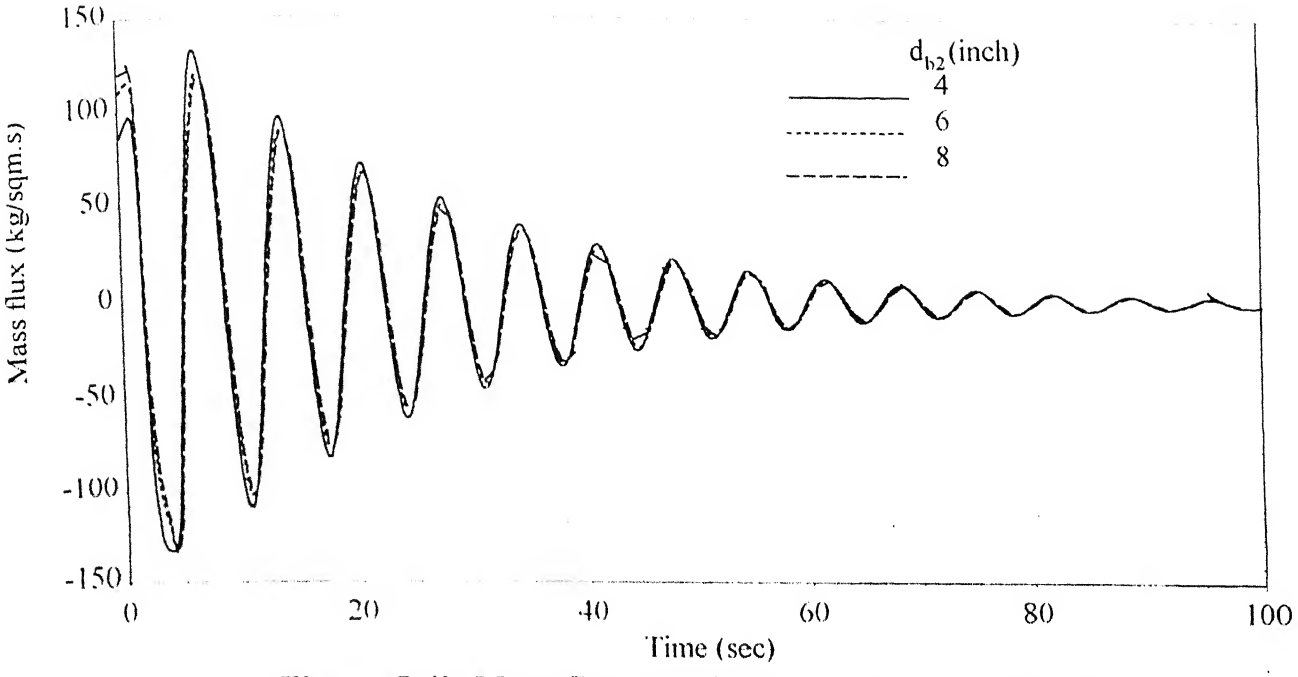

Figure 5.4i: Mass flux transience at node B for branch 1

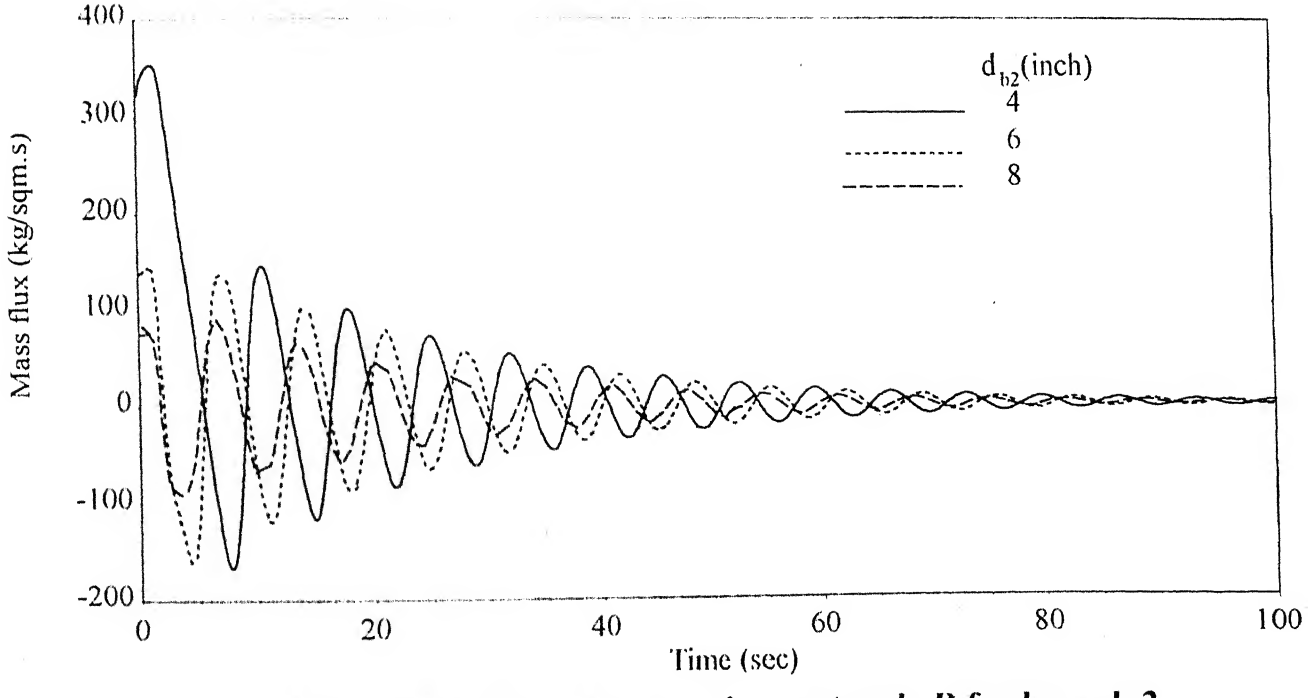

Figure 5.4j: Mass flux transience at node B for branch 2

(Effect of change in diameter of branch 2 on mass-flux transience)

(L_{fmb}=500 m ,L_{b1}= 500 m, L_{b2}=500 m, d_{mb}=12", d_{b1}=6" , P_{um}=10bar, m_{b1}= 2.5 kg/s m_{b2}=3kg/s)

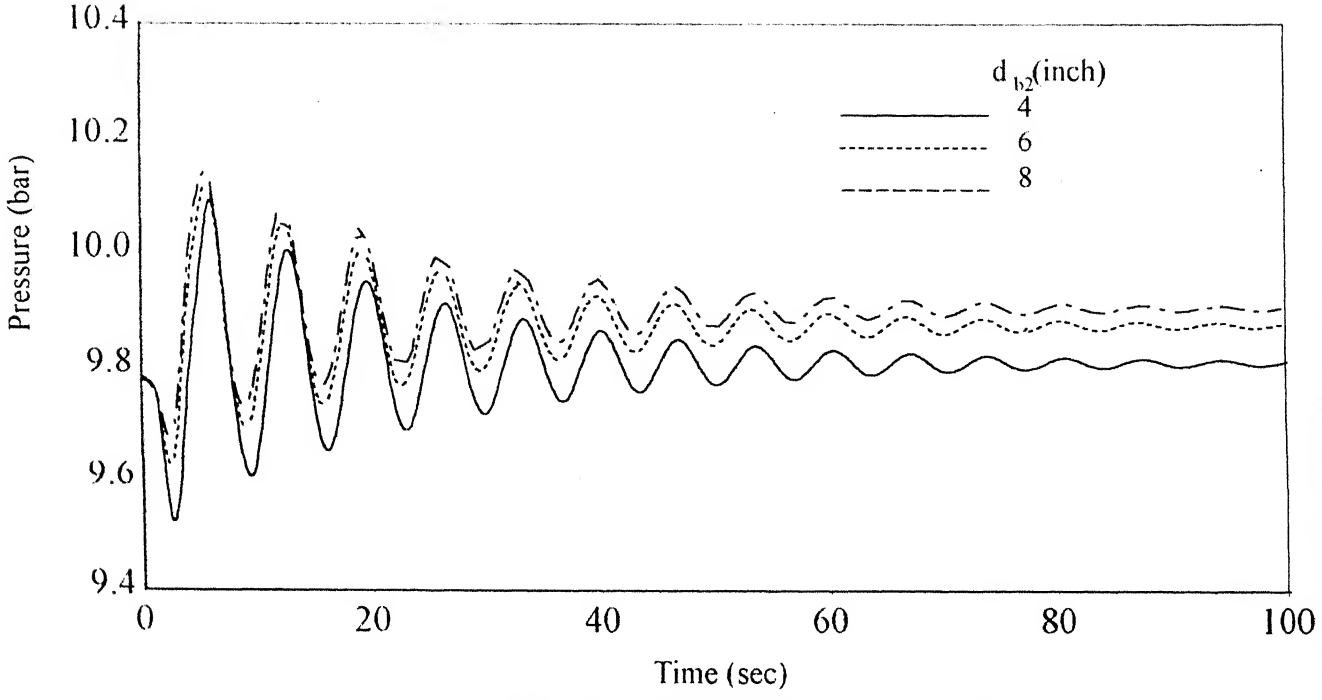

Figure 5.4k: Pressure transience at node A

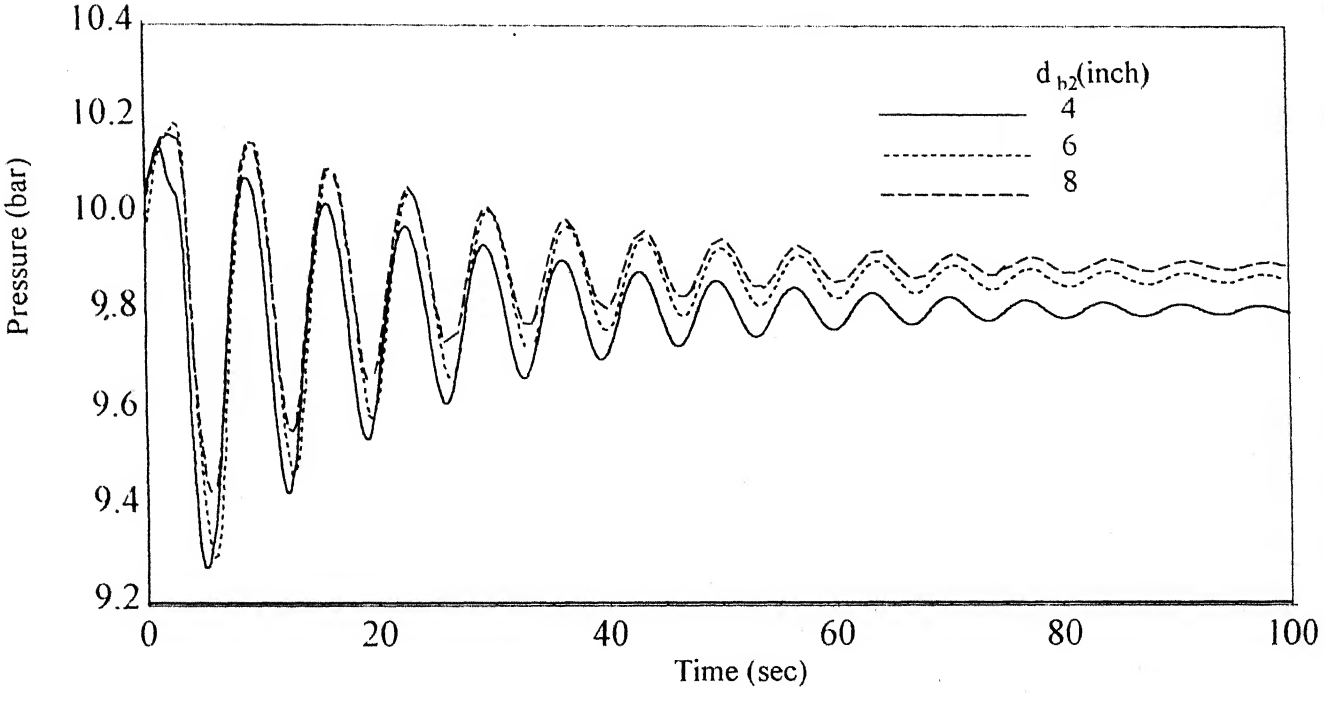

Figure 5.4l: Pressure transience at node B

(Effect of change in diameter of branch 2 on pressure transience)

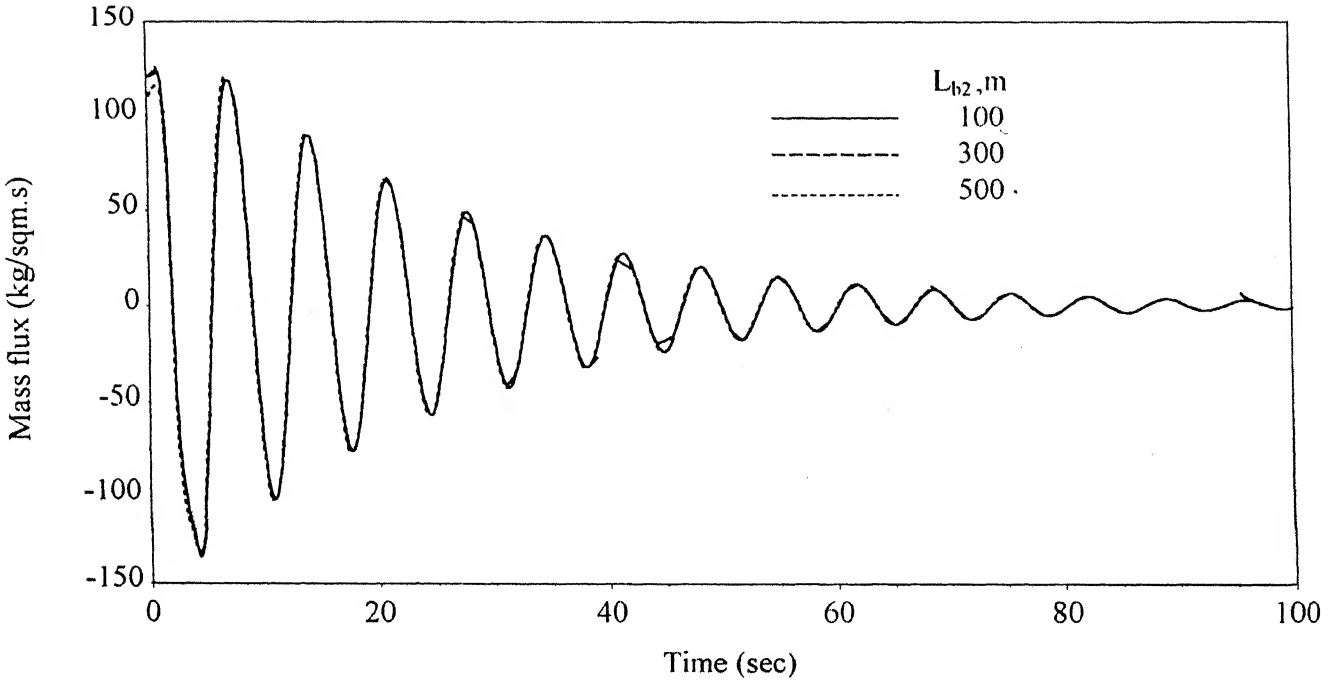

Figure 5.4m: Mass flux transience at node B for branch 1

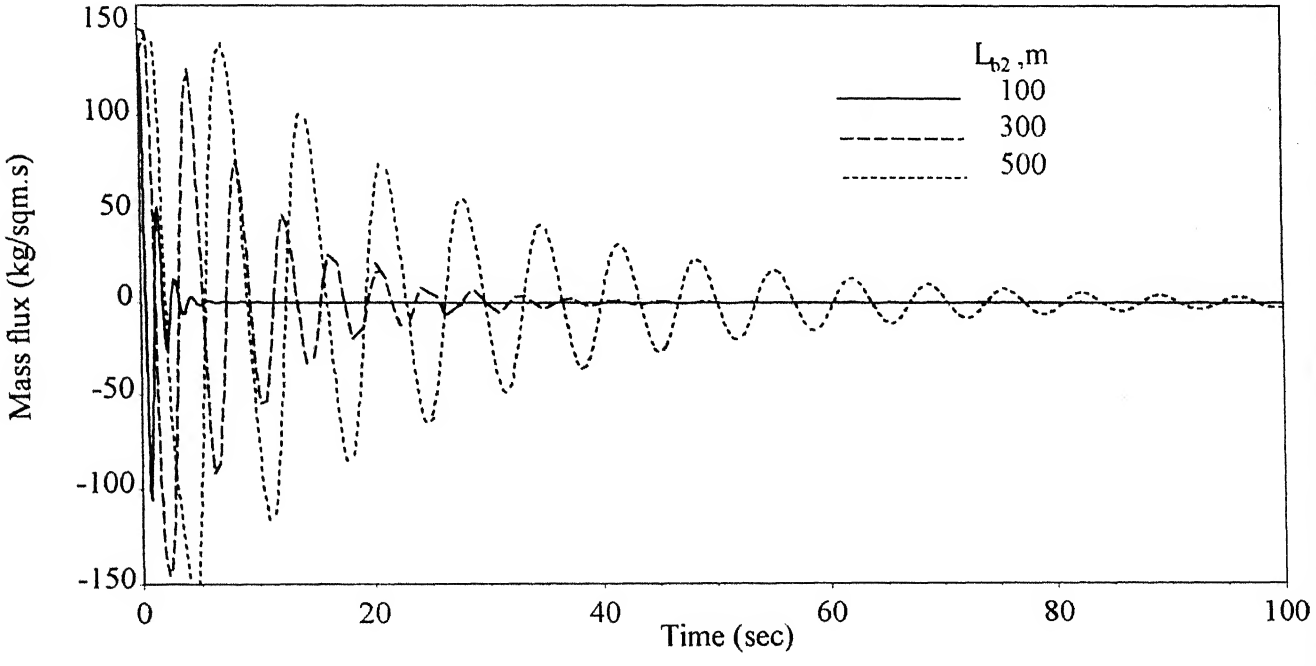

Figure 5.4n: Mass flux transience at node B for branch 2

(Effect of change in length of branch 1 on mass-flux transience)

(L_{mb}=500 m ,L_{b1}=500 m, d_{mb}=12", d_{b1}=6" ,d_{b2}=6" , P_{um}=10bar, m_{b1}= 2.5 kg/s m_{b2}=3kg/s)

Conditon: Compressor installed at the upstream end of main branch is closed completely and valves at nodes C and D are closed simultaneously

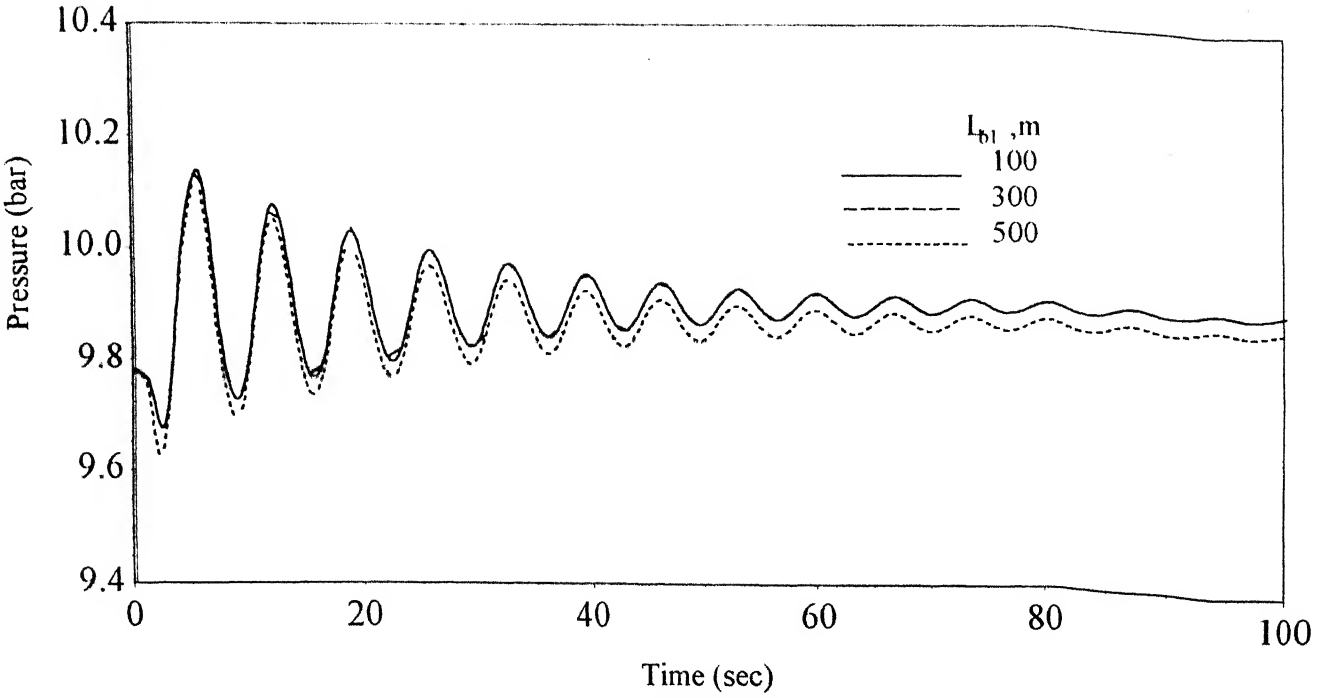

Figure 5.4o: Pressure transience at node A

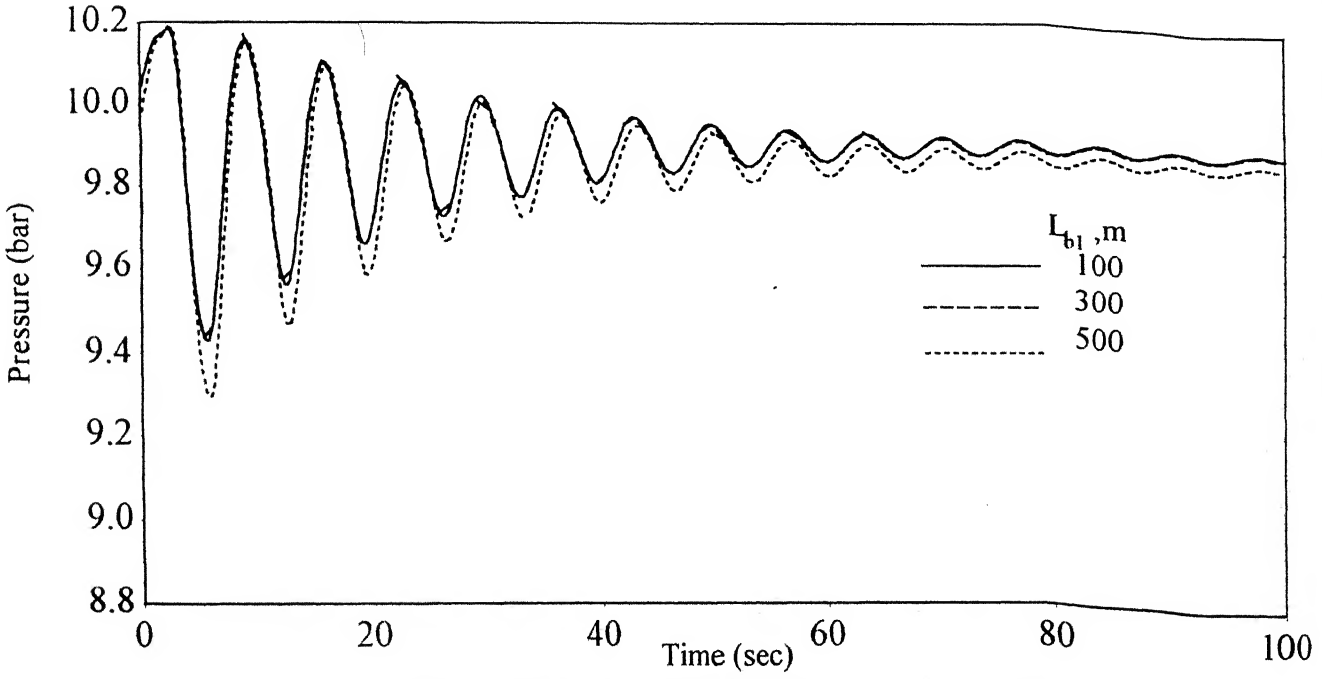

Figure 5.4p: Pressure transience at node B

(Effect of change in length of branch 1 on pressure transience)

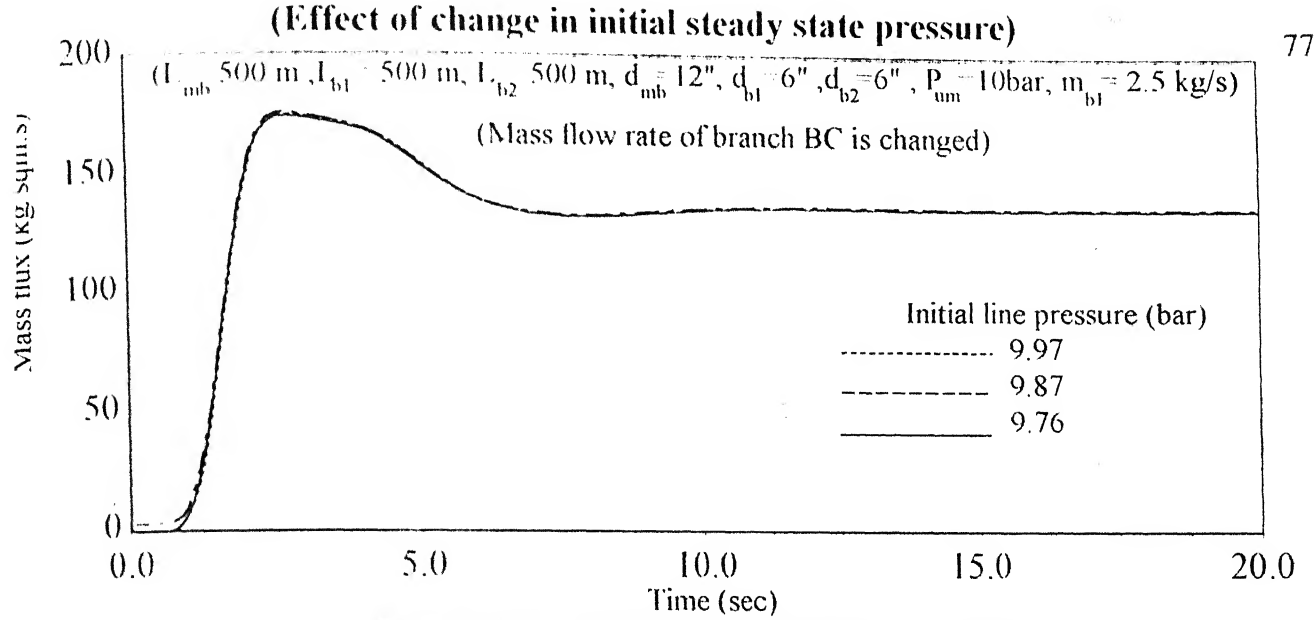

Figure 5.5a: Mass flux transience at node C

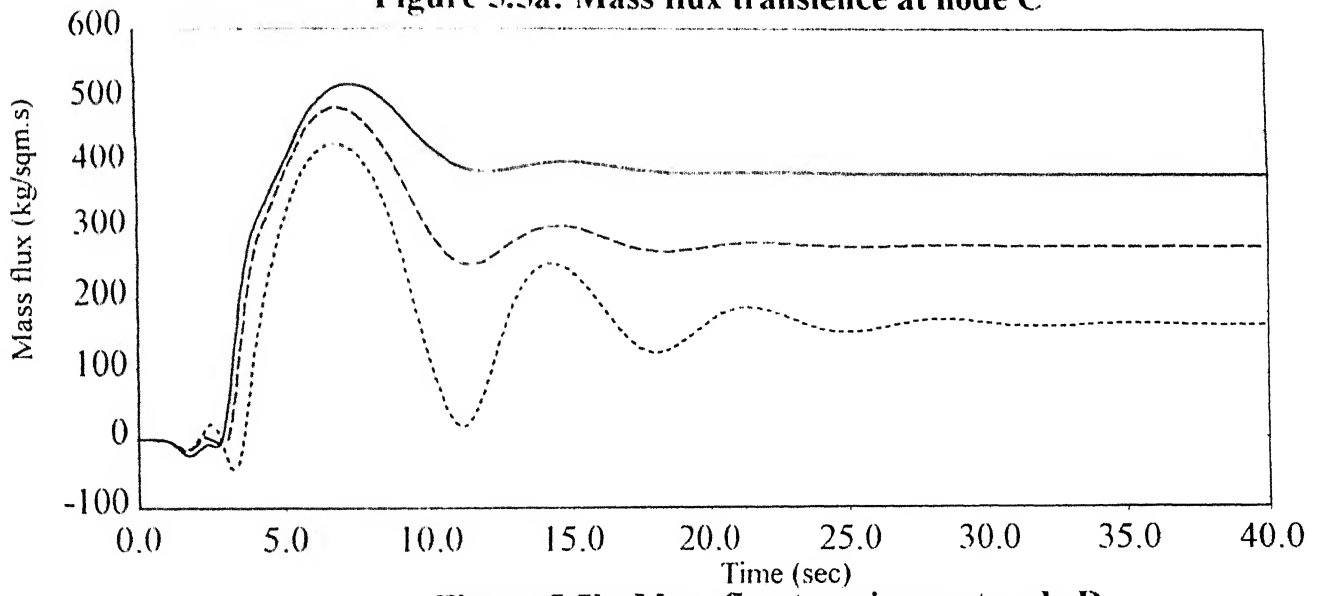

Figure 5.5b: Mass flux transience at node D

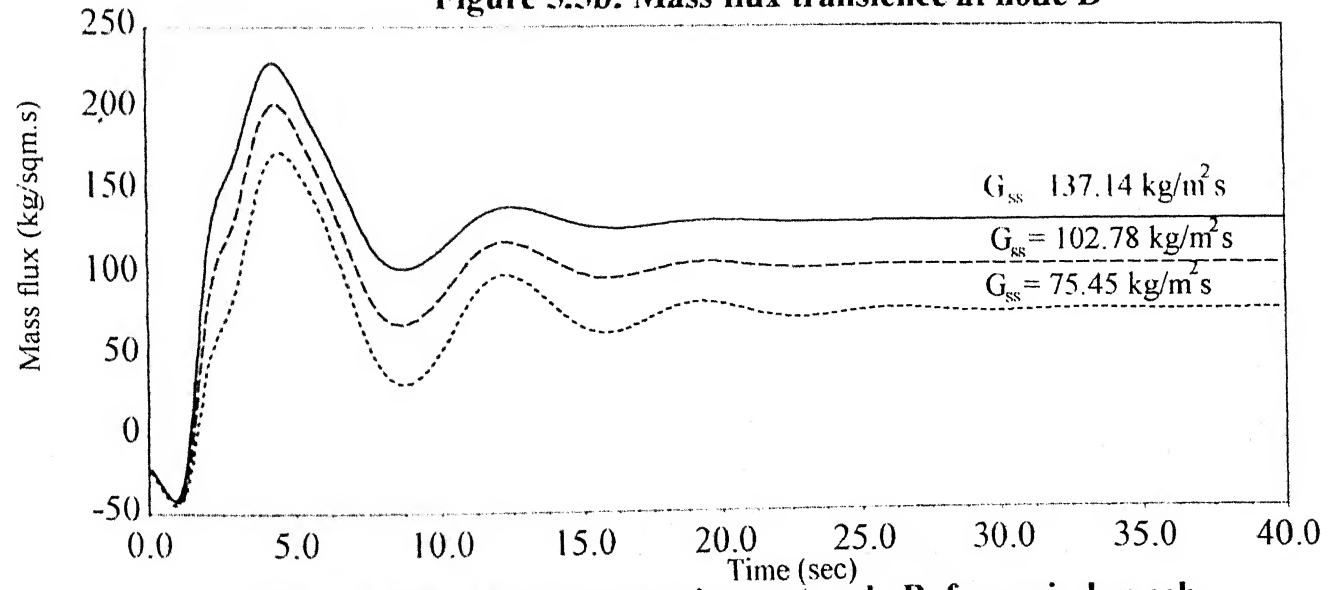

Figure 5.5c: Mass flux transience at node B for main branch

Condition:- Compressor at A starts from initial line pressure and valves

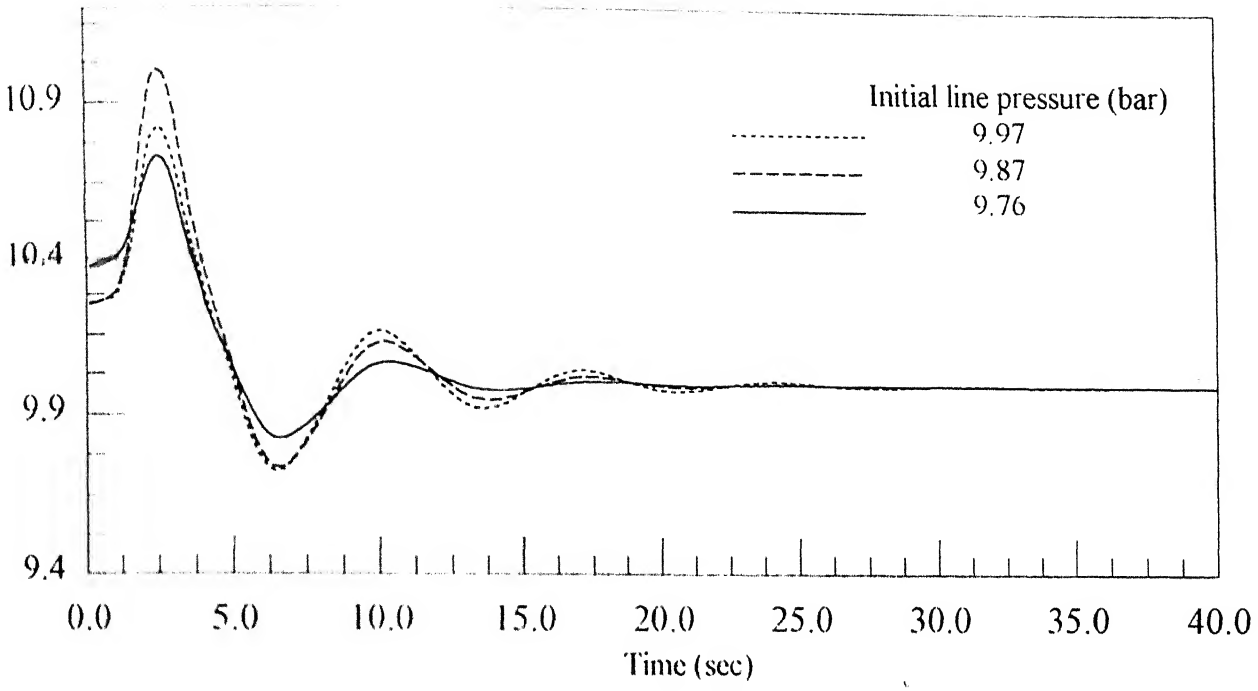

Figure 5.5d: Pressure transience at node A

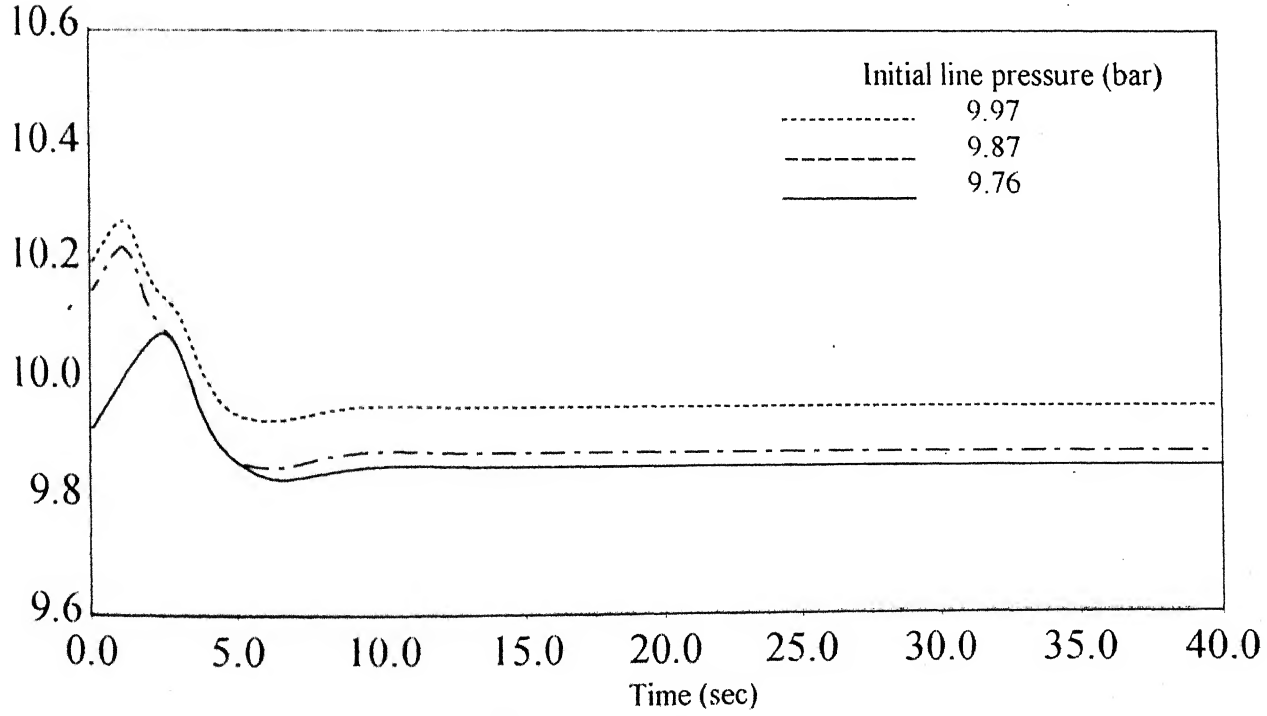

Figure 5.5e: Pressure transience at node B

(Effect of change in initial steady state pressure)

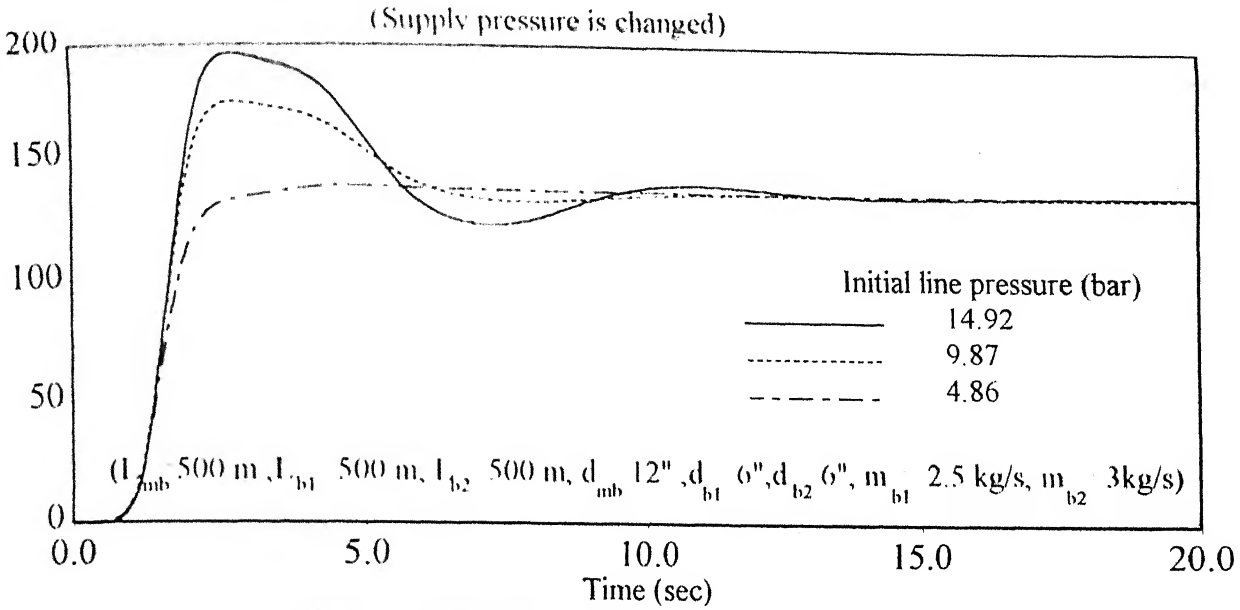

Figure 5.5f: Mass flux transience at node C

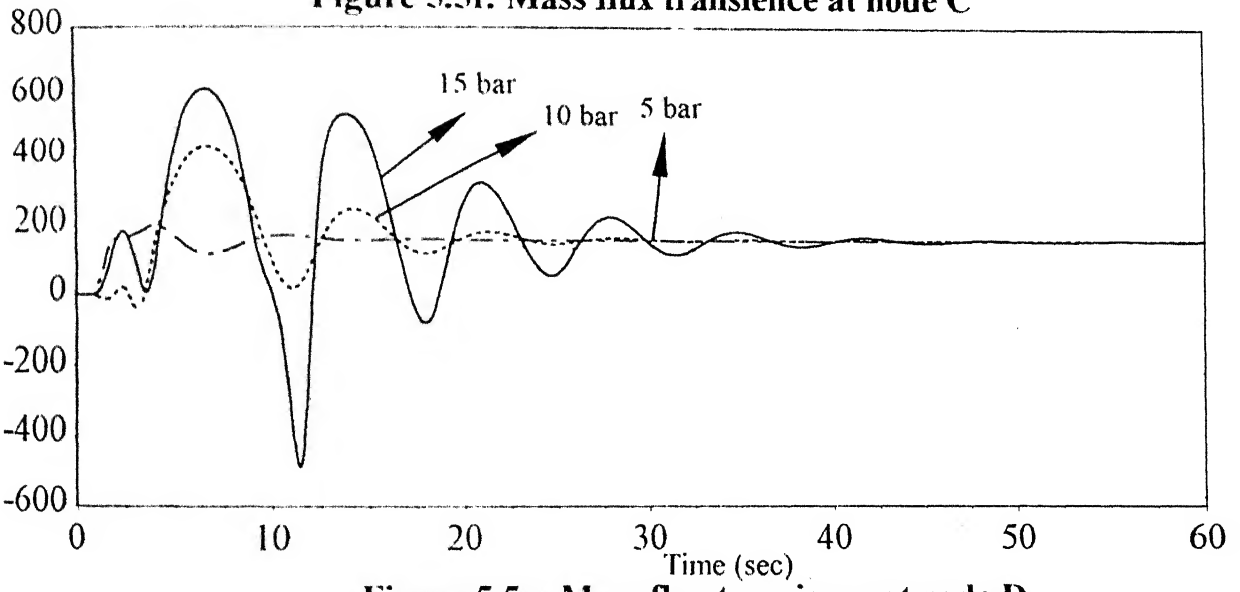

Figure 5.5g: Mass flux transience at node D

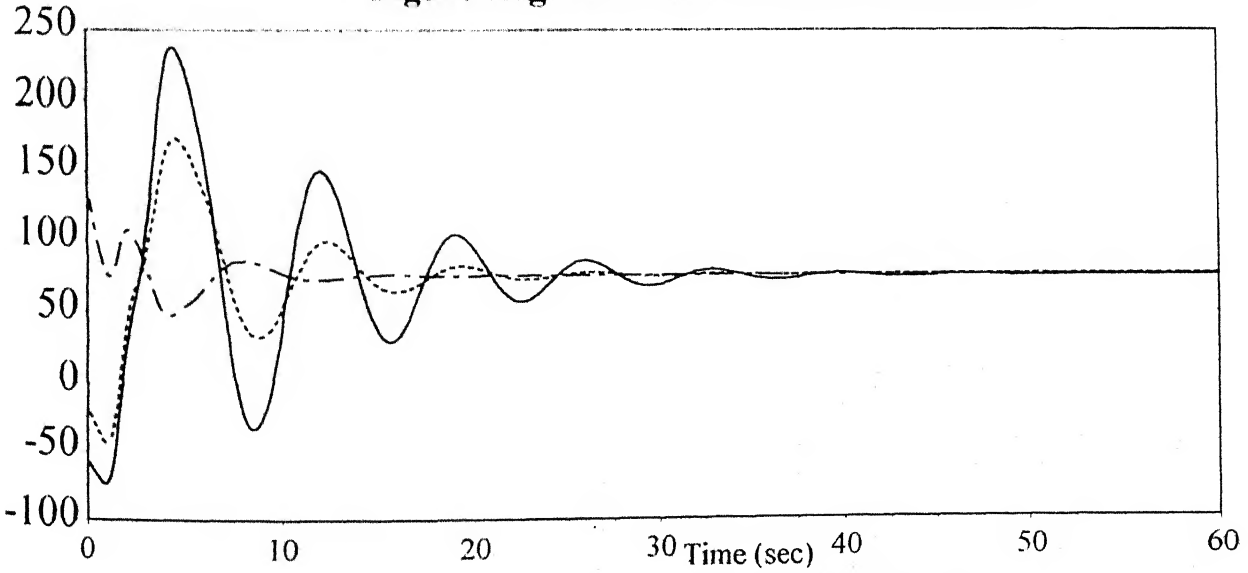

Figure 5.5h: Mass flux transience at node B for main branch (Effect of change in initial steady state pressure)

(Initial line pressure is 14.92 bar)

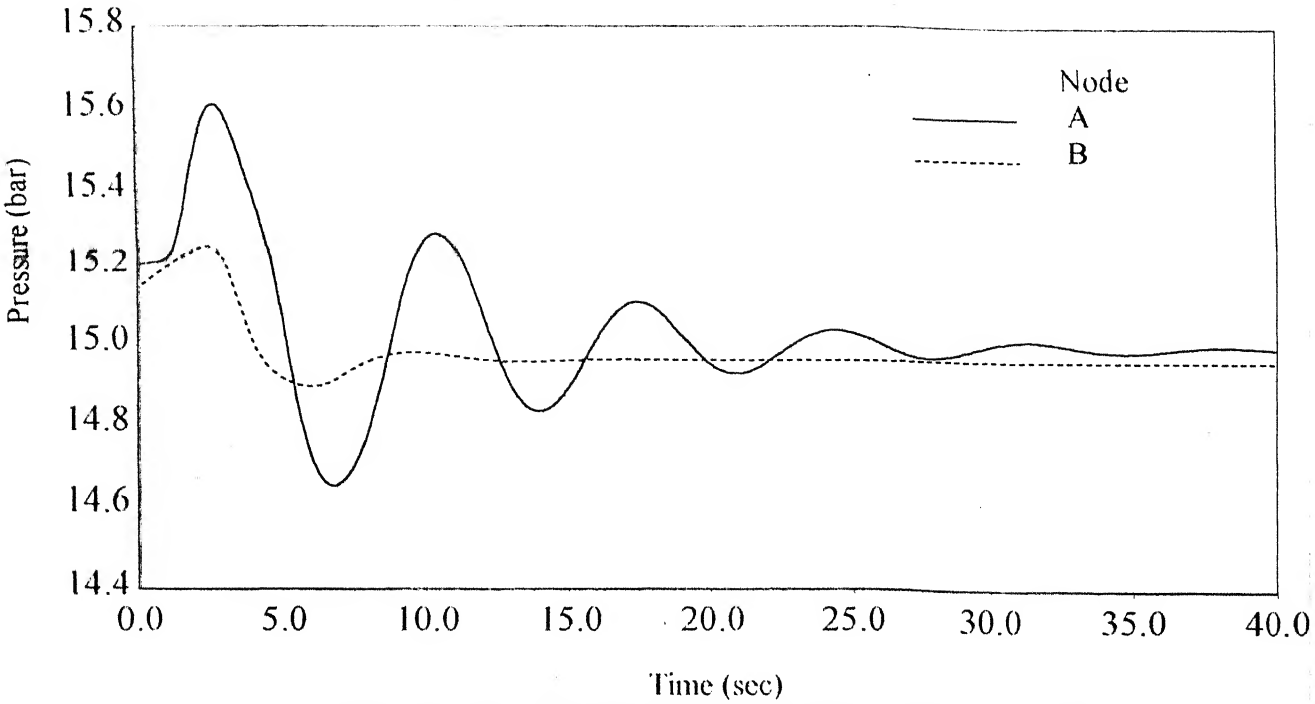

Figure 5.5i: Pressure transience at node A and B

(Initial line pressure is 4.86 bar)

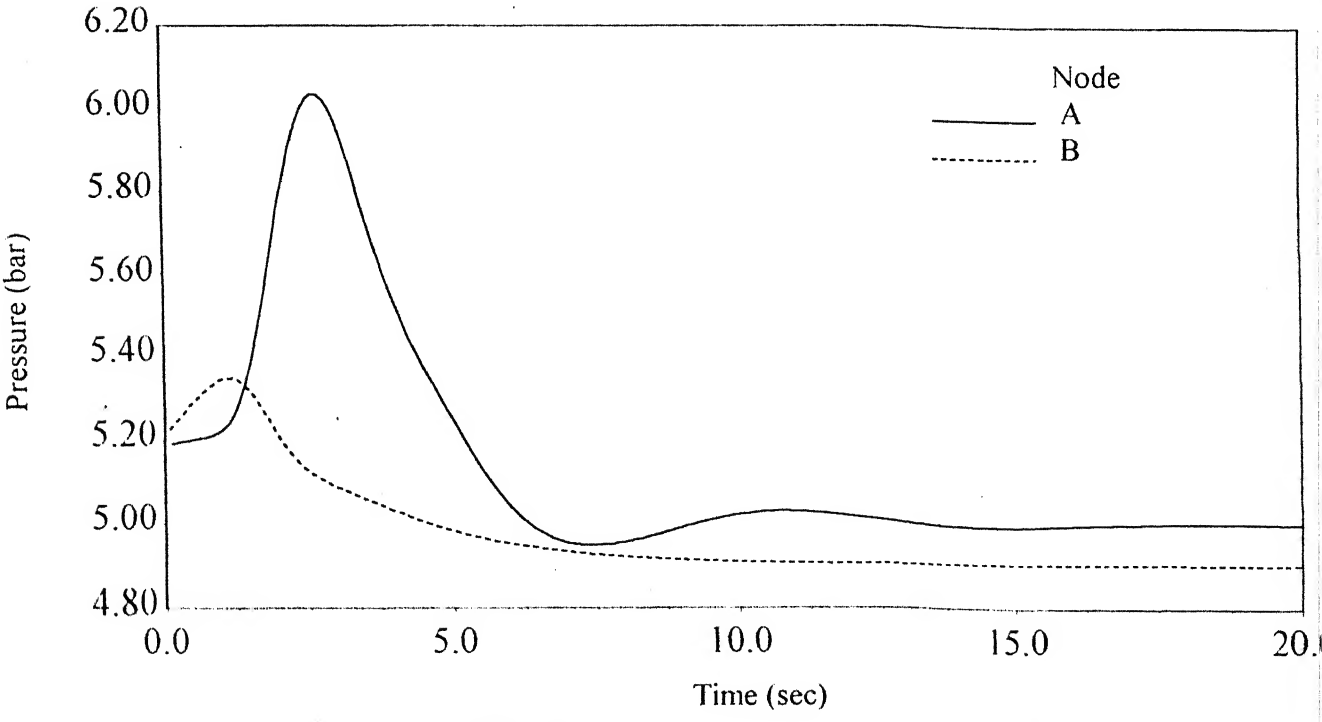

Figure 5.5j: Pressure transience at node A and B

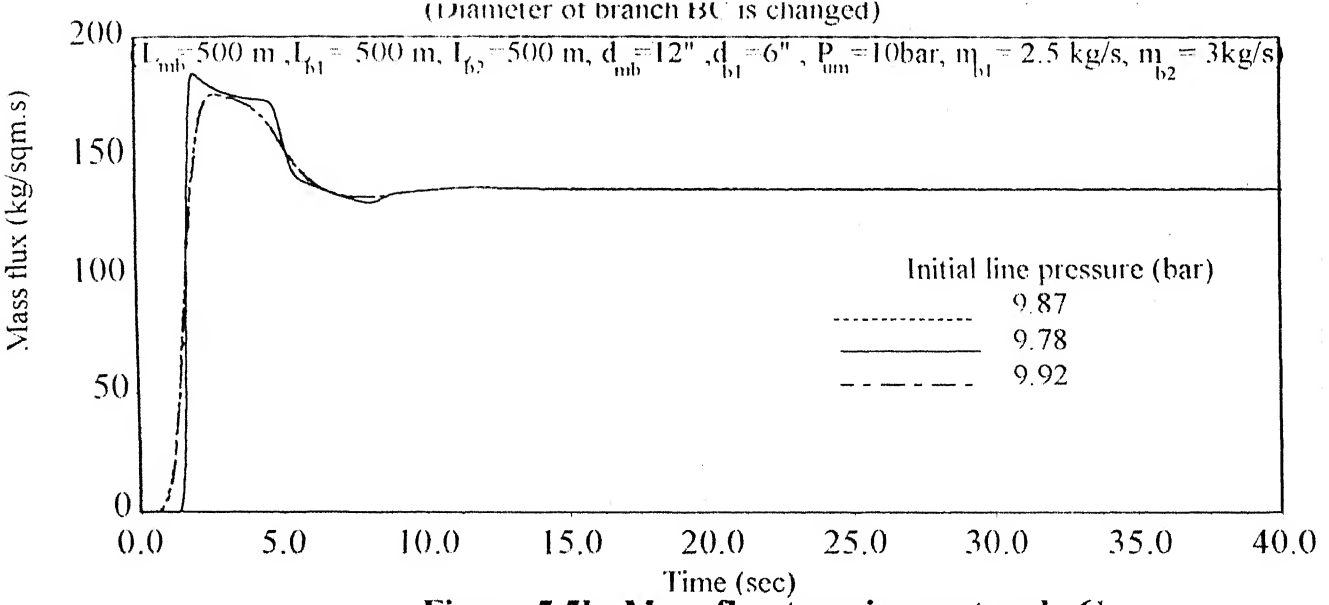

Figure 5.5k: Mass flux transience at node C

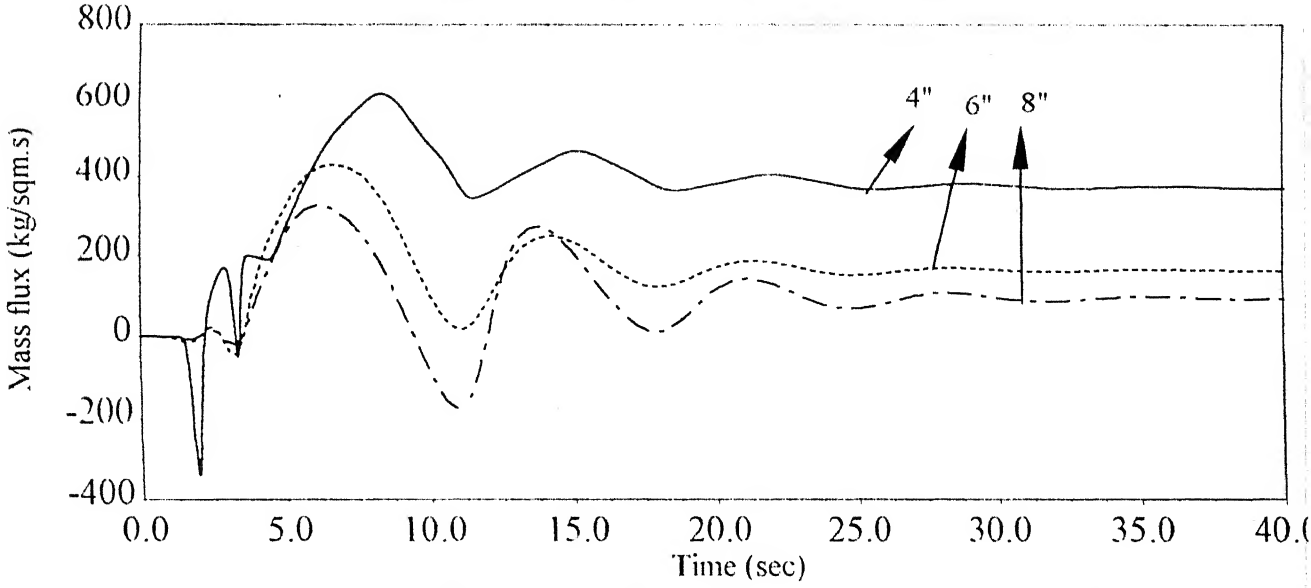

Figure 5.5l: Mass flux transience at node D

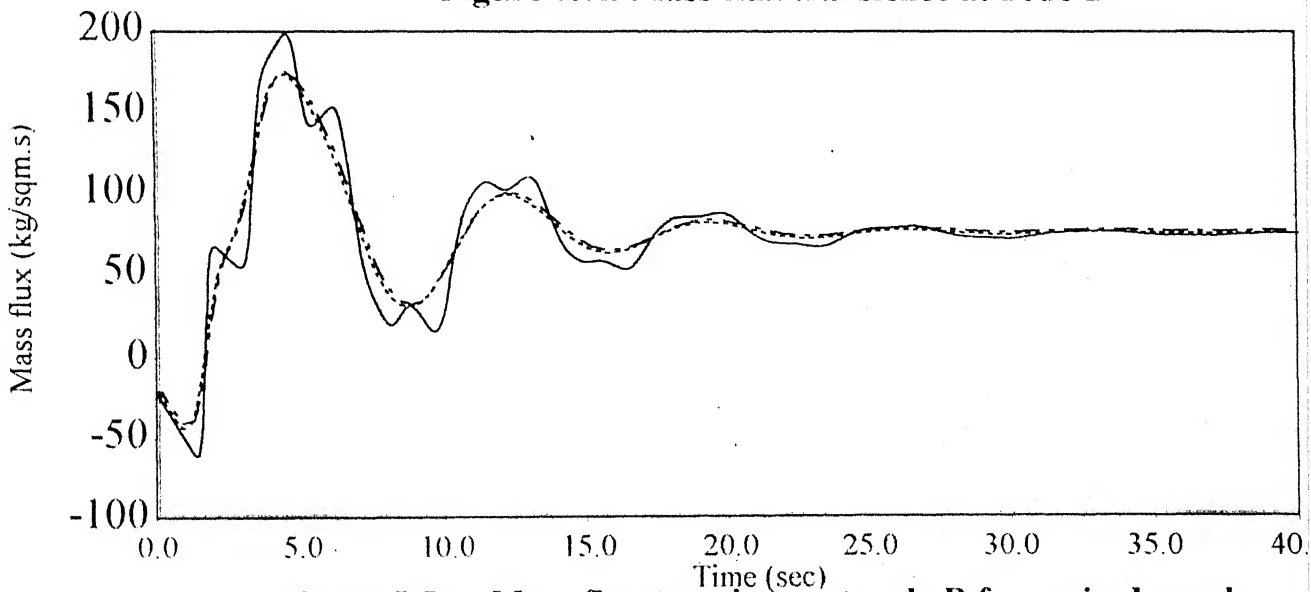

Figure 5.5m: Mass flux transience at node B for main branch
(Effect of change in initial steady state pressure)

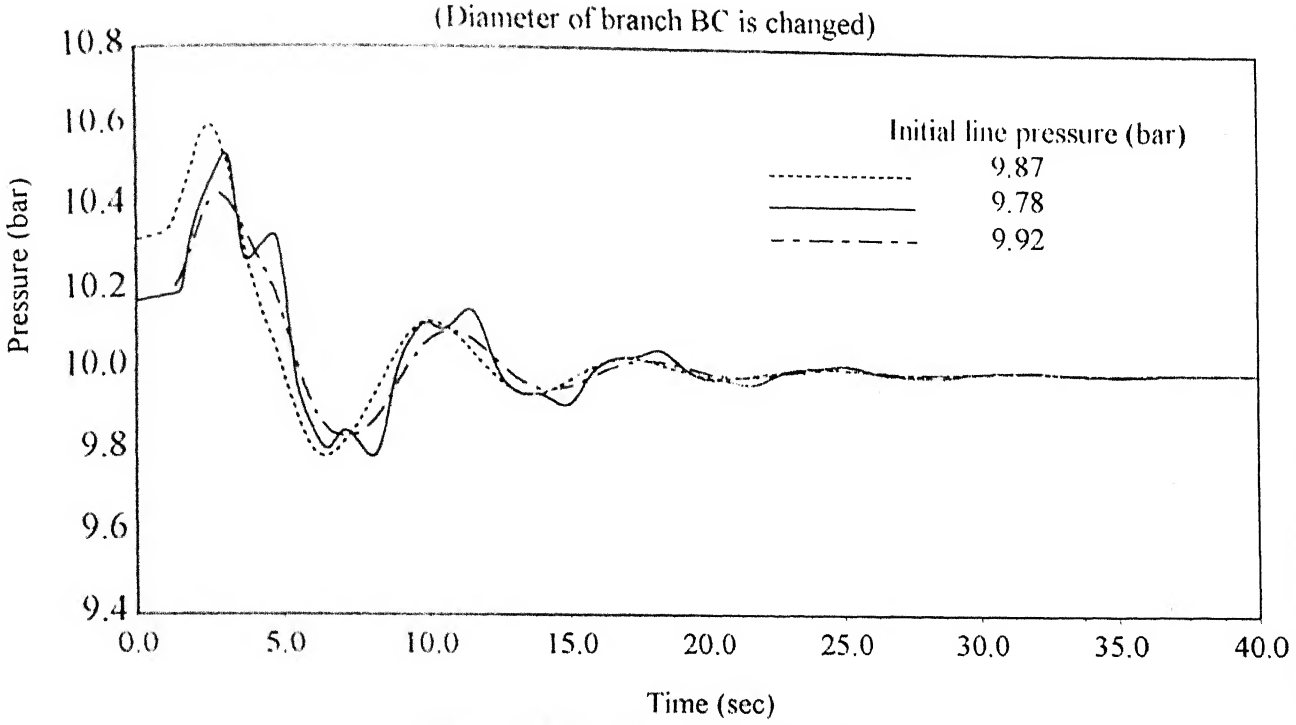

Figure 5.5n: Pressure transience at node A

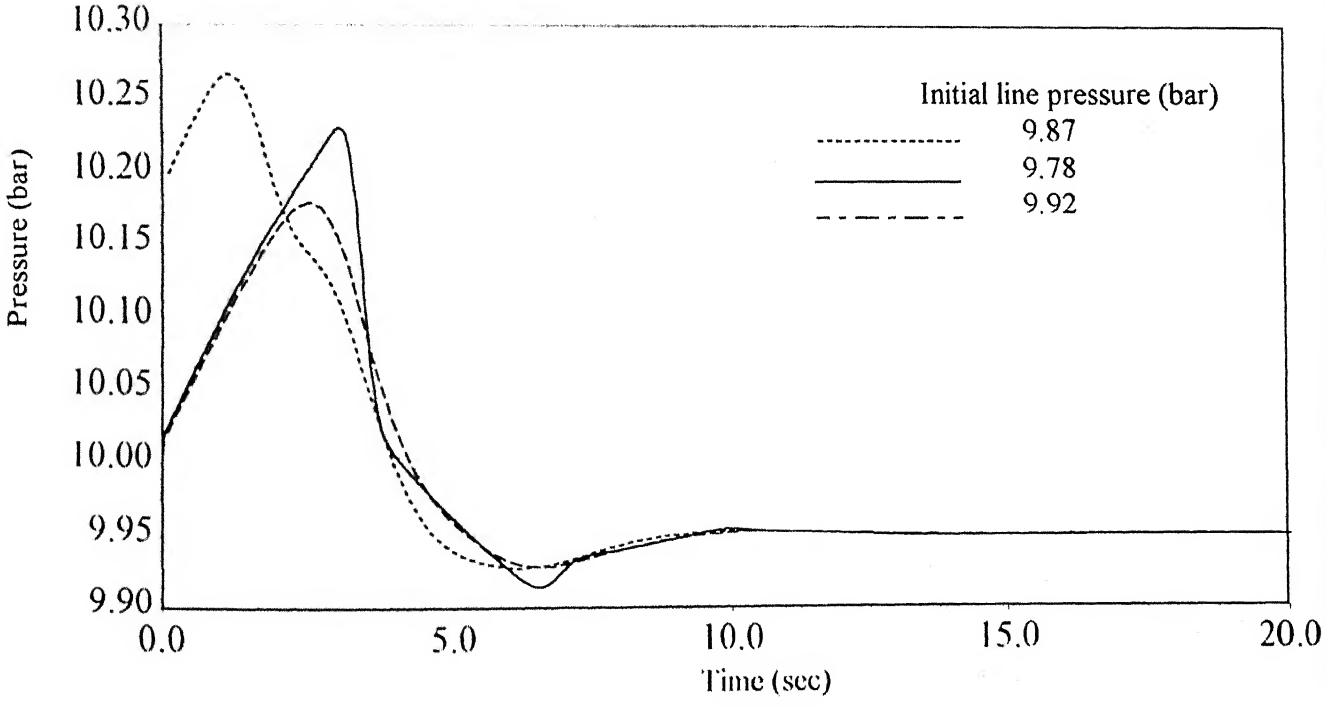

Figure 5.5o: Pressure transience at node B

(Effect of change in initial steady state pressure)

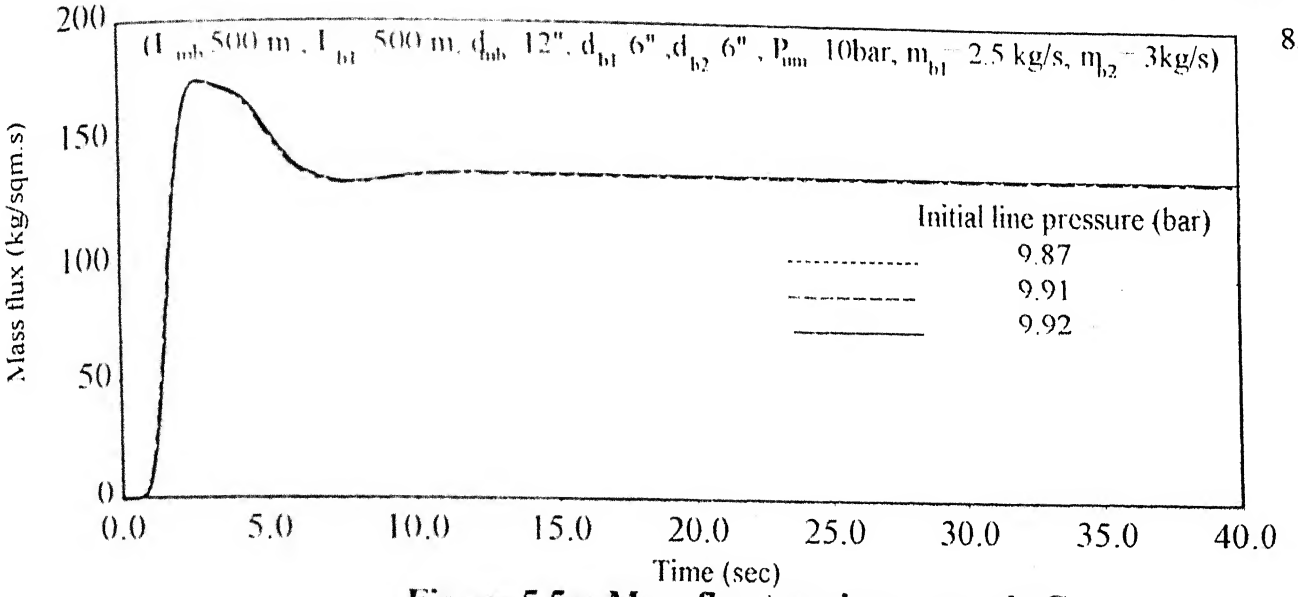

Figure 5.5p: Mass flux transience at node C

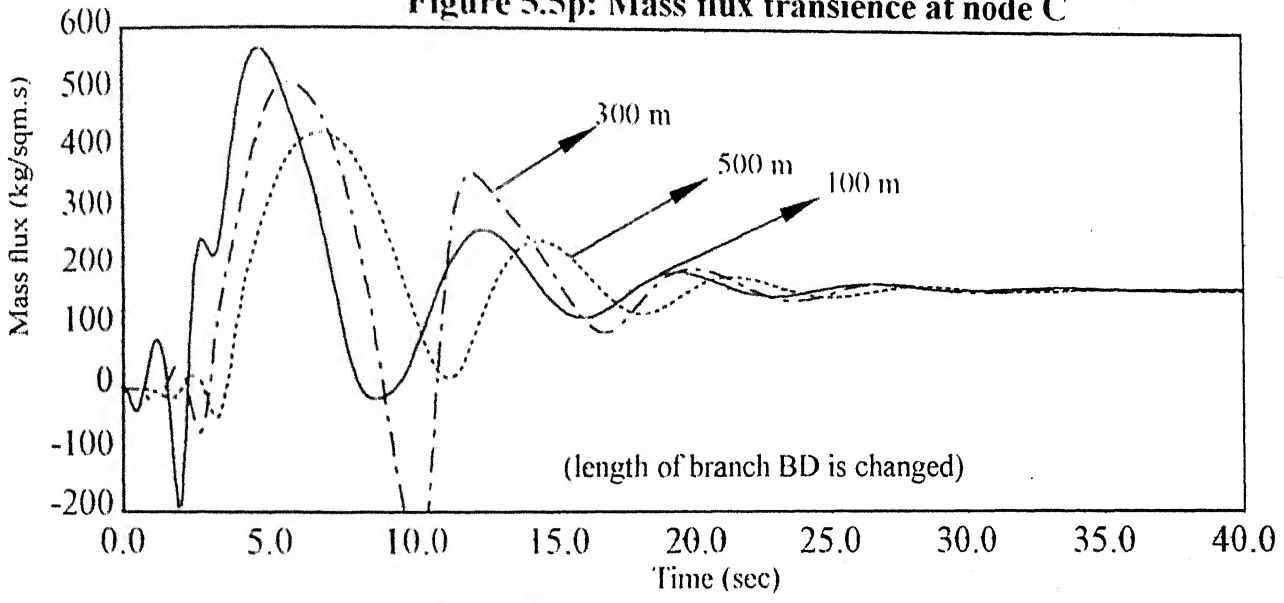

Figure 5.5q: Mass flux transience at node D

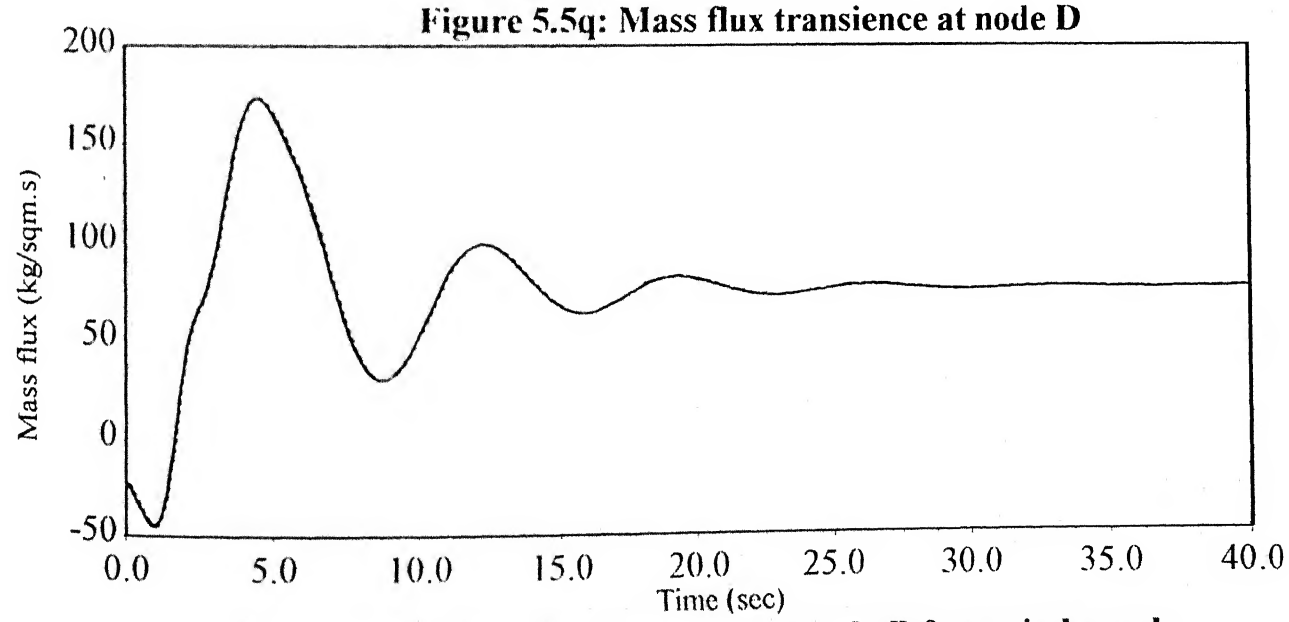

Figure 5.5r: Mass flux transience at node B for main branch (Effect of change in initial steady state pressure)

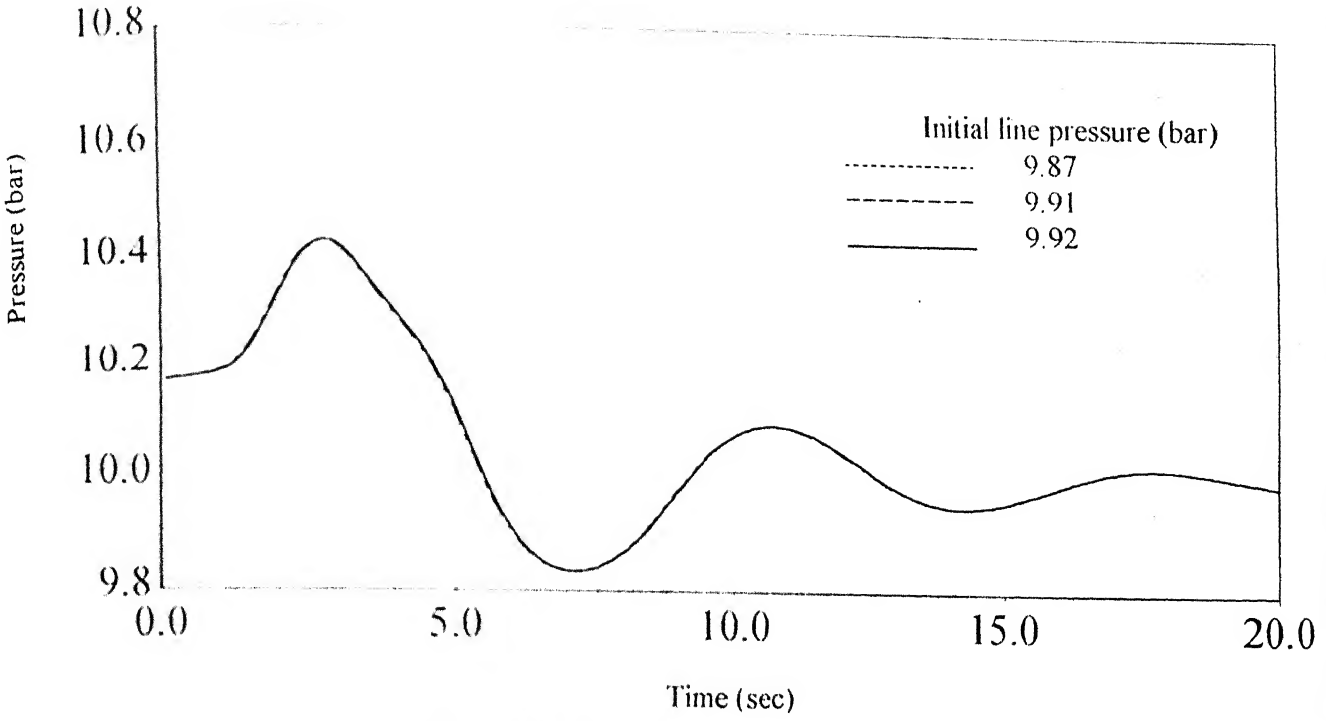

Figure 5.5s: Pressure transience at node A

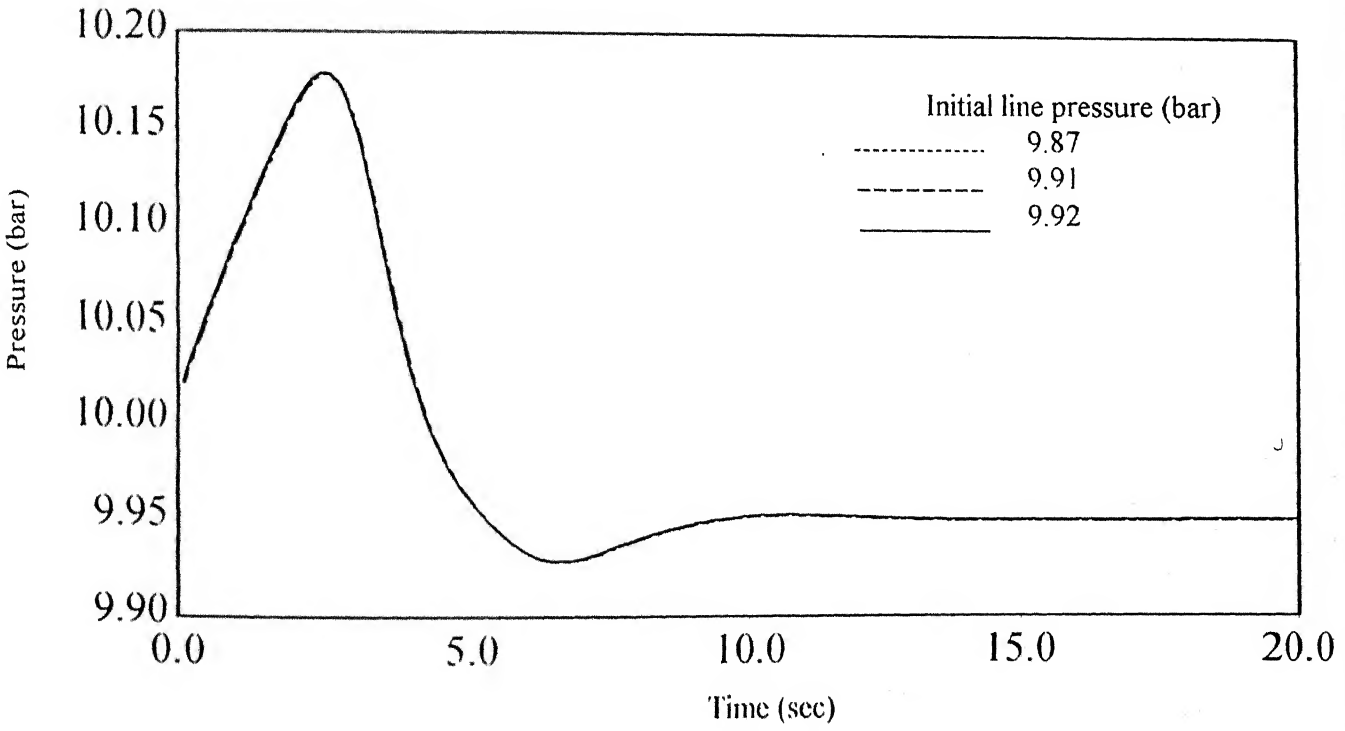

Figure 5.5t: Pressure transience at node B

(Effect of change in initial steady state pressure)

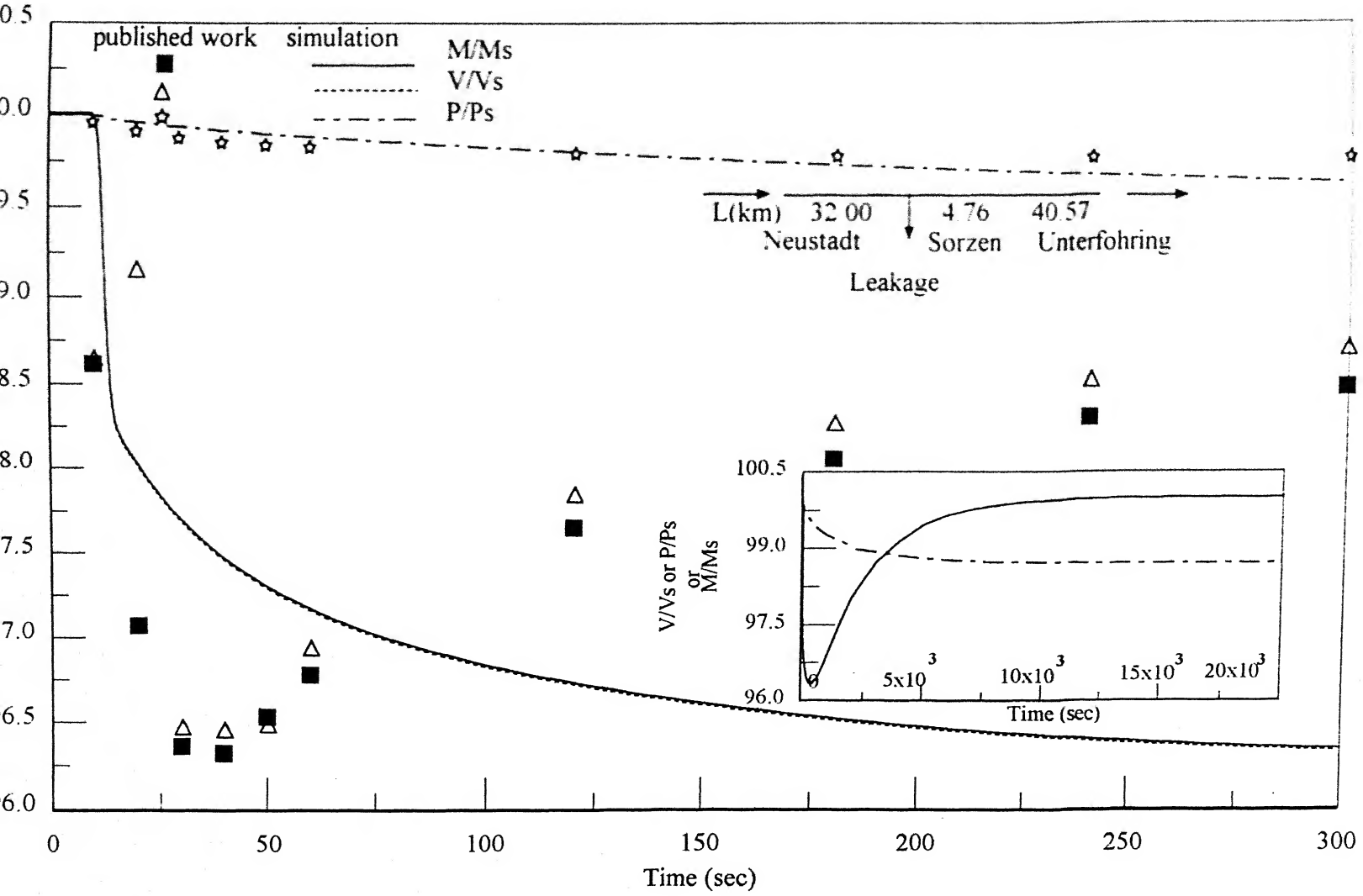

Figure 5.6: Leakage Analysis:- Velocity, pressure and flow-rate variations at Sorzen after leakage (The variations are given as percentages of the steady-state values)

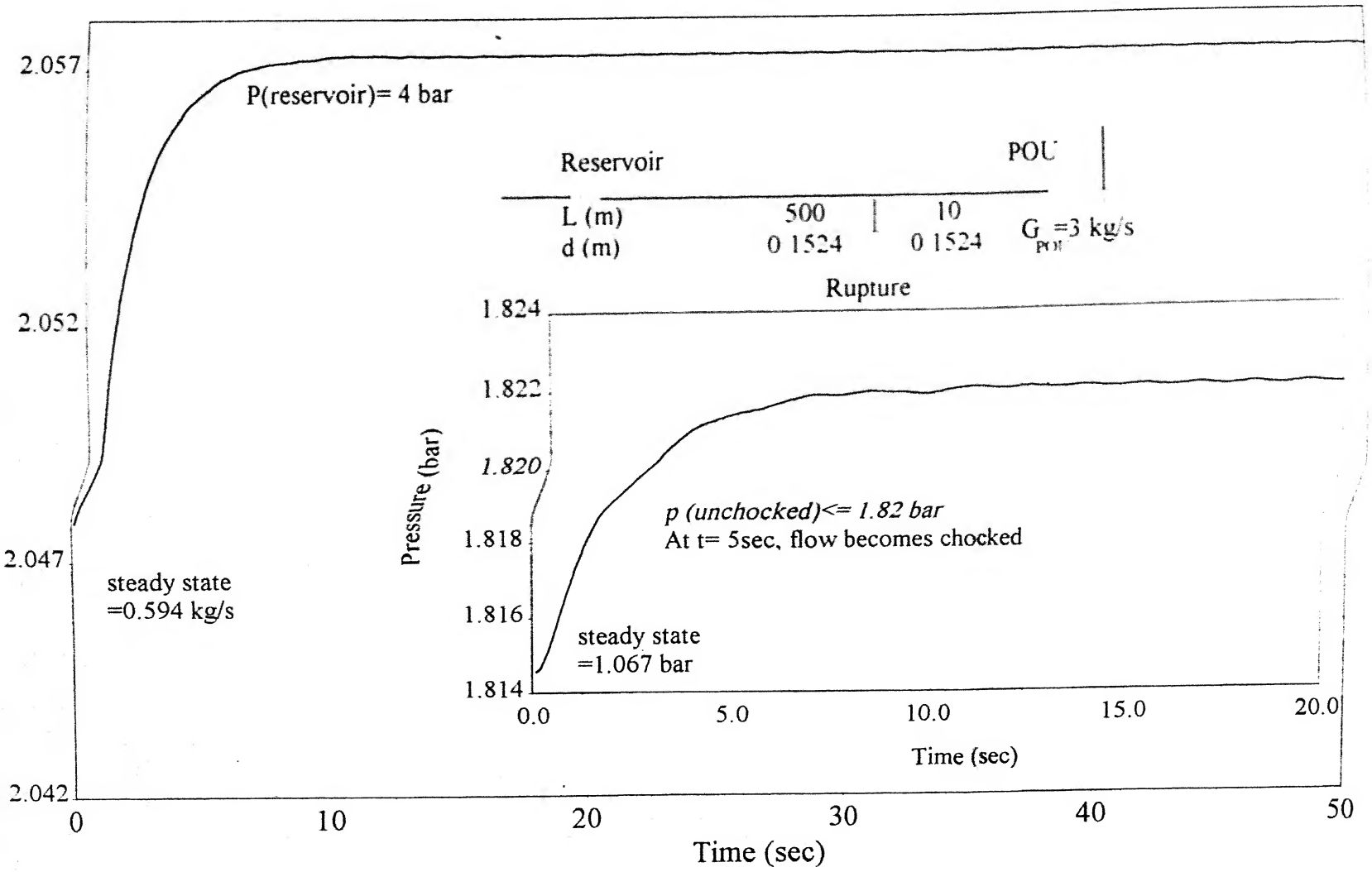

gure 5.7a: Rupture analysis: Simulation of gas flow at the outlet in a low pressure pipeline. The pressure at the position of the rupture is depicted in the inset

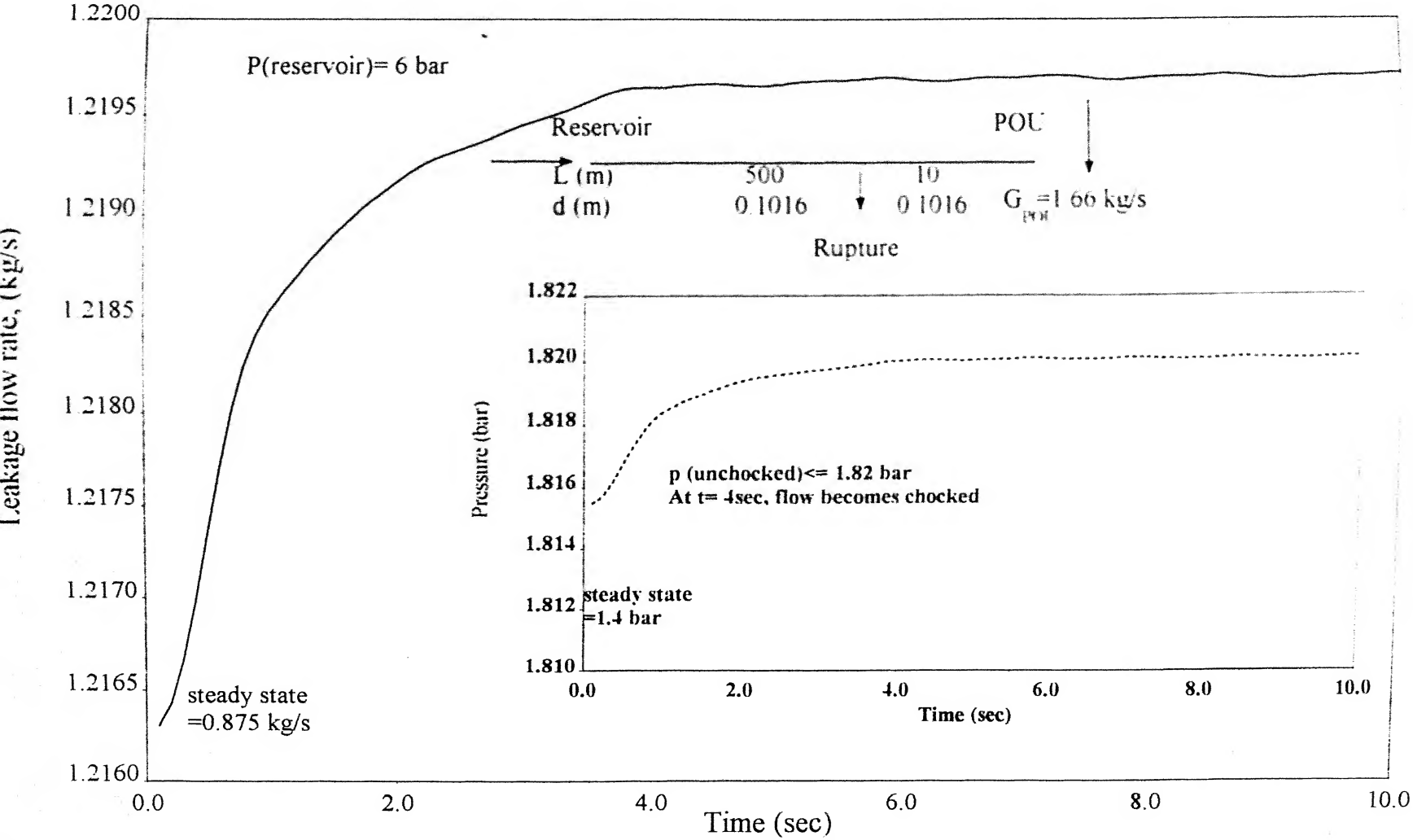

Figure 5.7b: Rupture analysis: Simulation of gas flow at the outlet in a low pressure pipeline. The pressure at the position of the rupture is depicted in the inset

Table 3

Simulation of outflow as well as pressure at the point of rupture in a high-pressure gas pipeline. During the whole simulation, the outflow pressure is greater than 1.82 times the pressure of the surroundings. The flow is thus sonic at the rupture.

Time (sec)	$P_{chocked}$ (bar)	P_0 (bar)	Q_m (kg/s)
1.0	4.50	8.1913	4.7989
1.5	3.75	6.8260	3.9990
2.0	3.50	6.3711	3.7325
2.5	3.30	6.0069	3.5192
3.0	3.20	5.8249	3.4126
3.5	3.10	5.6429	3.3059
4.0	3.00	5.4608	3.1993
4.5	2.90	5.2788	3.0926
5.0	2.85	5.1878	3.0393
5.5	2.80	5.0968	2.9862
6.0	2.77	5.0422	2.9541
6.5	2.75	5.0058	2.9326
7.0	2.72	4.9148	2.9007
7.5	2.70	4.9148	2.8793
8.0	2.70	4.9148	2.8793
8.5	2.70	4.9148	2.8793
9.0	2.70	4.9148	2.8793
9.5	2.70	4.9148	2.8793
10.0	2.70	4.9148	2.8793

Chapter 6

CONCLUSIONS

In this work, theoretical analysis has been carried out to study a wide range of scenarios concerning transient conditions in gas flow and pressure in a manifold consisting of a main branch dividing into various sub-branches. The model outlined herein enables to predict the transient behavior of pressure and mass-flux in a manifold when operating conditions such as pipe diameter and length, supply pressure or mass flow, number of sub-branches are altered. Transience situation in a manifold arising due to closure of a valve installed at the outlet end of one of the branches, compressor shut down and start up, leakage and rupture have been investigated.

The main findings of this work can be summarized as follows. When a valve at the downstream end of one of the sub-branches is closed completely, pressure and mass flux oscillations increases with increase in length and diameter of sub-branches. Increasing the supply pressure and mass flow rate in which the disturbance is brought about or by decreasing the mass flow rate in the neighborhood branches also result in increased mass flux and pressure transience.

In case of compressor shutdown due to power failure or malfunctioning, increased mass flow rate, supply pressure and larger pipe dimensions resulted in greater fluctuations in the manifold. In case of compressor start-up after the power is restored, initial line pressure affects the extent of transience in branches. A temporary surge in pressure and mass flux is observed, the magnitude of which depends upon length, diameter, supply pressure and mass flow rate. Higher mass flow rate, supply pressure and larger pipe dimensions cause increased fluctuations in pressure and mass flux.

A leakage in the pipeline has been simulated for a low-pressure pipeline. The simulated results have been compared with the published work. It appears that the velocity

and mass flow rates were much more sensitive to the change of supply pressure than the pressure at the location of the leakage. The maximum decreases in velocity and pressure were approximately 3 per cent and 0.3 per cent, respectively, at a position 4760m from the leakage.

The results of a simulation of outflow from an abrupt rupture are also described. The outflow of gas into the atmosphere has been predicted under chocked as well as un-chocked conditions.

Scope of Future Study

This work is limited to a manifold consisting of various sub-branches not interlinked with each other. The study should be extended to more realistic networks in which the sub-branches are interconnected to each other to form a closed loop network.

A constant supply pressure at the inlet of the main branch is assumed throughout the present work. A parametric study should be done to determine the transient response of gas mass flow-rate and supply pressure in the gas delivery line under the conditions of time varying pressure at the gas source. During transportation of liquefied gases, the temperature at the source may change due to cooling of the liquid in the container, which in turn will result in gradual decrease in vapor pressure or the inlet supply pressure. The gas in the pipeline may then condense leading to a two phase gas-liquid system which may affect the extent of transience in the system.

In-line instruments such as orifice-meter, venturi-meter, etc., or pressure and mass flow controlling devices such as compressors, boosters, etc. at various locations along the pipeline affects pressure and mass-flux which should also be investigated.

REFERENCES

Batey E.H., H.R.Courts and K.W.Hannah, 'Dynamic approach to gas-pipeline analysis', Oil and Gas J., 65-78, 1961

Bender E., 'Simulation of dynamic gas flow in networks including control loops', Comput. Chem. Eng., **3**, 611-613 (1979)

Bisgaard C., H.H.Sorensen and S.Spangenberg, 'A finite element method for transient compressible flow in pipelines', Int. J. Num. Methods in Fluids, **7**, 291-303 (1987)

Burnett R.R.,' Predicting and controlling transient pressures in long pipelines', Oil and Gas J.,**59**, 153-160, 1960

Fincham A.E. and M.H.Goldwater, 'Simulation models for gas transmission networks', Trans. of Inst. Of Measurement & Control, **1**, Jan-Mar 1979.

Guy J.J., 'Computation of unsteady gas flow in pipe networks', I. Chem.E., Symp. Series, **23**, 139-145 (1967)

Hati A., 'Transient analysis of a gas distribution system', M.Tech Thesis, Dept. of Chemical Eng., IIT Kanpur, Jan(2000).

Osiadacz A., 'Simulation of transient gas flows in networks', Int. J. Numer.Methods Fluid, **4**, 13-23 (1984)

Poloni M., D.E.Winterbone and J.R.Nichols, 'The calculation of pressure and temperature discontinuity in a pipe by the method of characteristics and the two-step differential Lax-Wendroff method', ASME FED, **62**, 1-7 (1987).

Rachford H.H., U.Rice and E.L.Ramsey, 'Application of variational methods to model transient flow in complex liquid transmission systems', J. Petroleum. Eng, AIME SPE, **5663**, 1-20 (1975).

Schmidt G. and A.Weimann, 'Instationare gasnetzberech-nung mit dem programming, GANESI. GWF GAS/Erdgas, **118**, 53-57 (1977).

Simpson A.R. and Z.Y.Wu, 'Computer modeling of hydraulic transients in pipe networks and the associated design criteria', MODSIM 97, Int. Congress on Modeling and Simulation, Hobart, Tasmania, Australia, Dec (1997).

Wylie E.B. and V.L.Streeter, 'Fluid Transients ', McGraw-Hill, NY, 271-285 (1978).

Watters G.H., 'Analysis and control of unsteady flow in pipelines', Butterworth publishers, Stoneham, M.A. (1984).

Wylie E.B. and V.L.Streeter, 'Fluid Transients in Systems', Wiley and Sons, NY (1993).

Appendix

Calculation of final steady state pressure in case of compressor shut down.

Since the system is isolated after the compressor at A and the valves at C and D are closed, one can apply the ideal gas equation to find the fixed number of moles trapped inside the system. The system in this case is a two branch manifold.

Using ideal gas law equation

$$PV=nRT \tag{A1}$$

Where P= pressure, N/m^2

V= volume, m^3

n=number of moles, kmole

Equation (A1) can be written as for a differential volume as

$$P.dV= dn.RT \tag{A2}$$

$$dn=\frac{Pdv}{RT} \tag{A3}$$

$$n=\frac{1}{RT}\int Pdv \tag{A4}$$

$$n=\frac{A}{RT}\int Pdl \qquad [V= A.l] \tag{A5}$$

$$\sum n=\frac{Al}{RT}\sum P \qquad \text{[all grids are equispaced]} \tag{A6}$$

$$P_{ss}=\frac{RT\sum n}{V} \tag{A7}$$

Thus, the total number of moles present in the system can be determined by knowing the pressure profiles in each of the pipes at the instance of closing the valves. Knowing the total moles enables us to know the final steady state pressure.

For a particular case of compressor shut down in case of a two branch manifold, the calculations are carried out as follows:

($L_{mb}=L_{b1}=L_{b2}=500$ m, $d_{mb}=12"(0.3048$ m), $d_{b1}=d_{b2}=6"(0.1524$ m), $P_{um}=10$ bar, $m_{b1}=2.5$ kg/s, $m_{b2}=5$ kg/s).

$\sum P$ (for branch 1)=38977.929 bar

$\sum P$ (for branch 2) = 36889.851 bar

$\sum P$ (for main branch) = 39818.246 bar

$\sum n$ (for branch 1) = 3.5×10^5 Kmoles

$\sum n$ (for branch 2) = 3.3×10^5 Kmoles

$\sum n$ (for main branch) = 14.4×10^5 Kmoles

$\sum n$ (total) = 21.3×10^5 Kmoles

The final steady state pressure, P_{ss} = 9.799 bar which is close to the value obtained from the graph (Figure 5.4c)(9.87 bar)